The effect of the f-component of the pseudopotential on selected properties of 5d transition metal systems.

by

Daniel Cunnama

Submitted in fulfillment of the requirements
for the degree of Master of Science in the
School of Physics,
University of KwaZulu-Natal

Pietermaritzburg
August, 2008

Declaration

I declare that this work is a result of my own research, except where specifically indicated to the contrary, and has not been submitted for any other degree of examination to any other university.

Signed: _____ Date: _____

D. C. Cunnama

Supervisor: _____ Date: _____

Prof. N. Chetty

Supervisor: _____ Date: _____

Dr. R. Lindebaum

Abstract

Cohesive energies, bulk moduli, and equilibrium lattice constants have been calculated for the $5d$ transition atoms (Hf, Ta, W, Re, Os, Ir and Pt) in face–centred cubic crystal lattices. We have used the *ab initio* pseudopotential method for the total energy calculations within the local density approximation. Two calculations have been performed for each element, one using only the s, p and d angular momentum components and another including the s, p and d components as well as the unoccupied $5f$ orbital in the ionic pseudopotentials. The pseudo–wave functions and charge densities of the valence electrons have been represented by a basis of plane waves. For the $5d$ metals the changes in the electronic structure of the solid are small and they produce small changes in the bulk properties.

Acknowledgments

I would like to acknowledge the support of my supervisors Prof. Nithaya Chetty and Dr. Robert Lindebaum, who have supported me both academically and financially. I am extremely grateful for all of their patience and guidance in completing this work. I would like to acknowledge financial support from the National Institute of Theoretical Physics.

I would also like to thank my parents, Margie and Errol, for their incredible support and unwavering confidence throughout the past two years, and for always being there with a kind ear and a helping hand.

Finally to my many friends who have supported me and kept me grounded over the past two years, a huge thank you. And to my friends and colleagues at the University of KwaZulu-Natal for their support and understanding, and particularly Mr Allard Welter for all of his advice and assistance.

Contents

List of Figures

List of Tables

Chapter 1

Introduction

The application and interpretation of predictions of quantum theory are still very active areas of research, with the limits being constantly tested, but there can be no doubt that the quantum–mechanical theory of electrons and ions can be used to accurately describe most of low-energy physics, chemistry and biology. One famous example of this accuracy is the calculation of the gyromagnetic ratio of the electron, a figure which agrees with the experimental result to the limit of the measurement, nowadays some 12 significant figures [8]. Quantum theory has yet to be shown to fail in these regimes and has proven correct in describing a wide range of phenomena including the energy levels of atoms, the covalent bond and the distinction between metals and insulators [9]. This gives us good reason to believe that by solving the quantum–mechanical equations of a system we can achieve a greater understanding of a large number of physical phenomena related to the properties of real world systems.

One such example, and the basis of this thesis, is the understanding of the electronic structure of matter. The ability of quantum mechanics to predict the total energy of a system of electrons and nuclei allows us to gain a great deal of information about the system. The quantum–mechanical calculation of the total energy of a simple one-atom system from the Hamiltonian has allowed quantum theory to be tested very rigorously. The extension to more complicated systems is fairly straightforward. Thus quantum theory allows us to predict the total energies of many-body systems with a good degree of accuracy.

This ability to predict the total energy of a system of electrons and nuclei enables us to determine computationally any physical property of the system related to the total energy. For example, the equilibrium lattice constant of a crystal will occur at a value that coincides with the minimum of the total energy and surfaces and defects of a solid also adopt structures that minimize the total energy. In order to predict the equilibrium lattice constant, one would simply run a series of total energy calculations at various volumes to determine the total energy as a function of volume. The results are then plotted as shown in Fig. 1.1 and a smooth curve fitted through the points, the theoretical value for the lattice constant is the value at the minimum of this curve. These total energy techniques have been successfully used to predict with great accuracy equilibrium lattice constants, bulk moduli, piezoelectric constants, phase-transition pressures and temperatures [10, 11, 12].

Moreover, in recent years first principles or *ab initio* methods that require only

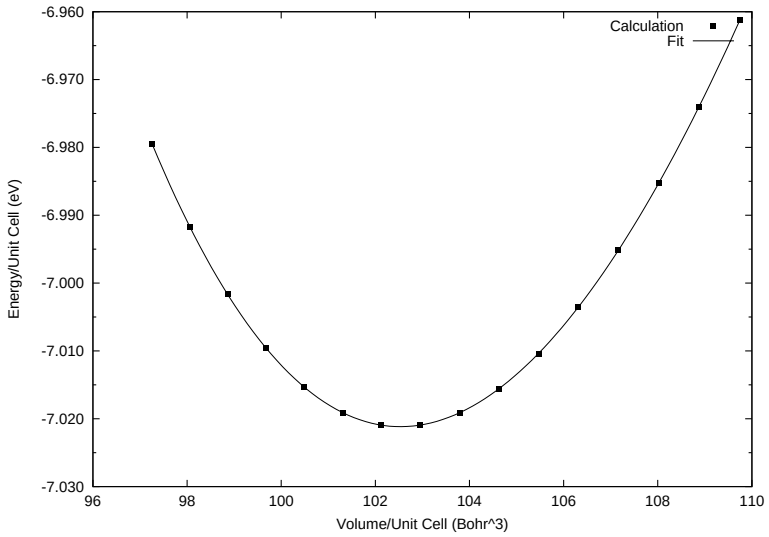

Figure 1.1: A plot illustrating how a Birch-Murnaghan curve [1] is fitted to a plot of cohesive energy versus volume.

a description of the ions present to calculate a wide range of physical properties, have become feasible with the increasing availability of more powerful computers. Many of these methods have been known for decades and have been continuously refined and improved. A couple of decades ago most *ab initio* methods would only have been able to simulate systems with a few atoms, so their applicability to useful systems was extremely limited. Nowadays, however, systems containing many thousands of atoms can be studied, mostly using the total-energy pseudopotential method, see Section 2.1. By pushing the limits of quantum mechanical calculations in this way it is possible to tackle a large number of interesting problems in many different fields of science.

Total energy pseudopotential calculations do require a large amount of compu-

tational time even for relatively small systems and this increases rapidly with increasing system size; it is therefore imperative to use the most efficient algorithms, especially for calculations involving heavier atoms. How this is achieved will be discussed in the following chapters where it will be seen that one of the techniques pivotal to this work is that of pseudopotentials.

As recently as the early 1990's it was believed that computations involving large atoms such as the transition row elements would be unmanageable with pseudopotentials in a plane-wave representation [9]. Work by Alan and Teter, 1987 [13], Bar-Yam et al 1989 [14], Rappe et al 1990 [15], Vanderbilt 1990 [16], Troullier and Martins 1991 [17]) showed that pseudopotential calculations could be performed for systems containing larger atoms by using a managable number of plane waves in the basis set. This allowed large total energy calculations to be performed using these new pseudopotentials and enabled a much larger variety of systems to be studied than was previously possible.

1.1 Motivation

It is well known that the magnetic properties of the lanthanides and actinides are as a result of partially filled f orbitals which are highly localized. Many total energy pseudopotential calculations neglect to include these f orbitals when they are not partially occupied and treat them instead as similar in character to the tightly bound s orbitals. One such example is the case of the $5d$ transition atoms which

have partially filled $5d$ orbitals and empty $5f$ orbitals. These empty orbitals are unbound and therefore are difficult to describe, a method for this is discussed in Chapter 6.

In this work we investigate the effect of including this empty, unbound $5f$ orbital on some physical properties of the $5d$ transition atoms. By doing so we attempt to gain insight into the effect of the inclusion of unbound orbitals on total energy pseudopotential calculations and the possible causes of deviations observed in the electronic structure of the bulk solids.

1.2 Organization

An overview of total energy pseudopotential calculations and the Hartree-Fock approximation which is fundamental to these calculations is presented in Chapter 2 together with a brief introduction to Density Functional Theory. In Chapter 3 we discuss approximations and methods for dealing with a large number of coupled equations and crystal structures. We introduce and discuss the pseudopotential approximation and its application to total energy calculations in Chapter 4. And finally in Chapters 5 and 6 we present our results for the case excluding the f component and the case including it along with a discussion of these results.

Chapter 2

Theoretical background

2.1 Total energy pseudopotential calculations

In describing the properties of matter from theoretical methods the fundamental equation is the Hamiltonian for a system of electrons and nuclei:

$$\hat{H} = -\frac{\hbar^2}{2m_e}\sum_i \nabla_i^2 - \sum_{i,I}\frac{Z_I e^2}{\mid \mathbf{r}_i - \mathbf{R}_I \mid} + \frac{1}{2}\sum_{i\neq j}\frac{e^2}{\mid \mathbf{r}_i - \mathbf{r}_j \mid} - \sum_I \frac{\hbar^2}{2M_I}\nabla_I^2 + \frac{1}{2}\sum_{I\neq J}\frac{Z_I Z_J e^2}{\mid \mathbf{R}_I - \mathbf{R}_J \mid} \tag{2.1}$$

where electron masses and positions are denoted by lowercase subscripts and nuclear masses and positions by uppercase subscripts.

In order to accurately describe the effects of all the interactions one has to include the difficult electron-electron Coulomb interactions. The development of approximate methods that are able to describe electronic correlations with sufficient accuracy to be able to predict various properties of matter is central to electronic structure theory. For the moment, the effects of external fields and relativity are

excluded, but these are able to be included later.

The kinetic energy term involving the masses of the nuclei in (2.1) may be neglected due to the large difference between the masses of the nuclei and the electrons and the fact that the forces acting on both the nuclei and electrons are the same. What this means is that the electrons will respond practically instantaneously to the motion of the nuclei, and therefore the kinetic energy of the nuclei can be ignored. This is the well–known Born-Oppenheimer or adiabatic approximation [18] and it reduces the many-body problem to the dynamics of the electrons with some frozen-in configuration of the nuclei.

So ignoring the nuclear kinetic energy the Hamiltonian (2.1) can be written as

$$\hat{H} = \hat{T} + \hat{V}_{ion-elec} + \hat{V}_{elec-elec} + \hat{V}_{ion-ion} \tag{2.2}$$

By utilizing Hartree atomic units, ie. $\hbar = m_e = e = 4\pi\epsilon_0 = 1$, the various terms in equation (2.2) can be written in the following simplified terms:

The kinetic energy operator for the electrons is

$$\hat{T} = -\frac{1}{2}\sum_i \nabla_i^2 \tag{2.3}$$

The potential energy acting on the electrons due to ions is

$$\hat{V}_{ion-elec} = -\sum_{i,I} \frac{Z_I}{\mid \mathbf{r}_i - \mathbf{R}_I \mid} \tag{2.4}$$

The electron-electron interaction potential is

$$\hat{V}_{elec-elec} = \frac{1}{2}\sum_{i\neq j}\frac{1}{\mid \mathbf{r}_i - \mathbf{r}_j \mid} \tag{2.5}$$

The ion–ion interaction is

$$\hat{V}_{ion-ion} = \frac{1}{2}\sum_{I\neq J}\frac{Z_I Z_J}{\mid \mathbf{R}_I - \mathbf{R}_J \mid} \tag{2.6}$$

Because of the adiabatic approximation however the term (2.6) is often included as the classical interaction of the nuclei with one another in an extra term consisting of $\hat{V}_{ion-ion}$ and any other terms that contribute to the total energy of the system but are not directly related to the problem of describing the electrons.

Importantly, it can be shown that the Hamiltonian (2.2) remains a good approximation when the Coulomb interaction is replaced by a pseudopotential for the core electrons. Pseudopotentials will be discussed in detail in Chapter 3.

2.1.1 Independent-electron approximations

The Schrödinger equation cannot be solved exactly for atoms containing more than one electron although the principles behind the calculation are well understood. The number of particles and the variety of forces involved make the problems extremely complicated. Various approximations have been developed, some with considerable success.

The first quantitative calculations on many electron-systems were performed in the late 1920's by Douglas Hartree [19]. These calculations assumed that each elec-

tron moved independently in an average electric field due to the nuclei and the other electrons, and ignored correlations between the positions of the electrons. Hartree defined a different potential for each electron by subtracting a specific term depending on each electron's orbital. The Hartree-Fock method [20] was later developed in which this self-interaction term is defined by an effective Hartree potential thereby ensuring the potential is independent of the orbital.

These approaches, namely Hartree-like or non-interacting and Hartree-Fock are the two fundamental independent-particle approximations. Both assume the electrons are uncorrelated, obeying only the Pauli exclusion principle. Where they differ is that the Hartree-Fock method includes the electron-electron Coulomb interaction in the energy, while ignoring the correlation that arises in the wavefunction due to those interactions. Non-interacting theories have an effective potential that incorporates some effects of the real interaction but do not include an explicit term in the effective Hamiltonian.

2.1.2 The Hartree-Fock approximation

The Hartree-Fock approximation is based on the independent-particle approximation. The approximate Hamiltonian can therefore be written as the sum of the single particle Hamiltonians:

$$H_{approx.} = \sum_{i=1}^{N} h(i), \tag{2.7}$$

where N is the number of electrons in the system. The simplest form of an eigen-

function of H_{approx} will be the product

$$\Psi = \psi_a(1)\psi_b(2)\psi_c(3)\psi_d(4)\ldots, \tag{2.8}$$

where $\psi_a, \psi_b, \psi_c, \ldots$ are single electron states and a, b, c,... represent their quantum numbers.

In order to satisfy the Pauli exclusion principle, the total wavefunction, ψ, must be antisymmetric with respect to the interchange of any two electrons. We can form a wave function with this property by antisymmetrising the above product function

$$\Psi = \frac{1}{\sqrt{N!}} Det\{\psi_a(1)\psi_b(2)\psi_c(3)\psi_d(4).....\psi_x(N).\} \tag{2.9}$$

This is known as a Slater determinant [21]. The Hartree-Fock equations for the single–electron states are [20]:

$$\left[-\frac{1}{2}\bigtriangledown^2 + V_{ion}(\mathbf{r}) + \sum_{j,\sigma}\int d^3\mathbf{r}'\psi_j^{\sigma *}(\mathbf{r}')\psi_j^{\sigma}(\mathbf{r}')\frac{1}{\mid \mathbf{r}-\mathbf{r}' \mid}\right]\psi_i^{\sigma}(\mathbf{r})$$
$$-\sum_j \int d^3\mathbf{r}'\psi_j^*(\mathbf{r}')\psi_i(\mathbf{r}')\frac{1}{\mid \mathbf{r}-\mathbf{r}' \mid}\psi_j(\mathbf{r}) = \varepsilon_i\psi_i(\mathbf{r}), \tag{2.10}$$

where the exchange term acts only between electrons of the same spin and is therefore only summed over the orbitals with the same spin, σ.

The Hartree-Fock theory is not always an improvement though; in some cases it yields less satisfactory results than the Hartree theory. This is because the electrostatic correlation due to the Coulomb repulsion of the electrons has not been taken into account in the Hartree-Fock approximation and this cancels the exchange effect to some extent. For single atoms and molecular solids the Hartree-Fock approximation yields fairly good results, however for the homogenous electron gas the prototypical metal it fails for a number of reasons. The electrons that contribute most to

the metallic properties are those close to the Fermi energy, and these electrons are calculated to have infinite velocities within Hartree-Fock theory; furthermore the density of states function which should closely resemble that of a free electron gas instead approaches zero at the Fermi energy.

It is therefore apparent that we need to more closely examine the exchange and correlation energies.

2.1.3 Exchange and correlation

The wave function of a many-electron system must always be antisymmetric under the exchange of two electrons since electrons are Fermions. The antisymmetry requirement of the wavefunction means that electrons that have the same spin are spatially separated due to the Pauli exclusion principle and this therefore reduces the Coulomb energy of the system. This reduction in energy due to antisymmetry is known as the exchange energy and as shown above it can be included as an exchange term in the Hartree-Fock approximation. The term correlation energy refers to the difference between the many-body energy of an electronic system and the energy of the system calculated by the Hartree-Fock approximation. This difference occurs when the Coulomb energy is decreased below the Hartree-Fock value due to electrons of opposite spins being spatially separated and therefore increasing their kinetic energy at the expense of the Coulomb energy. It is extremely difficult to calculate the correlation energy of a complex system because correlation affects both kinetic and potential energies. Therefore an approximation is required. The

first quantitative form for the correlation of a homogenous gas was proposed by Wigner [22], [23] and the first calculation was performed in 1957 by Gell–Mann and Breuckner [24]. Much work has been done on the correlation energy since then [25] including work by Ceperly and Alder [26] and Hedin and Lundqvist [27].

2.2 Density functional theory

2.2.1 Introduction

Density functional theory (DFT) techniques are amongst the most widely used *ab initio* methods in computational material science and solid state physics. The reason for this is both their high computationally efficiency and their accuracy. The importance of density functional theory was recognised in 1998 when Walter Kohn, one of its creators, was awarded the Nobel prize in Chemistry.

In contrast to the Hartree-Fock approach, which begins by describing a system of individual electrons interacting with each other and the nuclei, density functional theory begins by considering the entire electron system. So rather than using the many–electron wavefunction as the fundamental variable of the system, the electron density is used instead.

A similar approach to density functional theory was first proposed by Thomas(1927) [28] and independently by Fermi(1928) [29]. It was not until 1964 that Hohenberg and Kohn [30] formulated and proved a theorem that put these ideas on solid math-

ematical grounds. The proofs of Hohenberg and Kohn are discussed in the following sections.

In density functional theory the total energy is decomposed into three contributions: a kinetic energy, a Coulomb energy due to the classical electrostatic interactions between the charged particles in the system, and the exchange–correlation term that includes all many–body interactions. As discussed earlier exact expressions for the many–body exchange and correlation interactions are unknown and approximations are required.

2.2.2 The local density approximation (LDA)

One approximation to the exchange–correlation interactions is the local density approximation(LDA). In the LDA the exchange-correlation energy of an electronic system is derived from the known results of the electron interactions in a system of constant density; the theory of a homogenous electron gas. If the electron density at each point in a molecule or solid is well defined, it is assumed that an electron at that point experiences the same effect from the combination of the surrounding electrons as if the density of the surrounding electrons had the same values throughout the entire space. The exchange–correlation energy is then the integral over the contributions from each volume element, which depends on the local electron density. The local density approximation is exact for a perfect metal, as it has a constant electron density. It will become less accurate when dealing with systems with variable electron density. For transition metals which have a high electron

density the LDA is fairly well suited. In our work on transition metals we make use of the Perdew and Zunger [31] parameterization which is based on the quantum Monte Carlo calculations of Ceperly and Alder [26].

2.2.3 Reasons for the success of the LDA

The local density approximation relies on the assumption that the electron density varies slowly. It has been shown empirically however that even in the case of rapid variation the expression is highly accurate [32] . One of the reasons for this accuracy is the fact that the approximation gives the correct sum-rule for the exchange-correlation hole which is basically the equivalent of the charge of one electron excluded from the neighbourhood of the electron.

The second reason for the accuracy of the local density approximation is that there is an fortuitous cancellation in the errors of the exchange and correlation energy. The correlation energy is typically around one tenth the magnitude of the exchange energy. Therefore a 10% error in the exchange energy is somewhat compensated for by the 100-200% error in the correlation energy.

2.2.4 Basic density functional theory

In 1964 Hohenberg and Kohn [30] proved that the total energy of an electron gas, including the exchange and correlation energy, is a unique functional of the electron density and that all of the ground state expectation values depend uniquely on the

ground state density. This has the important effect of reducing the many-electron wavefunction from being 3N–dimensional for N particles to being just 3 dimensional. This has obvious computational advantages.

Kohn and Sham [33] then showed how it is possible to replace the many-electron problem by an exactly equivalent set of self–consistent one–electron equations.

The first Hohenberg-Kohn theorem

The theorem is divided into two parts.

Theorem 1. *The external potential $V_{ext}(\boldsymbol{r})$ is determined, within a trivial additive constant, by the electron density $\rho(\boldsymbol{r})$*

Proof

Notice firstly that the constant will simply shift the eigenenergies by a constant and the Schrödinger equation with Hamiltonians H and $H + const$ will give the exact same eigenfunctions.

The theorem is proved by contradiction:

- First, let us assume we have an exact ground state density $\rho(\mathbf{r})$.
- Now we assume that the ground state is nondegenerate (i.e. there is only one wavefunction for this state).
- Suppose that for the given electron density there are two distinct external potentials: $V_{ext}(\mathbf{r})$ and $V'_{ext}(\mathbf{r})$, which would obviously produce two different Hamiltonians: $H = T + V_{ee} + V_{ext}$ and $H' = T + V_{ee} + V'_{ext}$ respectively, and two different wavefunctions for the ground state: Ψ and Ψ' respectively.

These have energies $E_0 = \langle\Psi|H|\Psi\rangle$ and $E_0' = \langle\Psi'|H'|\Psi'\rangle$. We assume the wave functions are normalized, $\langle\Psi|\Psi\rangle = \langle\Psi'|\Psi'\rangle = 1$.

- If Ψ' is not the ground state it is always larger than the ground state wavefunction. Applying the Hamiltonian to both wavefunctions implies:

$$E_0 = \langle\Psi|H|\Psi\rangle < \langle\Psi'|H|\Psi'\rangle. \tag{2.11}$$

The strict equality in (2.12) follows if the ground-state is non-degenerate, this is not a necessary restriction and the proof can be readily extended to degenerate cases [34, 35]. The last part of (2.11) can be written:

$$E_0 < \langle\Psi'|H|\Psi'\rangle = \langle\Psi'|H - H'|\Psi'\rangle + \langle\Psi'|H'|\Psi'\rangle, \tag{2.12}$$

or, because the two Hamiltonian operators differ only in the external potential and $\langle H\rangle = \int \rho(\mathbf{r})V d\mathbf{r}$,

$$\begin{aligned} E_0 &< \langle\Psi'|T + V_{ee} + V_{ext} - T - V_{ee} - V'_{ext}|\Psi'\rangle + E'_0 \\ &< \int \rho(\mathbf{r})[V_{ext}(\mathbf{r}) - V'_{ext}(\mathbf{r})]d^3\mathbf{r} + E'_0. \end{aligned} \tag{2.13}$$

- Now we calculate the expectation value of the energy for the wavefunction Ψ with the Hamiltonian H' and again apply the variational theorem:

$$\begin{aligned} E'_0 < \langle\Psi|H'|\Psi\rangle &= \langle\Psi|H' - H|\Psi\rangle + \langle\Psi|H|\Psi\rangle \\ &= \int \rho(\mathbf{r})[V'_{ext}(\mathbf{r}) - V_{ext}(\mathbf{r})]d^3\mathbf{r} + E_0. \end{aligned} \tag{2.14}$$

- By adding equations (2.13) and (2.14) we obtain the contradiction:

$$E_0 + E'_0 < E'_0 + E_0. \tag{2.15}$$

Hence there cannot be two different external potentials that give the same ground state electron density: the ground state electron density uniquely specifies the external potential V_{ext}.

□

Since the complete ground state energy is a functional of the ground state electron density, so must be its individual components and we can write

$$E[\rho] = V_{ext}[\rho] + T[\rho] + V_{ee}[\rho]. \tag{2.16}$$

By grouping together all the functionals other than $V_{ext}[\rho]$:

$$E[\rho] = V_{ext}[\rho] + F_{HK}[\rho] = \int \rho(\mathbf{r}) V_{ext}(\mathbf{r}) d^3\mathbf{r} + F_{HK}[\rho]. \tag{2.17}$$

One should note that the electron density $\rho(\mathbf{r})$ uniquely determines the Hamiltonian operator, which characterizes all states of the system (ground and excited). This means that all the properties of all states are determined by the ground state density, this is as a result of the second Hohenberg-Kohn theorem which we will discuss in the following section. Consequently, density functional theory is usually referred to simply as a ground state theory. Note also that only the ground state density contains information about the positions and charges of the nuclei, the density of an excited state cannot be used in mapping an external potential.

The energy variational principle

We have now shown that we can deduce all the properties of interest from the ground state density, but we cannot yet be sure that a specific density is in fact

the ground state density. The second Hohenberg–Kohn theorem provides a way for this problem to be tackled. In words the theorem states that the functional, $F_{HK}[\rho] = T[\rho] + V_{ee}[\rho]$, provides the lowest energy if and only if the input density is the true ground state density, ρ_0. This of course is the variational principle.

Theorem 2. *For a trial density* $\tilde{\rho}(\boldsymbol{r})$ *such that* $\int \tilde{\rho}(\boldsymbol{r})d^3(\boldsymbol{r}) = N$*,*

$$E_0 \leq E[\tilde{\rho}], \tag{2.18}$$

where $E[\tilde{\rho}]$ *is the energy functional* (2.17) *with* $\rho \to \tilde{\rho}$*.*

In other words, if there exists some density that represents the correct number of electrons N, the total energy E calculated from this density cannot be lower than the true energy of the ground state, E_0. The ground state energy can then, in principle, be calculated exactly from the electron density using the variational method.

Proof

In order to prove this theorem we first note that Theorem 1 ensures that $\rho(\mathbf{r})$ determines its own external potential, $V_{ext}(\mathbf{r})$, Hamiltonian H, and wavefunction Ψ. This wavefunction is taken as a trial function for the problem having an external potential $V_{ext}(\mathbf{r})$. Following from this an energy functional $E[\rho]$ can be defined in which the external potential is unrelated to another density $\tilde{\rho}(\mathbf{r})$,

Thus we arrive at:

$$E[\rho] = F_{HK}[\tilde{\rho}] + \int \tilde{\rho}(\mathbf{r})V_{ext}(\mathbf{r})d^3\mathbf{r}. \tag{2.19}$$

The variational principle asserts,

$$\langle\tilde{\Psi}|F_{HK}|\tilde{\Psi}\rangle + \langle\tilde{\Psi}|V_{ext}|\tilde{\Psi}\rangle > \langle\Psi|F_{HK}|\Psi\rangle + \langle\Psi|V_{ext}|\Psi\rangle, \tag{2.20}$$

where Ψ is the wavefunction associated with the correct ground state density $\rho(\mathbf{r})$. this leads too,

$$F_{HK}[\tilde{\rho}] + \int \tilde{\rho}(\mathbf{r}) V_{ext}(\mathbf{r}) d^3\mathbf{r} > F_{HK}[\rho] + \int \rho(\mathbf{r}) V_{ext}(\mathbf{r}) d^3\mathbf{r}, \tag{2.21}$$

And therefore

$$E[\tilde{\rho}] \geq E_0[\rho] \tag{2.22}$$

This is the desired result.

□

If we knew an exact form of F_{HK}, then by minimizing the total energy of the system with respect to variations in the density one would obtain an exact equation for the ground state electron density and energy.

For a variable number of electrons if we assume differentiability of $E[\rho]$ and vary it with respect to density, the ground state density would satisfy the following equation [36]:

$$\delta \left\{ E[\rho] - \mu \left[\int \rho(\mathbf{r}) d^3\mathbf{r} - N \right] \right\} = 0, \tag{2.23}$$

where μ is the Lagrange multiplier associated with the restriction that the density yield the correct number of electrons N. From (2.23) we obtain:

$$\mu = \frac{\delta E[\rho]}{\delta \rho(\mathbf{r})} = V_{ext}(\mathbf{r}) + \frac{\delta F_{HK}[\rho(\mathbf{r})]}{\delta \rho(\mathbf{r})}. \tag{2.24}$$

The quantity μ is the chemical potential.

This Hohenberg-Kohn functional, F_{HK}, depends only on the density: its form does not depend on the external potential $V_{ext}(\mathbf{r})$, and it is therefore universal. Once we

have an explicit form, approximate or exact, for F_{HK}, we can apply this method to any system.

The two Hohenberg-Kohn theorems form the mathematical basis of density functional theory.

2.2.5 The Kohn-Sham approach

About a year after Hohenberg and Kohn published their groundbreaking paper, Kohn and Sham suggested a method for how the universal functional presented above could be approached [30]. The basis for their idea was the observation that most of the problems with density functionals are associated with the way the kinetic energy is determined. In order to alleviate this problem, Kohn and Sham developed the concept of a non-interacting reference system which was constructed from a set of orbitals so that the major contribution to the kinetic energy can be calculated fairly accurately. The remainder is combined in a term with the non-classical contributions to the electron-electron repulsion, which are also unknown, but typically fairly small. In this way as much information as possible is calculated exactly , leaving only a small part of the total energy that has to be approximated.

The Kohn-Sham Equations

For non-interacting electrons, $F_{HK}[\rho] = T[\rho]$, where $T[\rho]$ is the electron kinetic energy, but the functional $T[\rho]$ is unknown and therefore so is $F_{HK}[\rho]$. The ground state energy for non-interacting electrons in any external potential can however be solved for trivially, and we can then use this information to tackle the problem of

interacting electrons.

In the non-interacting case the total energy has contributions from both the kinetic and potential energies(see (2.16) and (2.17),

$$E[\rho] = T[\rho] + V_{ext}[\rho] = T[\rho] + \int V_{ext}(\mathbf{r})\rho(\mathbf{r})d\mathbf{r}. \tag{2.25}$$

We can write the ground state of the system as a Slater determinant with spin-orbitals satisfying the single-particle Schrödinger equation [37],

$$\left[-\frac{\nabla^2}{2} + V_{ext}(\mathbf{r})\right]\psi_m(\mathbf{r}) = \varepsilon_m\psi_m(\mathbf{r}). \tag{2.26}$$

The ground state density is then given by a sum over occupied states

$$\rho(\mathbf{r}) = \sum_{m}^{occ} |\psi_m(\mathbf{r})|^2, \tag{2.27}$$

where the spin orbitals $\psi_m(\mathbf{r})$ are normalized so that the density satisfies the correct normalization condition for the number of particles N.

So by multiplying (2.26) by Ψ^* and integrating we can write:

$$\sum_{m}^{occ} \varepsilon_m = T[\rho] + \int V_{ext}(\mathbf{r})\rho(\mathbf{r})d^3\mathbf{r}. \tag{2.28}$$

Now we need to look at the case of interacting electrons. The energy functional (2.16) for a many-electron system with the electronic interactions included can be written,

$$E[\rho] = T[\rho] + \int V_{ext}(\mathbf{r})\rho(\mathbf{r})d^3\mathbf{r} + \frac{1}{2}\int\int \frac{\rho(\mathbf{r}_1)\rho(\mathbf{r}_2)}{|\mathbf{r}_1 - \mathbf{r}_2|}d^3\mathbf{r}_1 d^3\mathbf{r}_2 + E_{xc}[\rho(\mathbf{r})], \tag{2.29}$$

where the last term, the exchange–correlation term, is the term that by definition takes into account all the contributions not considered in the first three terms. Here

$T[\rho]$ is the kinetic energy of the noninteracting electron gas. Note that we cannot at this stage write the kinetic energy and electron-electron interaction as the sum of two terms depending only on density, this is why $T[\rho]$ has been split off and the remaining part of the kinetic energy included in E_{xc}.

Varying equation (2.29) with respect to density, we obtain an equation similar to (2.24) only with a more complicated potential V_{eff},

$$\mu = \frac{\delta T[\rho]}{\delta \rho} + \frac{\delta E[\rho]}{\delta \rho} + \int \rho(\mathbf{r}') \frac{1}{|\mathbf{r} - \mathbf{r}'|} d^3\mathbf{r}', \tag{2.30}$$

where we can write

$$V_{eff}(\mathbf{r}) = V_{ext}(\mathbf{r}) + V_{xc}(\mathbf{r}) + V_{Hartree}(\mathbf{r}). \tag{2.31}$$

The analogue of equation (2.26) is then

$$\left[-\frac{\nabla^2}{2} + V_{eff}(\mathbf{r}) \right] \psi_m(\mathbf{r}) = \varepsilon_m \psi_m(\mathbf{r}), \tag{2.32}$$

and therefore we have

$$\sum_m^{occ} \varepsilon_m = T[\rho] + \int V_{eff}(\mathbf{r}) \rho(\mathbf{r}) d^3\mathbf{r}. \tag{2.33}$$

And by substituting equation (2.31) into (2.29) we obtain

$$E[\rho] = T[\rho] + \int [V_{eff}(\mathbf{r}) - V_{Hartree}(\mathbf{r}) - V_{xc}(\mathbf{r})] \rho(\mathbf{r}) d^3\mathbf{r} + \frac{1}{2} \int \int \frac{\rho(\mathbf{r}_1)\rho(\mathbf{r}_2)}{|\mathbf{r}_1 - \mathbf{r}_2|} d^3\mathbf{r}_1 d^3\mathbf{r}_2 + E_{xc}[\rho(\mathbf{r})], \tag{2.34}$$

These equations were first derived by Walter Kohn and Lu Jue Sham [33]. The exact form of the exchange–correlation potential which, if it is known, should work for all materials and is simply a functional of the density. So we conclude that

- If the energy functional is split according to (2.29) the exchange–correlation term, containing all the unknown contributions, is independent of the external potential.

- The ground state energy can be found by the solution of minimization problem of the energy functional (2.34) with respect to the electron density $\rho(\mathbf{r})$.

- The Kohn-Sham orbitals (one–electron orbitals) are a mathematical construction devised in order to simplify the problem and in principle do not have any obvious physical meaning. In practice however they are commonly thought of as single-particle physical eigenstates. It is often stated that the orbitals are meaningless but a rigorous perturbative treatment due to Görling [38] shows that the Kohn-Sham eigenvalue differences obtained from (2.29) are a reasonable approximation to excitation energies.

The Kohn-Sham equations basically map a system of interacting electrons onto a system of non-interacting electrons moving in an effective potential due to all the other electrons. These equations need to be solved in a self-consistent way so that the occupied states generate a charge density that will produce the potential used in the construction of the equations. Most of the work involved in a total-energy pseudopotential calculation is in solving the Kohn-Sham equations (2.31) once the exchange-correlation energy is approximated.

Chapter 3

Solving the electronic problem

3.1 Kohn-Sham and Hartree-Fock equations

In the previous chapter it was shown that certain observables of the many–body problem may be mapped into equivalent observables in a single–particle problem. There remains however, the formidable task of solving a set of N coupled, three–dimensional, partial differential equations self consistently. The two basic methodologies introduced in the previous chapter, Hartree-Fock and Kohn-Sham, are the result of a simplification of the 3N–dimensional many–body problem into manageable, but approximate, schemes. The solution of either of these schemes involves two important tasks: how to treat the electron–nuclear interaction, and finding a way to represent the single–particle orbitals.

3.1.1 The electron–nuclear interaction

The electron–nuclear interaction is described by the bare Coulomb potential[1]:

$$V_{ext} = -e^2 \sum_{I=1}^{P} \frac{Z_I}{|\mathbf{r} - \mathbf{R}_I|}, \tag{3.1}$$

However, a distinction has to be made between two classes of electrons: valence electrons, that participate actively in chemical bonding, and core electrons, that are tightly bound to the nuclei and do not participate in bonding. The core states are not completely insensitive to the molecular or crystal field and in some cases a third class of electrons, called semi–core electrons, is introduced. These semi–core electrons do not participate in chemical bonding but have energies similar to those of the valence states and react to the presence of the environment. Note that there is no such thing as classes of electrons as all electrons are identical, the terminology above refers to the approximate single–particle electronic states rather than the electrons themselves.

All–electron methods

All–electron methods deal explicitly with all the electrons in the system, but due to the different characteristics of the electronic states, they are usually treated in different ways. Core electrons can be taken to be frozen as in the isolated atom situation, or they can be seen as separate from valence electrons only in the presence of the environment. One method, based on dividing the space into spherical regions around the atoms, is known at the augmented plane wave method. In this method

[1] see Section 2.1

the basis functions are constructed to be continuous and differentiable across the boundaries of the separate regions. The solutions at the boundaries are augmented with the partial waves inside every sphere leading to an energy–dependent set of basis functions. These basis functions are much more flexible than those based on fixed, energy-independent orbitals. Fixed methods are typically represented by a minimal number of basis functions and therefore greatly reduce the computational burden. Plane wave methods will be discussed further in section 3.2.3.

3.1.2 Classes of basis sets

In order to represent the Kohn-Sham orbitals (equation 2.32) a choice of basis set needs to be made. The four main types of basis sets may be grouped as follows

Extended basis sets: the basis functions are delocalized, either independent of the nuclear positions or centred on them, and cover all space. These basis sets are useful for condensed phases of matter such as solids or liquids, they are however inefficient for molecular systems.

Localized basis sets: the basis functions are localized and are centred on either the nuclear positions or on bonds. They are mainly used for molecular systems or in periodic systems.

Mixed basis sets: in this case both extended and localized basis sets are used in order to take the best of both: they do, however, carry the technical difficulties associated with both sets.

Augmented basis sets: an extended or atom-centred basis set is combined with atomic-like wave functions in spherical regions around the nuclei. This method is very accurate and since the basis functions are flexible, fewer of them are needed to achieve convergence of the basis set. They are however more complicated to construct.

3.2 Condensed phases

A crystal is an ordered state of matter in which a small number of atoms (a basis) is repeated periodically in space. It may be completely described by a primitive, or Wigner-Seitz, unit cell (that contains the whole symmetry of the system) and the rules specifying the repetition of that cell. The set of translations, which generates the entire periodic crystal is called the Bravais lattice. It is often convenient to describe the solid in terms of its symmetry properties rather than its unit cell. For example, a body centred cubic (bcc) unit cell can be described as a simple cubic cell with two atoms in the basis. This conventional unit cell is twice as large as the primitive unit cell.

It is not possible to study an infinite number of electrons on a computer and this is avoided by utilizing Bloch's theorem [39] which relates the properties of the electrons in an infinite periodic system to those of the electrons in the unit cell.

3.2.1 Bloch's theorem

Bloch's theorem states that in a periodic solid each electronic wavefunction can be written as the product of a cell–periodic part and a wave–like part:

$$\psi_i(\mathbf{r}) = e^{i\mathbf{k}\cdot\mathbf{r}} f_i(\mathbf{r}). \tag{3.2}$$

The cell periodic part of $f_i(\mathbf{r})$ can be expressed in a Fourier series as an expansion of plane waves whose wave vectors are reciprocal lattice vectors of the crystal,

$$f_i(\mathbf{r}) = \sum_{\mathbf{G}} c_{i,\mathbf{G}} e^{i\mathbf{G}\cdot\mathbf{r}}. \tag{3.3}$$

The vectors $\mathbf{k}$ in (3.2) define the reciprocal lattice of the Bravais lattice, they satisfy $e^{i\mathbf{k}\cdot\mathbf{r}} = 1$ for all lattice point position vectors $\mathbf{r}$. The reciprocal lattice vectors $\mathbf{G}$ are defined by $\mathbf{G}\cdot\boldsymbol{l} = 2\pi m$ for all $\boldsymbol{l}$ where $\boldsymbol{l}$ is a lattice vector of the crystal and m is an integer.

Each electronic wavefunction can therefore be written as the sum of plane waves,

$$\psi_i(\mathbf{r}) = \sum_{\mathbf{G}} c_{i,\mathbf{G}} e^{i(\mathbf{k}+\mathbf{G})\cdot\mathbf{r}}. \tag{3.4}$$

3.2.2 The Brillouin zone and k-point sampling

The first Brillouin zone (usually referred to simply as the Brillouin zone) is the Wigner-Seitz cell of the reciprocal lattice: it is defined by planes that are the perpendicular bisectors of a vector from the origin to the nearest points in the reciprocal lattice. Construction of the Brillouin zone is illustrated below.

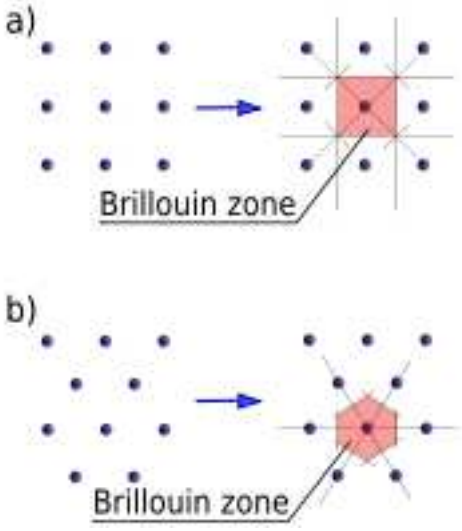

Figure 3.1: The first Brillouin zones (a) for a square lattice and (b) for a hexagonal lattice. Image source: Downloaded from [2]

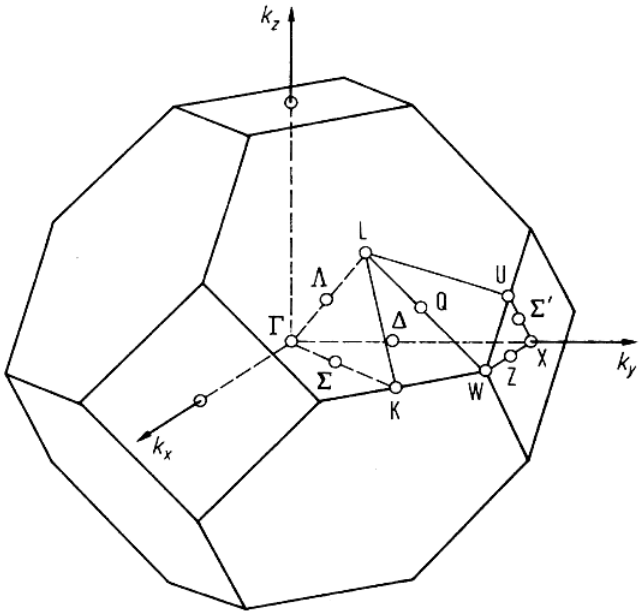

Figure 3.2: The Brillouin zone for the face centered cubic lattice. High symmetry points and lines are labeled according to Slater [3]. Image source: Downloaded from [4].

k-point sampling

The first Brillouin zone may be mapped out by a set of **k** points determined by the boundary conditions that apply to the bulk solid [40]. Electronic states are only allowed at these **k** points, the density of which is proportional to the volume of the solid. The essentially infinite number of electrons in the periodic solid are accounted for by an infinite number of **k** points, and a finite number of occupied states exist at each **k** point. The basis set required to represent the electronic wavefunctions at an infinite number of **k** points would of course be infinite.

The Bloch theorem allows us to reduce this problem to calculating a finite number of wavefunctions at an infinite number of **k** points within the Brillouin zone. The occupied states at each **k** point each contribute to the electronic potential of the bulk solid so in principle an infinite number of calculations are still required to calculate this potential. The wavefunctions at **k** points that are very close together will be almost identical however, so it is possible to represent the electronic wavefunctions over a region of space by the wave functions at a single **k** point. In this way we can calculate the electronic states at a finite number of **k** points in order to calculate the electronic potential and therefore we can determine the total energy of the solid.

Calculating the electronic states at special sets of **k** points in order to obtain accurate approximations of the electronic potential and the contributions of filled electronic bands to the total energy has been done using several methods [40, 41, 42]. The electronic potential and total energy of insulators or semi-conductors may be

approximated fairly accurately using these methods requiring only a small number of **k** points. Metallic systems are much more difficult to approximate because a very dense set of **k** points is required to define the Fermi surface precisely.

Errors in the total energy due to **k**–point sampling can easily be reduced by using a denser set of **k** points; this of course increases the computational time required to calculate the electronic wavefunctions and so a compromise must be reached.

The special k–point technique

The method of choice in the current work is the special **k**–point technique. This method is very well suited to the plane–wave representation. A discrete set of **k** points where the electronic states are to be calculated are selected within the irreducible part of the Brillouin zone. These points are selected to characterize the shape of the reciproca–space unit cell. The group symmetry operations of a crystal map some of the **k** points onto others: the charge density at such points is related and therefore only one calculation is required for all points connected in this way. This symmetry property is used to generate a special set of **k** points using the method designed by Monkhorst and Pack [42].

3.2.3 Plane waves

The simple wavefunctions for free electrons in a periodic crystal can be easily expanded in terms of plane waves. The planes waves are the exact solution if the potential due to the atoms is neglected. In the case of the nearly free-electron the

potential is relatively smooth and can thus be treated as a perturbation. Atomic nuclei, however, generate a potential that is far from smooth. The hydrogen atom is the simplest case and has a potential which goes as $-1/r$ and therefore diverges at the origin. The wavefunction for the $1s$ orbital has a cusp at the origin and decays exponentially with distance. For heavier atoms the wave functions for the core states are even more complicated and a plane wave expansion of a real crystal is near impossible due to the number of plane wave components required.

Augmented plane waves

The plane wave approach is appealing for its simplicity and a possible solution to the problem was suggest by Slater in 1937 [43]. He suggested the augmentation of the plane wave solution with the solutions to the atomic problem in spherical regions around the atoms. The potential was then assumed to be spherically symmetric inside the spheres and zero outside. This is known as the augmented plane wave solution.

An augmented plane wave is constructed such that it is identical to the original plane wave outside a certain radius R,

$$\phi_{\mathbf{k}} = e^{i\mathbf{k}\cdot\mathbf{r}}. \tag{3.5}$$

Within the sphere of radius R the potential is assumed to have spherical symmetry so that the augmented plane wave can be constructed in such a way that the wavefunction is continuous at $r = R$.

The portion of the augmented plane wave outside the sphere does not satisfy the Schrödinger equation and at $r = R$ the wavefunctions do not join smoothly, i.e. the

gradients of the wavefunction at $r = R$ are discontinuous.

A superposition of augmented plane waves yields an approximation of the correct solution to the crystal Schrödinger equation. The expansion of the wavefunction will have the form:

$$\psi_{\mathbf{k}}(\mathbf{r}) = \sum_{\mathbf{G}} c_{\mathbf{G}} \phi_{\mathbf{k}+\mathbf{G}}(\mathbf{r}), \tag{3.6}$$

with the sum over all the reciprocal lattice vectors $\mathbf{G}$.

Orthogonalised plane waves

Orthogonalised plane waves were first introduced by Herring in 1940 [44, 45]. They were the basis for the first quantitative calculations of bands in materials other that *sp*-bonded metals. Orthogonalised plane waves are constructed by adding contributions from lower energy core states to a plane wave. This is to ensure the wavefunction is approximated as closely as possible. The plane wave is defined as

$$\phi_{\mathbf{k}} = e^{i\mathbf{k}\cdot\mathbf{r}} + \sum_{c} b_c \psi^c_{\mathbf{k}}(\mathbf{r}), \tag{3.7}$$

where the sum is over all core levels with wave vector $\mathbf{k}$. The orthogonality constant b_c is determined such that $\phi_{\mathbf{k}}$ is orthogonal to each core level $\psi^c_{\mathbf{k}}$,

$$b_c = -\int \psi^{c^*}_{\mathbf{k}} \phi_{\mathbf{k}} e^{i\mathbf{k}\cdot\mathbf{r}} d^3\mathbf{r} \tag{3.8}$$

This construction ensures that the wavefunction can then be expressed as a series of orthogonalised plane waves. This method does not provide energy values that are as accurate as the values yielded using augmented plane waves, but very few terms are required to obtain a sufficiently accurate representation of the wavefunction.

Plane–wave energy cut–off

Bloch's theorem implies that the electronic wave function at each $\mathbf{k}$ point in a periodic solid can be expanded as a plane–wave basis set. In principle an infinite basis set is required to represent the wavefunctions with complete accuracy. In practice, however, the Fourier coefficients $c_{\mathbf{G}}$ are larger at small energies and decrease with an increasing energy. This means that the plane–wave expansion can be truncated at a finite number of terms, including only plane waves with energies less than some energy cut–off.

$$\frac{\hbar^2}{2m}|\mathbf{k}+\mathbf{G}|^2 < E_{cut} \tag{3.9}$$

The truncation of the basis set will lead to an error in the computed physical quantities. This error can be reduced by increasing the chosen energy cut–off.

Plane-wave representation of Kohn-Sham equations

The expansion of the electronic wavefunctions in terms of a plane wave basis set allows the Kohn-Sham equations (2.32) to assume a fairly simple form when equation (3.4) is substituted into them and integrated over $\mathbf{r}$:

$$\sum_{\mathbf{G}'}\left[\frac{\hbar^2}{2m}|\mathbf{k}+\mathbf{G}|^2\delta_{\mathbf{G}\mathbf{G}'} + V_{ion}(\mathbf{G}-\mathbf{G}')\right.$$
$$\left.+V_H(\mathbf{G}-\mathbf{G}') + V_{XC}(\mathbf{G}-\mathbf{G}')\right] c_{i,\mathbf{k}+\mathbf{G}'} = \varepsilon_i c_{i,\mathbf{k}} \tag{3.10}$$

In this form, the kinetic energy is diagonal and the potentials are expressed in terms of their Fourier components. This equation is solved by diagonalization of the Hamiltonian matrix determined by the terms in square brackets. The cut–off energy will determine the size of the matrix. For large systems with both core and valence

electrons the matrix will become too large to solve. This problem is overcome by the pseudopotential approximation that will be discussed in the following chapter.

Advantages and disadvantages of plane waves

The plane wave expansion has a few main advantages. First, the kinetic term in the Hamiltonian is local in reciprocal space and the potential term is local in real space. This is taken advantage of by transforming the wavefunctions and density back and forth between real space and reciprocal space. Unfortunately this is not the case when non-local pseudopotentials are used together with a plane wave basis set. In this case the non-local pseudopotential component of the Kohn-Sham potential is usually computed in reciprocal space [46]. Second, by using fast Fourier transforms this transformation can be done very efficiently, thus greatly reducing the computational cost. The energy and force can also be calculated analytically and fairly simply. Finally, the plane–wave functions represent all regions of space with the same accuracy and there are no additional forces (Pulay forces [47]) on the nuclei arriving from the derivation of the basis set.

There are some disadvantages, such as the fact that charged systems cannot be studied by a standard plane wave approach unless some compensating background is added. Additionally, systems with wavefunctions that vary rapidly close to the nuclei will require a high energy cut–off and therefore many plane wave components. Localised basis sets are much better in this respect as they are designed to reproduce atomic wavefunctions. This becomes especially important in hydrogen, first–row

elements and transition metals, where the localised d and f states are difficult to represent.

Chapter 4

Atomic pseudopotentials

It was shown in the previous chapter that Bloch's theorem allows us to expand electronic wavefunctions in a periodic solid as a set of plane waves. However, for the tightly bound core orbitals a very large number of plane waves would be required to describe the rapid oscillations of the wave function close to the core. This of course would incur a large computational cost if an all-electron calculation was attempted. The pseudopotential approximation [48, 49, 11] allows the electronic wavefunctions to be expanded using a much smaller plane–wave basis set.

The pseudopotential approach exploits the fact that most of the physical properties of solids are largely dependent on the valence electrons and thus the core electrons are considered to be inert. The fundamental idea of a pseudopotential is to replace the strong Coulomb potential of the nucleus and the effects of the core electrons with a weaker ionic potential acting on the valence electrons. This is illustrated in figure 4.

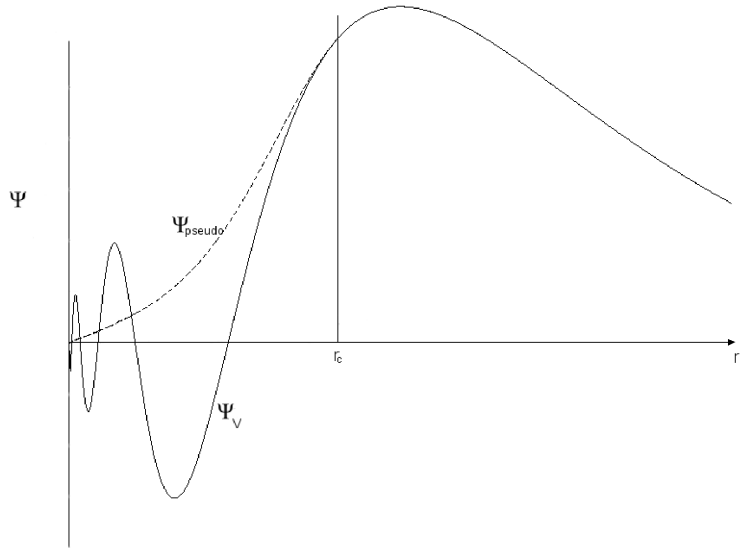

Figure 4.1: An illustration of the pseudopotential method. All-electron wave function (solid line) and corresponding pseudo wave function (dashed line) generated inside the core radius r_c.

The atomic wavefunctions are eigenstates of the atomic Hamiltonian, and as the Hamiltonian is Hermition, the atomic wavefunctions must all be orthogonal. The core states are localised near the nucleus, therefore the valence wavefunctions must oscillate rapidly in the core regions to maintain orthogonality with the core electrons. The pseudopotential is constructed so that it correctly describes the observable effects of the core electrons such as scattering properties and phase shifts. This must be done in such a way that there are no radial nodes in the core region.

4.1 Pseudopotential theory

The pseudopotential formalism grew out of the orthogonalised plane wave method, in which valence wave functions were expanded in a set of plane waves which are orthogonal to all of the core wavefunctions. Modern pseudopotential theory can be traced back to Philips and Kleinman [49], who, in 1959, showed that it is possible to construct a smooth valence wave function $\tilde{\psi}_v$ that is not orthogonalised to the core states, by combining a linear combination of the core states, ψ_c, and valence wave functions, ψ_v, in the following way:

$$|\tilde{\psi}_v\rangle = |\psi_v\rangle + \sum_c b_{cv}|\psi_c\rangle, \tag{4.1}$$

where $b_{cv} = \langle\psi_c|\tilde{\psi}_v\rangle \neq 0$.

Since $|\psi_v\rangle$ and $|\psi_c\rangle$ are orthogonal, applying $H|\psi_i\rangle = E_i|\psi_i\rangle$ to $|\tilde{\psi}_v\rangle$ gives:

$$\begin{aligned} H|\tilde{\psi}_v\rangle &= E_v|\psi_v\rangle + \sum_c E_c|\psi_c\rangle b_{cv} \\ &= E_v|\tilde{\psi}_v\rangle + \sum_c (E_c - E_v)\,|\psi_c\rangle b_{cv} \end{aligned} \tag{4.2}$$

or

$$\left\{H + \sum_c (E_v - E_c)|\psi_c\rangle\langle\psi_c|\right\}|\tilde{\psi}_v\rangle = E_v|\tilde{\psi}_v\rangle \tag{4.3}$$

Thus we have constructed an energy-dependent pseudo-Hamiltonian with the same eigenvalues of the original Hamiltonian but a smoother, nodeless wave function. The energy-dependent, non-local repulsive potential introduced is known as the Phillips-Kleinman pseudopotential [49], and is given by the sum of the true potential V and the repulsive potential of equation (4.3),

$$V_{PK} = V + \sum_c (E_v - E_c)|\psi_c\rangle\langle\psi_c|. \tag{4.4}$$

This pseudopotential is somewhat more complicated than the original potential but it is also much weaker so it can therefore be handled more easily than the full potential. The weak pseudopotential limit also closely resembles an electron gas that has been weakly perturbed by pseudopotentials, which describes alkali metals fairly accurately, but not many other metals. The pseudopotential is also often rapidly convergent in a plane wave basis set which is very useful for describing most semiconductors and metals with no d or f bands in the valence region.

The Phillips-Kleinman pseudopotentials do have some shortcomings however. For instance, for valence functions that are orthogonal to each of the core functions, such as oxygen $2p$ and iron $3d$, the pseudopotential reduces to the original potential. Another problem is that outside the core region the normalized wavefunction is proportional to, but not equal to, the original wavefunction. This leads to an incorrect valence charge distribution and thus to deviations in bonding properties. Therefore to perform an accurate self–consistent calculation the wavefunction must be constructed and then renormalized.

The Phillips-Kleinman construction, and the subsequent proof of the Phillips cancellation theorem [50] by Cohen and Heine [51], became an important tool both for the investigation of electronic band structures of solids and for understanding the behaviour of crystals. This method provided the justification required to describe the electronic structure of strongly bound valence electrons using a nearly-free electron model and weak potentials.

Based upon the orthogonalized plane wave equations and the Phillips-Kleinman approach many new methods for generating pseudopotentials have been developed. There are two basic approaches for the definition of potentials: empirical potentials, which are fitted to atomic or solid state data, and "*ab initio*" potentials, which are constructed to fit the valence properties calculated for the atom.

4.2 Empirical pseudopotentials

The first pseudopotentials developed in the 1960's were empirically based. In 1966 Ashcroft [52] suggested an empty core model in which the potential inside a cut–off radius r_c is zero. This is an example of a local pseudopotential, or a pseudopotential that uses the same potential for all the angular momentum components of the wave function. Local potentials vary only as functions of the distance from the nucleus. Non-local pseudopotentials depend on both the distance from the nucleus and the angular momentum, l. These are also known as l–dependent pseudopotentials.

The empty–core model was modified to have different core radii depending on the angular momentum quantum number. These were fitted to match experimental lattice parameters. This potential gave fairly good results for the cohesive energy and bulk moduli of various solids [52].

Heine and Abarenkov [53] developed another non-local potential that had a constant non–zero potential inside the core region. These were fitted to atomic data

by Animalu and Heine [54]. These pseudopotentials are discontinuous at r_c which leads to problems as the potentials are unphysical and their Fourier transforms are very complicated, making a plane–wave expansion difficult.

4.3 Norm–conserving pseudopotentials

There is a large amount of freedom in the construction of pseudopotentials, but as we have seen in the preceding sections both empirical methods and the non-empirical Phillips–Kleinman approach have important limitations. Another approach must therefore be considered.

In order to construct a good pseudopotential we require a pseudo–wave function that satisfies two important conditions. It should decay exactly as the all–electron wavefunction beyond some radius, and it should also be an eigenstate of a pseudo–Hamiltonian with the same eigenvalue as the all–electron wave function. The pseudopotential is then obtained by inverting the radial Schrödinger equation

$$\left\{-\frac{\hbar^2}{2m}\frac{d^2}{dr^2}+\frac{l(l+1)}{2r^2}+v(r)\right\}rR(\varepsilon,r)=\varepsilon rR(\varepsilon,r). \tag{4.5}$$

for that pseudo-wave function. Equation (4.5) is a second–order linear differential equation. By fixing ε the solution can be uniquely determined by the value of the wave function $R(\varepsilon,r)$ and its derivative $R'(\varepsilon,r)$ at a given point r_0. The two conditions stated above can then be satisfied by specifying the value of the radial

logarithmic derivative of the wave function at r_0 :

$$\cot \eta_l(\varepsilon) \propto \left[\frac{d}{dr} ln R^l(\varepsilon, r)\right]_{r_0} = \frac{1}{R^l(\varepsilon, r_0)} \left[\frac{dR^l(\varepsilon, r)}{dr}\right]_{r_0}, \tag{4.6}$$

together with the normalization condition this can be done for all values of angular momentum l. The quantities $\eta_l(\varepsilon)$ are the phase shifts of the partial waves.

Therefore we have the condition that if both the all–electron potential and pseudopotential are the same beyond some cut–off radius r_c, then the all–electron and pseudo–wave functions are proportional if the logarithmic derivatives are the same, that is, if

$$\frac{1}{R^l_{AE}(\varepsilon, r_c)} \left[\frac{dR^l_{AE}(\varepsilon, r_c)}{dr}\right]_{r_c} = \frac{1}{R^l_{PS}(\varepsilon, r_c)} \left[\frac{dR^l_{PS}(\varepsilon, r_c)}{dr}\right]_{r_c}. \tag{4.7}$$

The wave functions become equal when the pseudo–wave function is required to preserve the norm inside r_c:

$$\int_0^{r_c} r^2 [R^l_{AE}(\varepsilon, r)]^2 dr = \int_0^{r_c} r^2 [R^l_{PS}(\varepsilon, r)]^2 dr. \tag{4.8}$$

This property is known as norm–conservation. It was first introduced in the field of pseudopotentials by Hamann, Schlüter and Chiang in 1979 [55]. They proposed a method to construct non–local norm–conserving pseudopotentials to fit first–principles all–electron atomic calculations without explicitly referencing orthogonalization to the core states.

One important result of this work was the realization that the norm of the wave-

function also appears in an important identity related to the Friedel sum rule [56, 57]:

$$-\frac{1}{2}\left\{[rR^l(\varepsilon,r)]^2\frac{d}{d\varepsilon}\frac{d}{dr}\ln R^l(\varepsilon,r)\right\}_{r_c}=\int_0^{r_c}r^2[R^l(\varepsilon,r)]^2dr. \tag{4.9}$$

What this means is that the norm conservation condition (4.8) requires that the logarithmic derivatives of the all–electron and pseudo–wave functions vary in the same way, at least to first order. This implies that an external potential that would produce a small change in the eigenvalue would only produce a second-order change in the logarithmic derivative. Therefore the condition (4.7) becomes approximately valid for a range of eigenvalues around the reference energy, ε, which was used to obtain the wave function. This allows pseudopotentials derived from atomic calculations to be used in other environments such as molecules or crystals. When an atom is part of a larger structure its electrons feel the influence of the other atoms around it. The electronic eigenvalues will therefore be shifted from their atomic values, but because of the transferability of norm-conserving potentials, the all–electron and pseudo–wave functions will still coincide outside the cut–off radius.

The norm–conservation constraint ensures that pseudopotentials are useful in environments in which the eigenvalues do not deviate significantly from the eigenvalues used in the construction. This transferability is improved by reducing the cut–off radius because the pseudo-wavefunction will then approach the all-electron result. This is limited however by the condition that the pseudo–wave function must be nodeless. The cut–off radius must therefore be larger than the position of the outermost node of the all-electron wavefunction.

In order to construct "good" norm–conserving pseudopotentials Hamann, Schlüter and Chiang proposed the following list of requirements:

1. The eigenvalues of the pseudo–wave functions agree with those of the all–electron wave functions for the chosen electronic configuration of the atom.

2. The pseudo–wave function is nodeless and agrees with the all–electron wave function beyond a chosen core radius r_c.

3. The logarithmic derivatives of the all–electron and pseudo–wave functions agree at r_c.

4. The norm, or integrated charge, of the true and pseudo–wave functions inside the "pseudized" region ($r < r_c$) is the same (norm–conservation condition given by (4.8)):

$$\int_0^{r_c} |r\tilde{R}_{PS}(r)|^2 dr = \int_0^{r_c} |r\tilde{R}_{AE}(r)|^2 dr. \tag{4.10}$$

5. The first energy derivative of the logarithmic derivatives of the all–electron and pseudo wavefunctions agree at r_c, and therefore beyond r_c.

There are other constraints that can be applied in order to improve the smoothness of the pseudopotentials such as reducing the number of Fourier components. This is crucial for plane wave calculations as the energy cut–off and therefore the computational expense of the calculation are determined by the number of Fourier components.

4.4 Generation of pseudopotentials

The typical procedure for the generation of an ionic pseudopotential is as follows.

An all–electron atomic calculation is performed for an isolated atom in the ground state and some excited states given both the atomic configuration and an approximation for the exchange–correlation density functional. Each l, m state is treated independently except that the total potential is calculated self consistently. This allows us to obtain valence electron eigenvalues and wavefunctions for the atom, from which we can generate the pseudopotentials and pseudo–orbitals for the valence states.

The pseudopotential is finally obtained by subtracting the Hartree and exchange–correlation potentials which are calculated only for the valence electrons in their pseudo–orbitals:

$$V^l(r) = V^l_{total}(r) - V_{Hartree}(r) - V_{XC}(r). \tag{4.11}$$

An important point here is that the exchange–correlation functional, E_{XC}, used in the all-electron calculation has to be the same in the target calculation.

There is still some freedom in the choice of pseudopotentials beyond the norm–conservation requirements. These choices are typically between the accuracy and transferability of a pseudopotential, and the smoothness of a pseudopotential. Decreasing the cut–off radius will increase the accuracy and transferability as the wavefunction will be better described close to the atom. Increasing the cut–off radius will decrease the accuracy but lead to smoother pseudo–wave functions that require a far smaller plane–wave basis set. Typically cut–off radii are located around the

maximum of the valence wavefunction.

4.4.1 Relativistic corrections

In the case of heavy atoms the effects of special relativity have to be incorporated into pseudopotentials. This is because the core electrons in the deepest shells have very high energies. The kinetic operator in Schrödinger's equation therefore has to be replaced by Dirac's expression so that the solutions have well–defined total angular momentum and parity [58]. The total angular momentum is composed of orbital and spin components and since the electron spin is always a half, there are two values of the total angular momentum quantum number j for each orbital state l; $j = l \pm \frac{1}{2}$.

If the atomic wavefunctions are described in terms of the angular l and spin s components instead of the total angular momentum quantum number j, then the spin–orbit effects are included in a short range non–local term. The total pseudopotential then becomes [59, 60]:

$$\hat{V}_{PS} = \sum_l V_{PS}^l(r)\hat{P}_l = \sum_l \left[V_{PS(SR)}^l(r) + V_{PS(SO)}^l(r)\mathbf{L}\cdot\mathbf{S}\right]\hat{P}_l, \tag{4.12}$$

where

$$V_{PS(SR)}^l(r) = \frac{1}{2l+1}\left[lV_{PS}^{l-\frac{1}{2}}(r) + (l+1)V_{PS}^{l+\frac{1}{2}}(r)\right], \tag{4.13}$$

and $\hat{P}_l$ are the projection operators.

This is an average potential that includes scalar relativistic effects. It is appropriate whenever the spin–orbit effects on the valence electrons are very small. The

spin–orbit effects are described by a short range non–local term [11, 61],

$$V^{l}_{PS(SO)}(r) = \frac{2}{2l+1}\left[V^{l+\frac{1}{2}}_{PS}(r) - V^{l-\frac{1}{2}}_{PS}(r)\right]. \tag{4.14}$$

Relativistic corrections are only important in the core regions and therefore can be included directly into the pseudopotential in such a way that the solution of the non–relativistic Schrödinger equation contains relativistic effects. The exchange–correlation functional also needs to be changed in order to incorporate relativistic effects deep in the atomic core. A method was suggested by Bachelet *et al.* [61], in which the exchange energy density and potential are multiplied by density–dependant correction factors [62].

4.4.2 The Trouiller–Martins pseudopotential

In an attempt to generate smoother pseudopotentials that were more suitable for an expansion in terms of plane waves another form of pseudopotential was introduced by Troullier and Martins [17]. This work was a generalization of the work of Kerker [63] with some additional conditions imposed, namely:

1. The wavefunction and its first four derivatives have to be continuous at the cut-off radius as opposed to both Kerker's work and the work of Hamann, Schlüter and Chiang [55] in which only the first two derivatives were continuous.

2. Every odd derivative of the pseudopotentials is forced to be zero at $r = 0$.

3. The screened pseudopotential has a zero gradient at $r = 0$.

These conditions allow a pseudopotential of equal quality to that of Hamann, Schlüter and Chiang to be produced but at a much larger cut–off radius, therefore allowing a much faster convergence rate with a smaller plane wave basis set.

4.5 Separable form of atomic pseudopotentials

In 1982 Kleinman and Bylander [64] proposed a method that greatly reduced the computational effort required to evaluate the contribution of the non–local pseudopotential part to the Hamiltonian and energy of the target system. They introduced the term *semi–local* to denote a potential which is non–local in the angular momentum co–ordinates, l, but not in the radial co–ordinates, r.

This observation led Kleinman and Bylander to propose a different description of the non-local component of the pseudopotential. They constructed a pseudopotential operator that is separable in $\mathbf{r}$ and $\mathbf{r}'$,

$$\delta V(\mathbf{r}, \mathbf{r}') = \sum_i f_i(\mathbf{r}) g_i(\mathbf{r}'). \tag{4.15}$$

so that when evaluating the matrix elements $V_{ij} = \langle i|\hat{V}|j\rangle$ in a set of N basis functions the $\mathbf{r}$ integral, involving only the basis function ψ_i, and the $\mathbf{r}'$ integral, involving only the function ψ_j, can be calculated seperately. This reduces the number of integrals from N^2 to N, which is of course of computational advantage.

The general form for the pseudopotential is

$$V_{PS}(r) = \sum_{l} |Y_{lm}\rangle V^{l}_{PS}(r) \langle Y_{lm}|, \tag{4.16}$$

where Y_{lm} are spherical harmonics and V^l is the l^{th} angular momentum component of the pseudopotential acting on the wavefunction. Assuming all potentials with angular momentum greater than some chosen value l_{max} are equal to some arbitrarily chosen local potential, the pseudopotential becomes:

$$\begin{aligned} V_{PS}(r) &= \sum_{l=0}^{l_{max}} |Y_{lm}\rangle V^{l}_{PS}(r) \langle Y_{lm}| \quad + \quad \sum_{l=l_{max}+1}^{\infty} |Y_{lm}\rangle V^{loc}_{PS}(r) \langle Y_{lm}| \\ &= \sum_{l=0}^{l_{max}} |Y_{lm}\rangle \left(V^{l}_{PS}(r) - V^{loc}_{PS}(r) \right) \langle Y_{lm}| \quad + \quad \sum_{l=0}^{\infty} |Y_{lm}\rangle V^{loc}_{PS}(r) \langle Y_{lm}| \\ &= \sum_{l=0}^{l_{max}} |Y_{lm}\rangle \left(V^{l}_{PS}(r) - V^{loc}_{PS}(r) \right) \langle Y_{lm}| \quad + \quad V^{loc}_{PS}(r). \end{aligned} \tag{4.17}$$

The pseudopotential proposed by Kleinman and Bylander is

$$V_{PS} = \sum_{lm} \frac{|\delta V^{l} \psi^{0}_{lm}\rangle \langle \psi^{0}_{lm} \delta V^{l}|}{\langle \psi^{0}_{lm} | \delta V^{l} | \psi^{0}_{lm} \rangle} \quad + \quad V^{loc}_{PS}, \tag{4.18}$$

where the functions ψ^0_{lm} are the pseudo–eigenfunctions from which the original pseudopotential was constructed. The process of taking matrix elements of the semi–local pseudopotential with a basis of N plane waves scales as N^2, whereas using the separable form requires a process which scales as N. This result is a substantial saving in computational load for calculations involving many atoms in the unit cell.

4.5.1 Ghost states

The Kleinman–Bylander construction is not without its problems though. When introducing a separable form of norm–conserving pseudopotentials one has to ensure that this does not lead to unphysical "ghost" states. The Wronskian theorem

[65] states that atomic eigenfunctions are energetically ordered so that the energies increase with the number of nodes. Therefore the nodeless wavefunction should be the solution with the lowest energy. The Kleinman–Bylander Hamiltonian does not obey this theorem and therefore this is no longer guaranteed to be the case. These ghost states are single node states at energies below the true ground state eigenvalue which therefore undermine the transferability of the pseudopotential.

Gonze *et al.* [66] showed that the existence of these ghost states is related to the choice of the local component of the pseudopotential. These problems normally occur when the energies are large, but can be avoided by using more than one reference state, or by careful choice of the local component and cut–off radii in the semi–local pseudopotentials. Ghost states can be identified and analysed by investigating properties such as the logarithmic derivatives of the energy and the bound state spectra and observing deviations. For ghost states below the valence states Gonze *et al.* [66] proposed a set of criteria by which they could be identified.

Chapter 5

Pseudopotential calculations for the $5d$ transition metals

5.1 Introduction

The transition elements are those elements which have partially filled d or f shells in the neutral or cationic states. They are commonly referred to as transition metals as they possess the properties of metals, i.e. they have high melting points and are good conductors of heat and electricity. The transition metals are generally very hard and are widely used as simple substances and alloys because they form stable hard materials.

The transition metals are classified into the d-block metals and f-block metals. The d-block consists of the $3d$ elements from Scandium to Copper, the $4d$ elements from Yttrium to Silver, and the $5d$ elements from Hafnium to Gold. The f-block

consists of the lanthanoid elements from Lanthanum to Lutetium and the actinoid elements from Actinium to Lawrencium. The chemistry of these two blocks differs considerably.

In this work we will be investigating specifically the $5d$ elements from Hafnium to Platinum. These elements are used extensively in industry for various purposes:

Hafnium captures neutrons very efficiently and is used in nuclear reactor control rods.

Tantalum is extremely resistant to corrosion by air or water and is therefore a valuable alloying agent, It is also used in capacitors and tantalum carbide cutting tools.

Tungsten has the highest melting point of the d-block metals and therefore has important applications in electrical filaments such as those in household bulbs. It is also used in steel alloys and tungsten carbides are very common as cutting tools.

Rhenium is a rare metal but is also used in alloys and as a catalyst. It is used in photographic flashes and mass spectrometers.

Osmium is a rare metal which is extremely hard and one of the densest elements known. At this stage its commercial applications are limited but it is used as an alloying agent.

Iridium is also rare and expensive and extremely dense. It is also very resistant

to corrosion by water, air or acids. It is used as an alloy and also in the calibration of high pressure diamond anvils due to its extreme stability at high pressure and temperature.

Platinum is widely used in the manufacture of wires, electrodes and jewelery due to its silver colour and the fact that it is malleable and ductile. It is inert in air even at high temperatures and is used extensively as a catalyst both in industry and in motor vehicle catalytic converters.

5.2 Pseudopotential generation

In the generation of pseudopotentials for our calculations we have used the improved norm–conserving pseudopotential of Troullier and Martins [17] type in the fully separable Kleinman–Bylander [64] form. The local density approximation (LDA) using the Ceperly–Alder [26] exchange–correlation functional was employed.

The core electrons are treated in a scalar relativistic formalism and we treated as the valence states the $6s$, $6p$ and $5d$ orbitals. The cut–off radius in each case was chosen to be a distance of 80% between the last node and the outermost maximum of the corresponding wavefunctions. These choices for the core radii gave fairly accurate values for bulk properties when compared with experimental values. The core radii for each atom are shown in Table 5.1 and the consequent true and pseudo wavefunctions and the corresponding pseudopotentials are shown in Figures 5.1 to 5.14. These cut–radii compare well with those used in other publications and result in the fairly smooth pseudo wavefunctions presented below.

Table 5.1: A table of the cut-off radii used for generating the pseudopotentials for the valence orbitals.

	r_c (Bohr radii)		
Element	$6s$	$6p$	$5d$
Hf	2.57	3.33	1.46
Ta	2.47	3.17	1.37
W	2.38	3.05	1.30
Re	2.31	2.94	1.24
Os	2.22	2.85	1.18
Ir	2.41	3.14	1.15
Pt	2.13	2.81	1.10

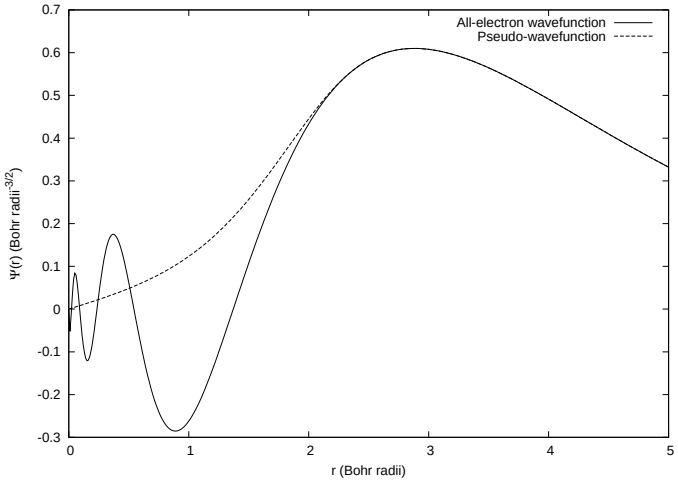

(a)

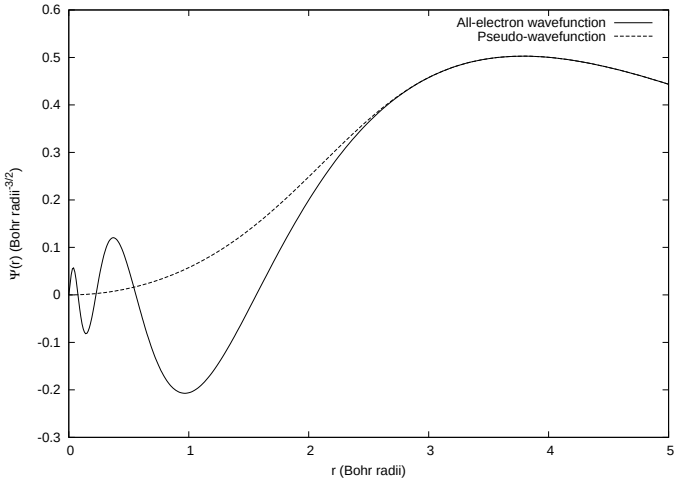

(b)

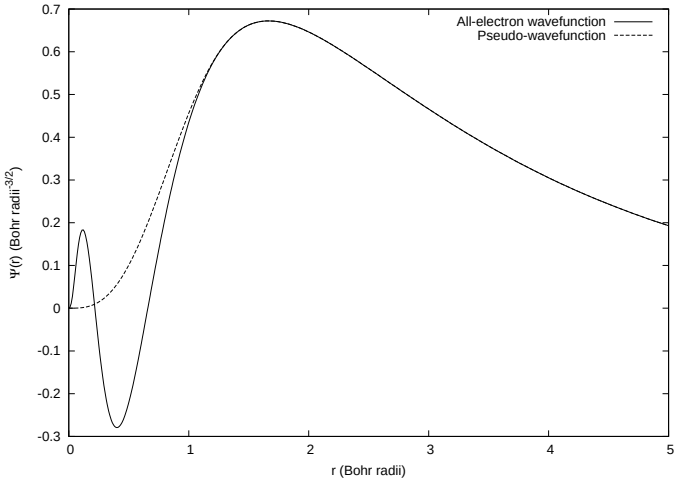

(c)

Figure 5.1: The all–electron and pseudo–wavefunctions for Hafnium. (a) $6s$, (b) $5p$, (c) $5d$

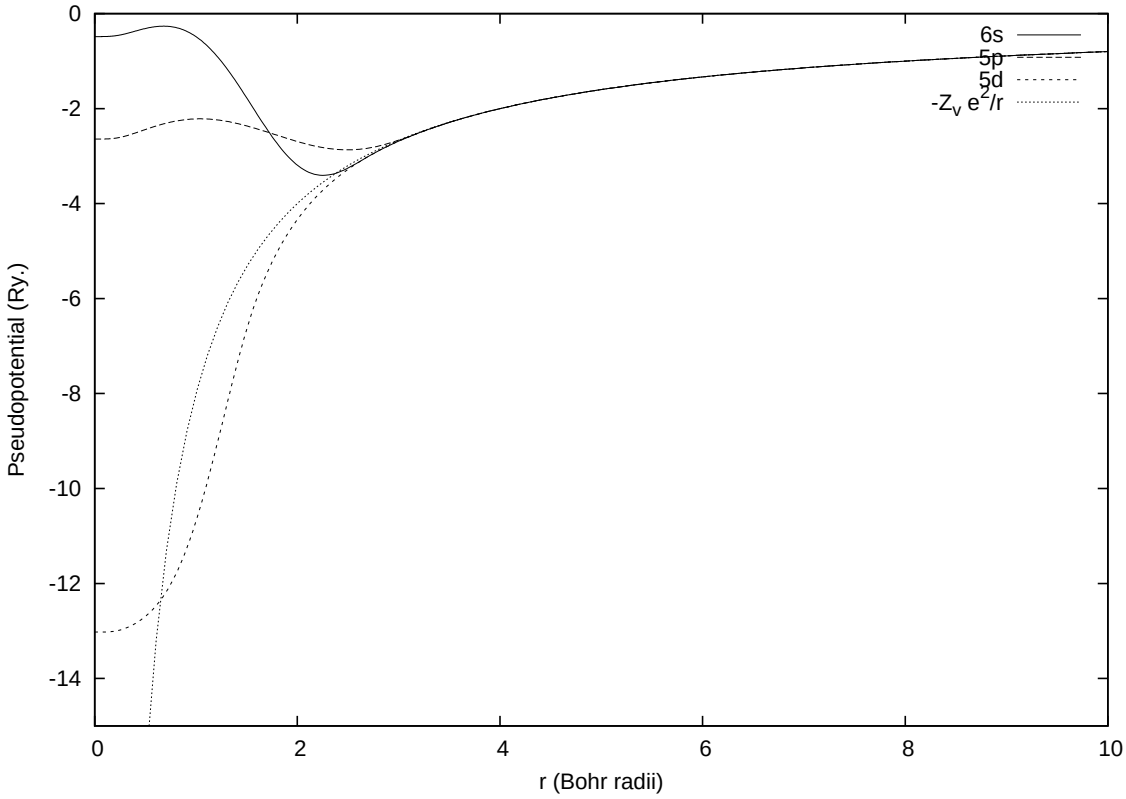

Figure 5.2: The pseudopotential for $l = 0$, 1 and 2 for Hafnium.

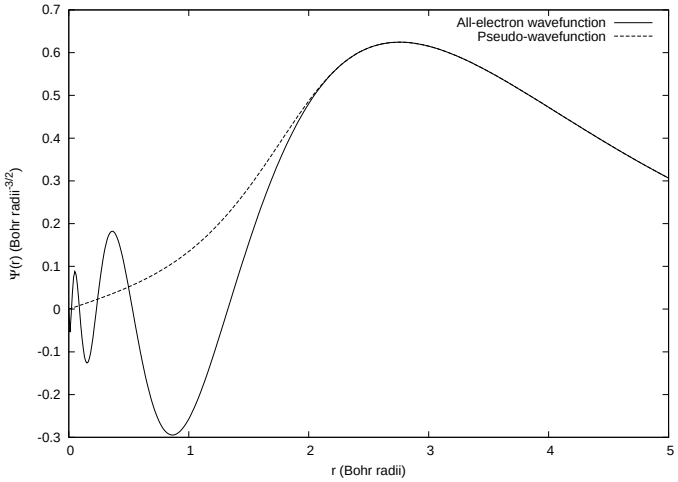

(a)

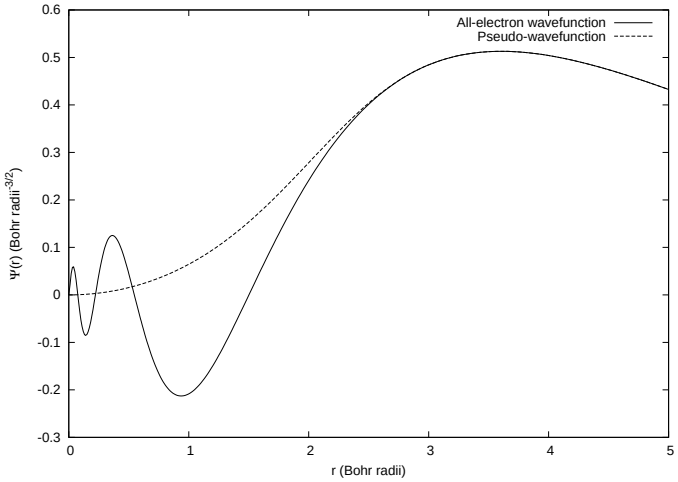

(b)

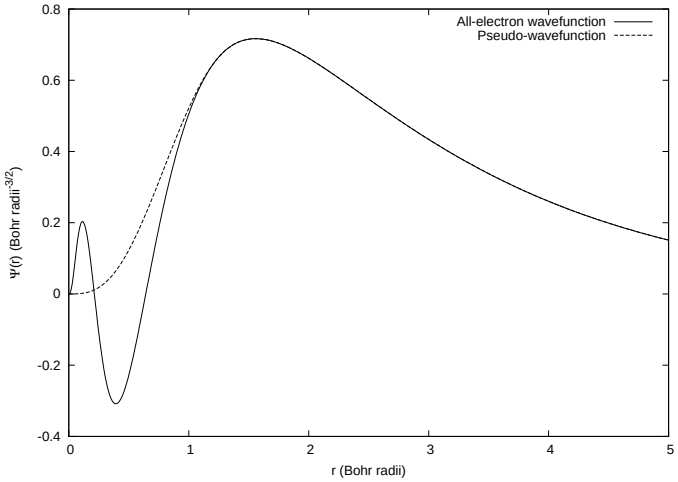

(c)

Figure 5.3: The all–electron and pseudo–wavefunctions for Tantalum. (a) $6s$, (b) $5p$, (c) $5d$

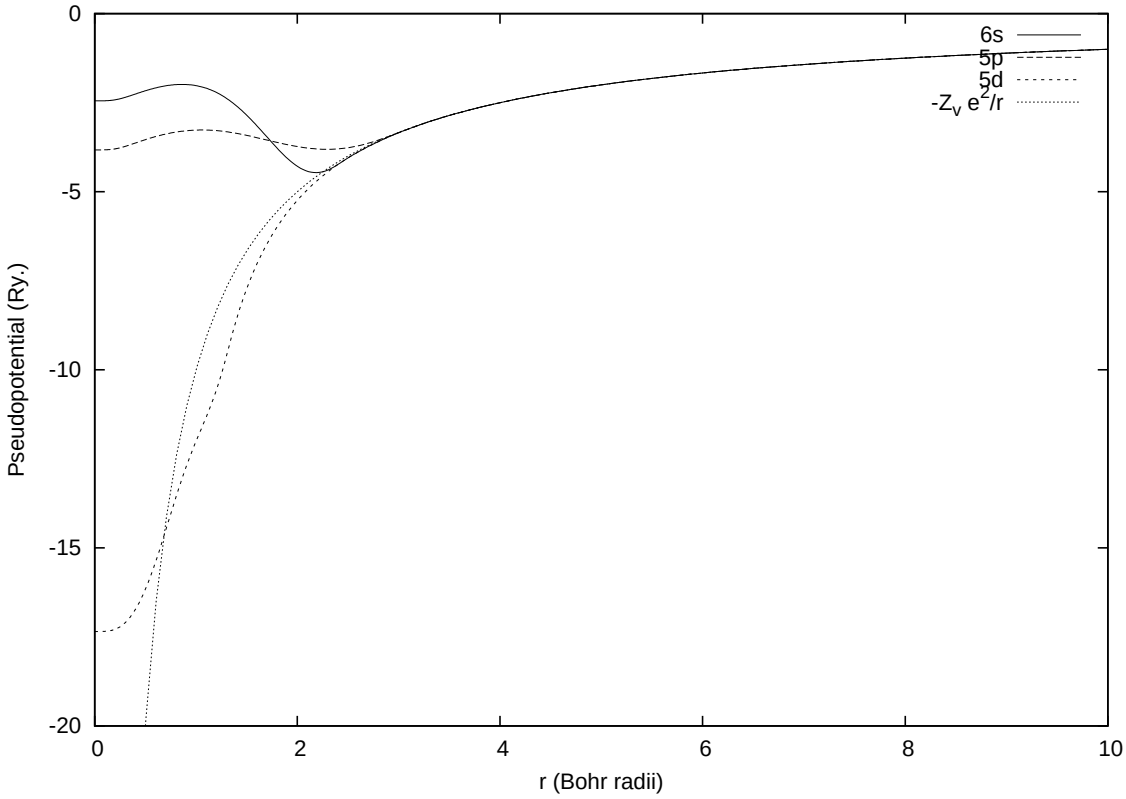

Figure 5.4: The pseudopotential for $l = 0$, 1 and 2 for Tantalum.

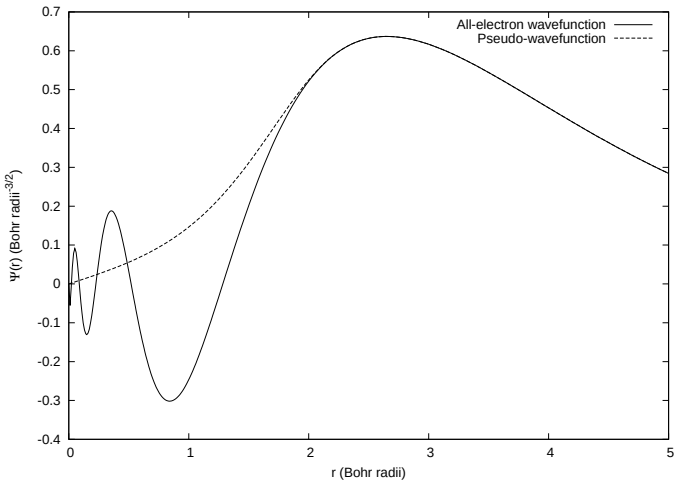

(a)

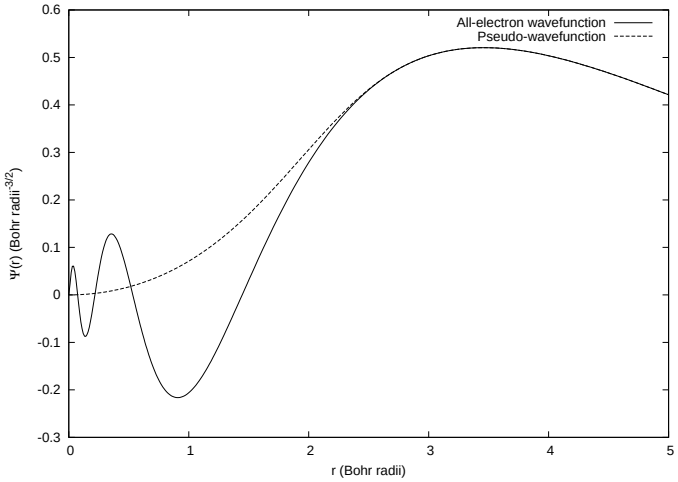

(b)

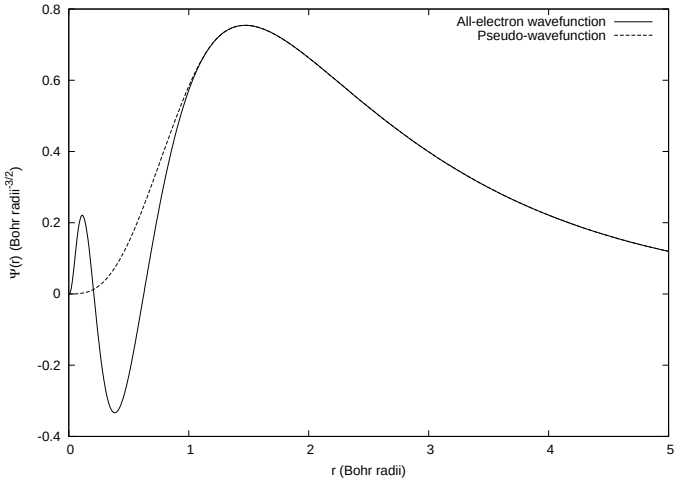

(c)

Figure 5.5: The all–electron and pseudo–wavefunctions for Tungsten. (a) $6s$, (b) $5p$, (c) $5d$

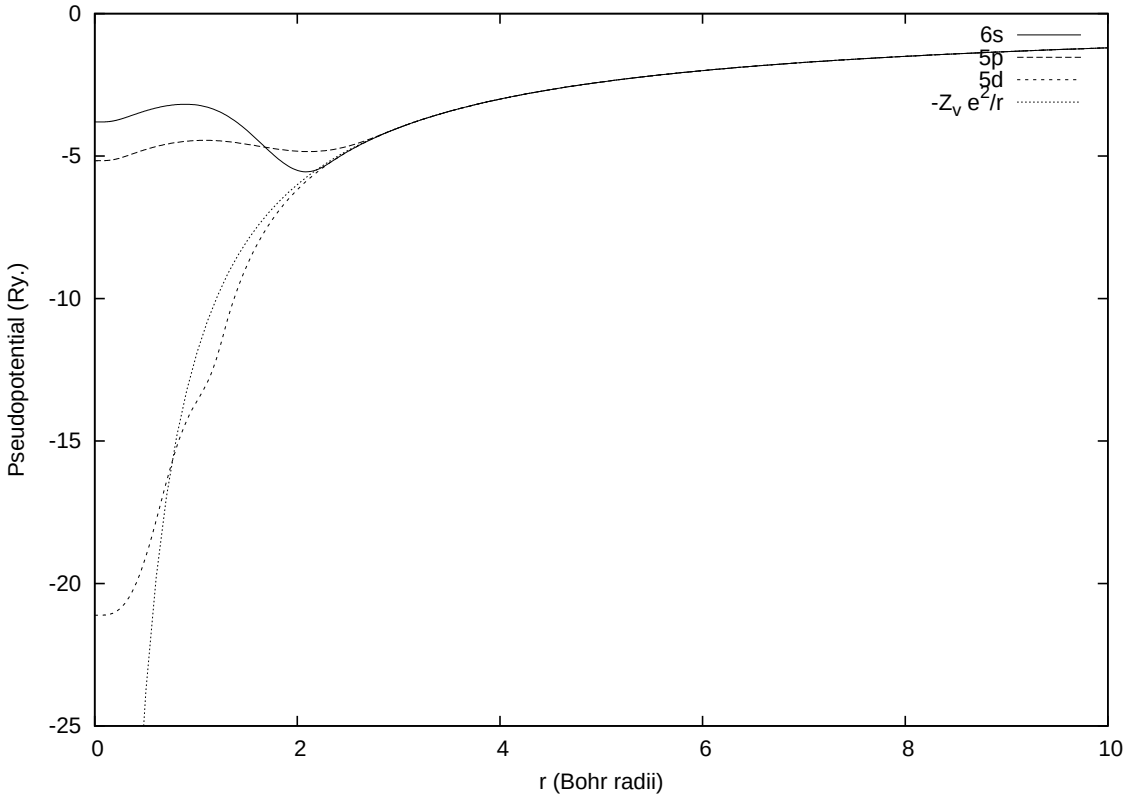

Figure 5.6: The pseudopotential for $l = 0$, 1 and 2 for Tungsten.

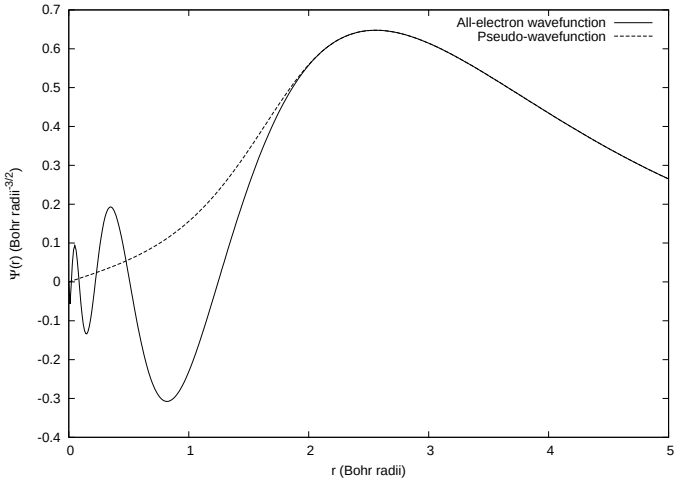

(a)

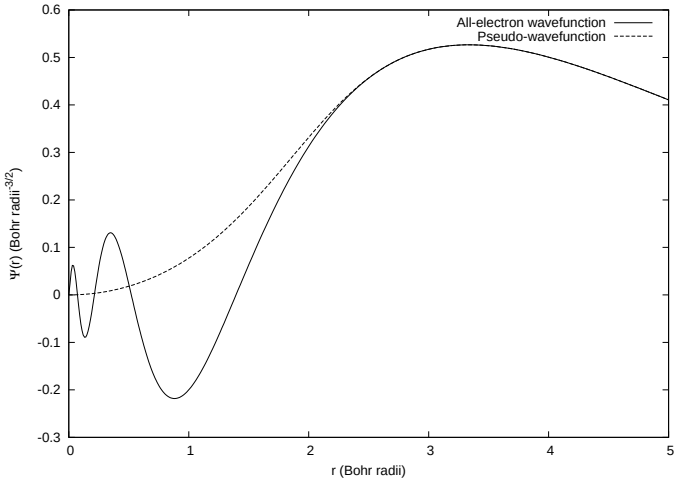

(b)

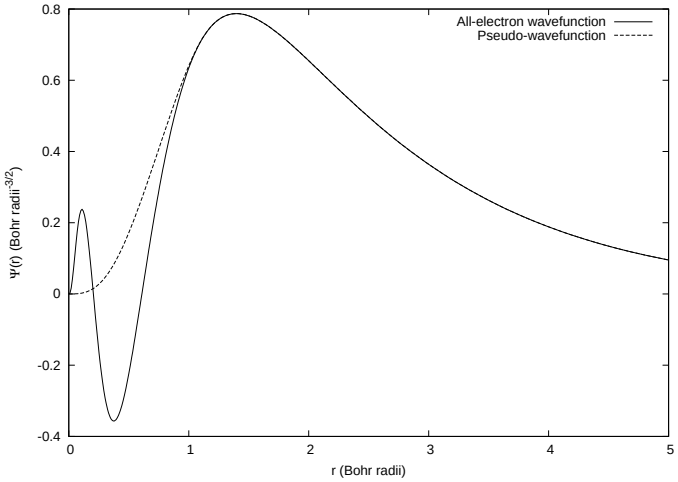

(c)

Figure 5.7: The all–electron and pseudo–wavefunctions for Rhenium. (a) $6s$, (b) $5p$, (c) $5d$

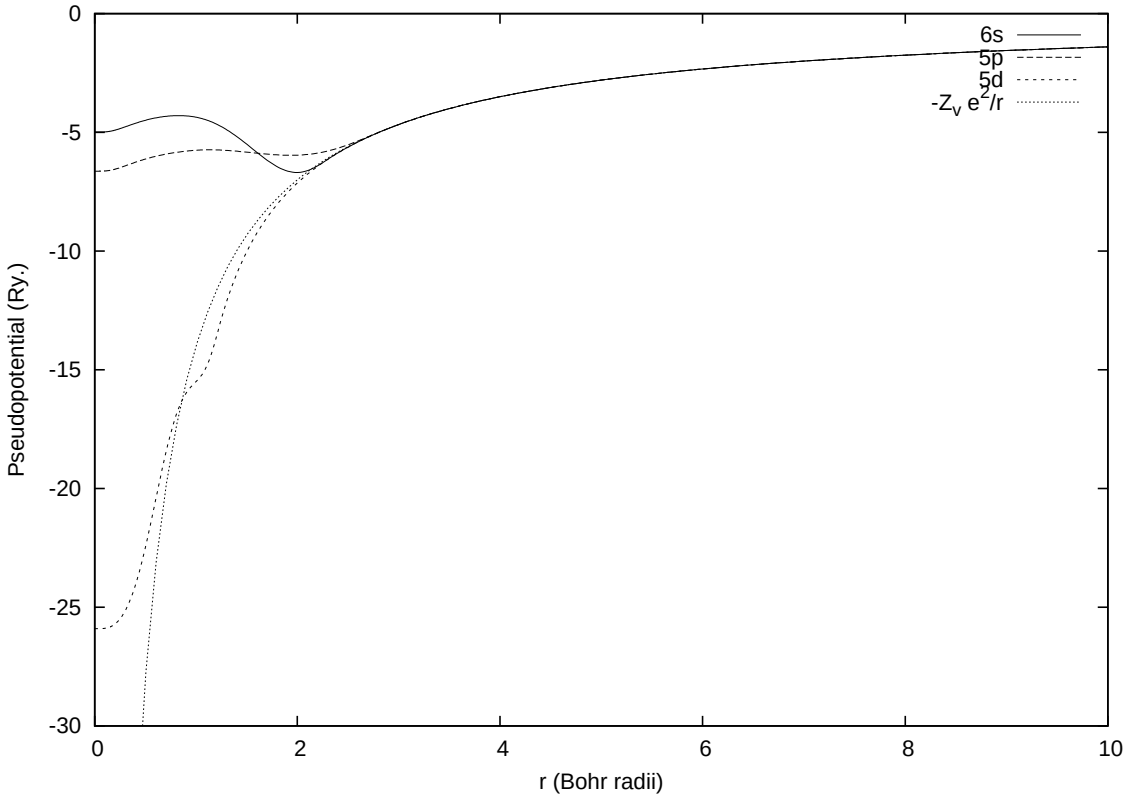

Figure 5.8: The pseudopotential for $l = 0$, 1 and 2 for Rhenium.

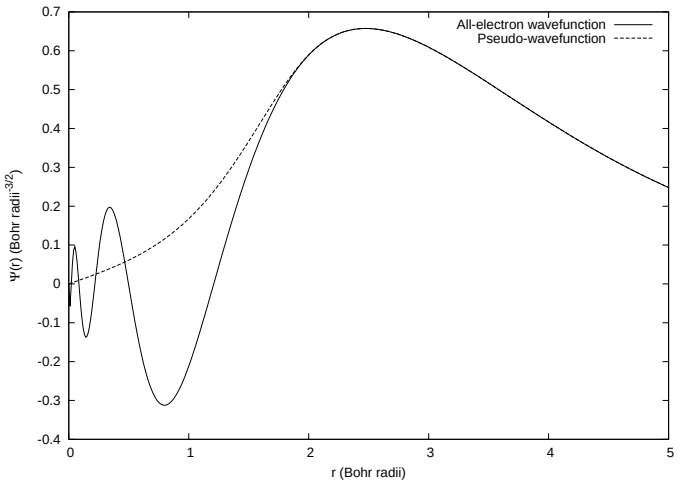

(a)

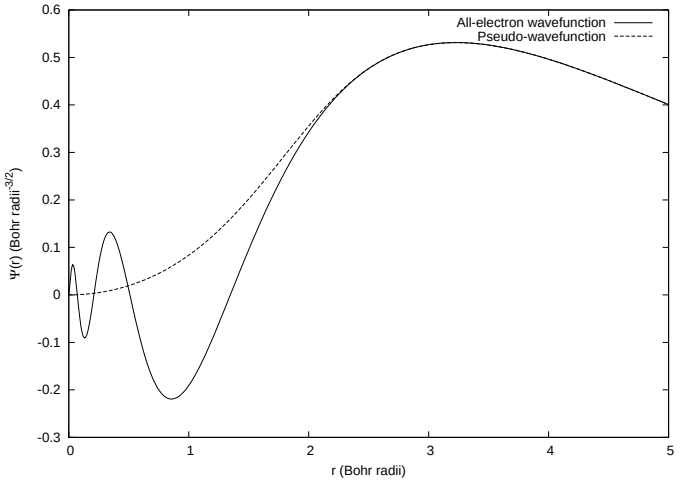

(b)

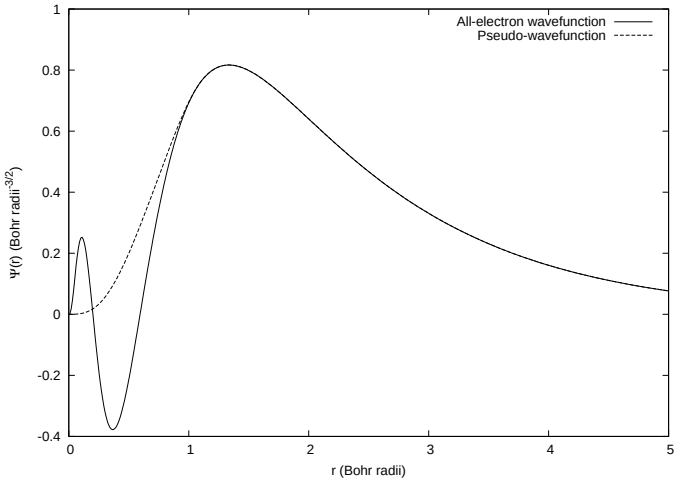

(c)

Figure 5.9: The all–electron and pseudo–wavefunctions for Tungsten. (a) $6s$, (b) $5p$, (c) $5d$

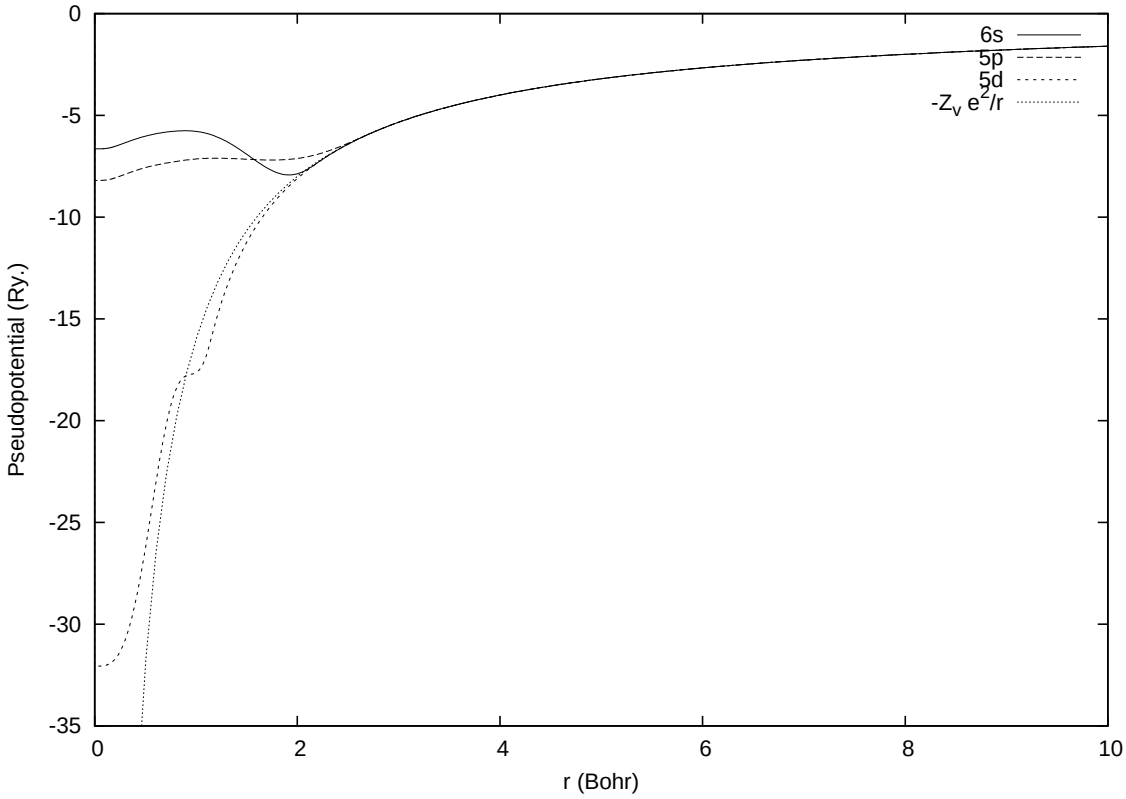

Figure 5.10: The pseudopotential for $l = 0$, 1 and 2 for Osmium.

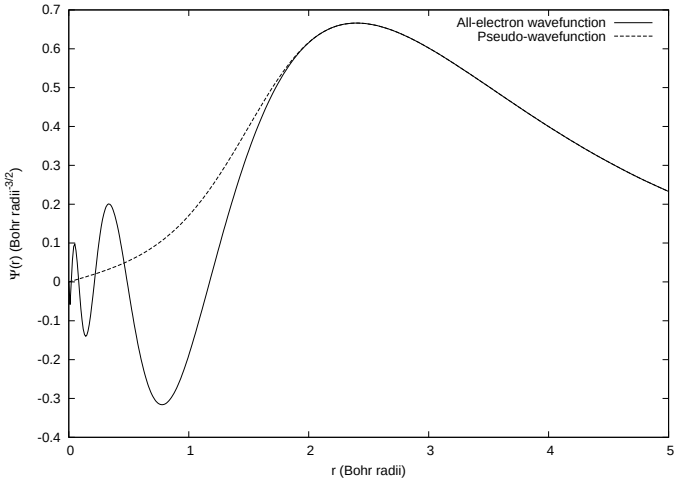

(a)

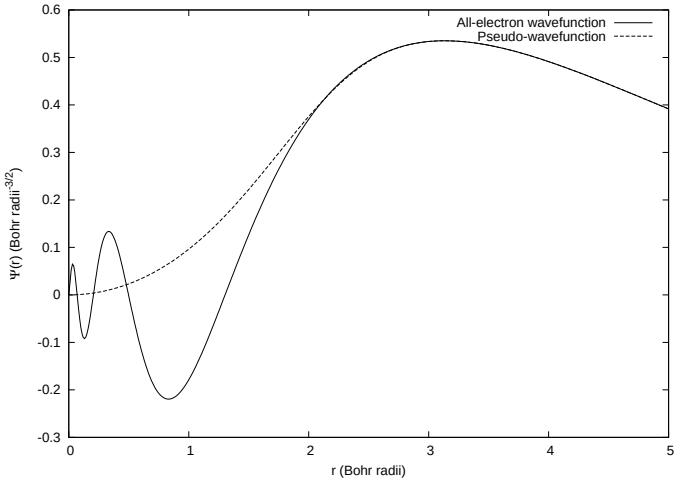

(b)

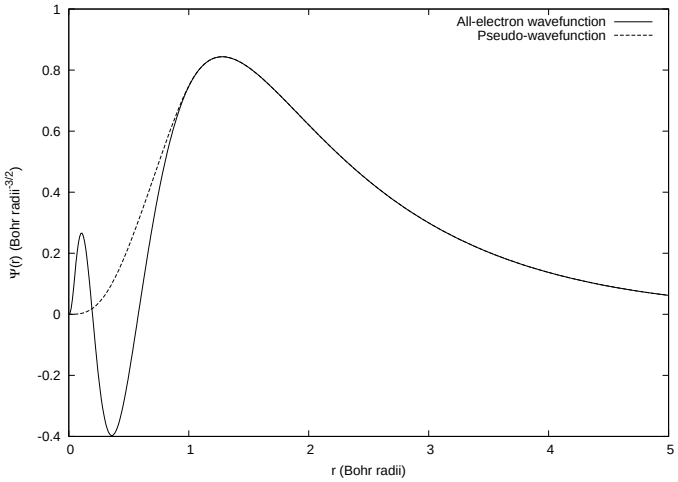

(c)

Figure 5.11: The all–electron and pseudo–wavefunctions for Iridium. (a) $6s$, (b) $5p$, (c) $5d$

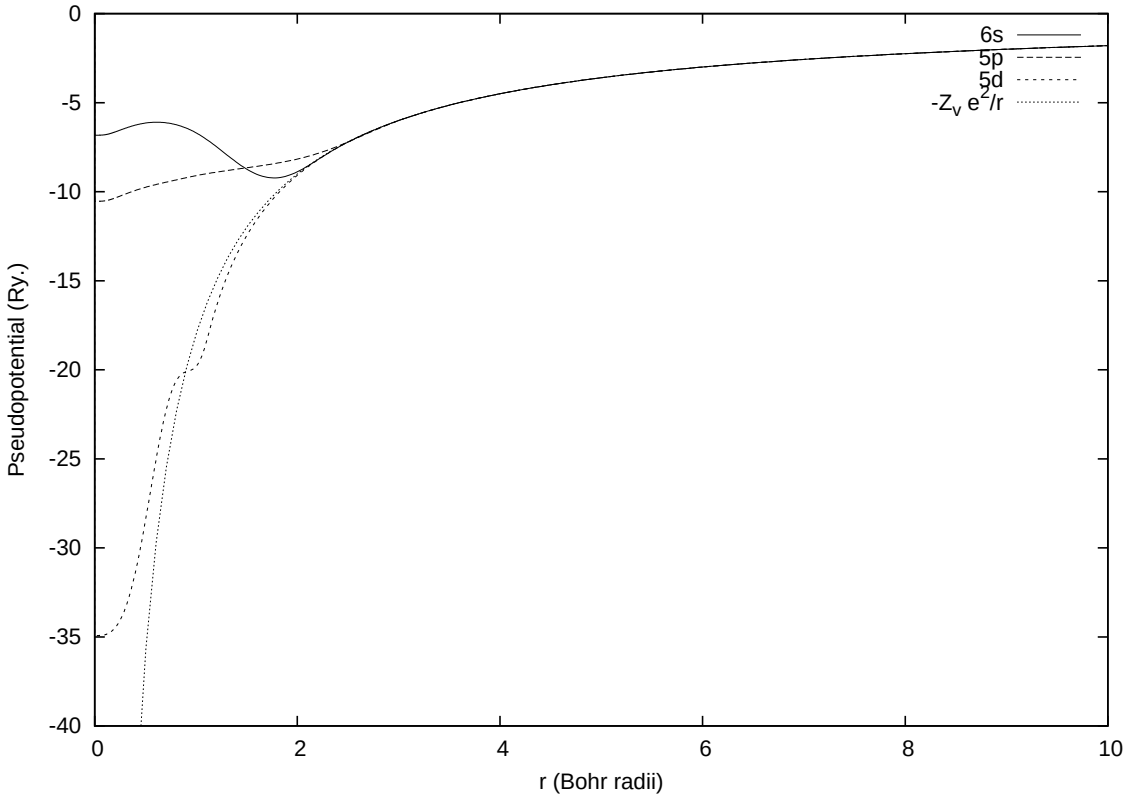

Figure 5.12: The pseudopotential for $l = 0$, 1 and 2 for Iridium.

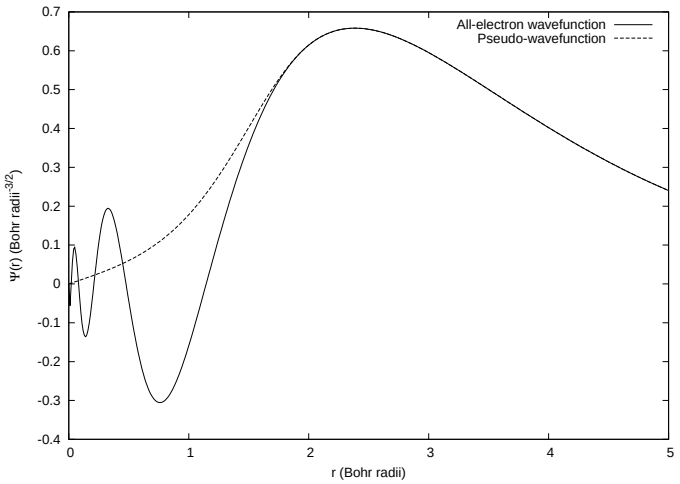

(a)

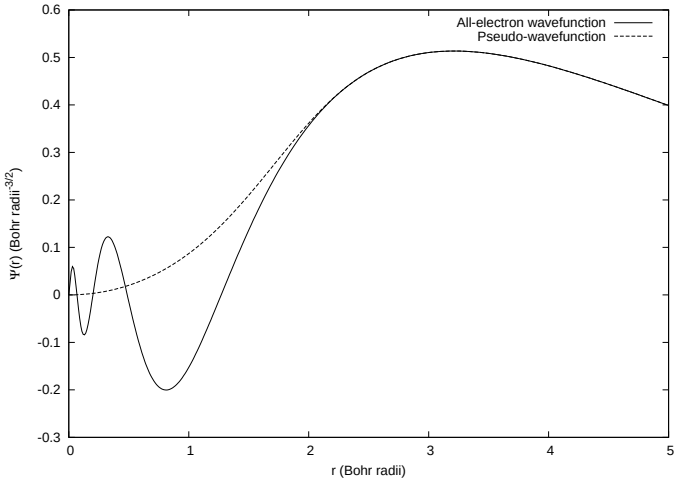

(b)

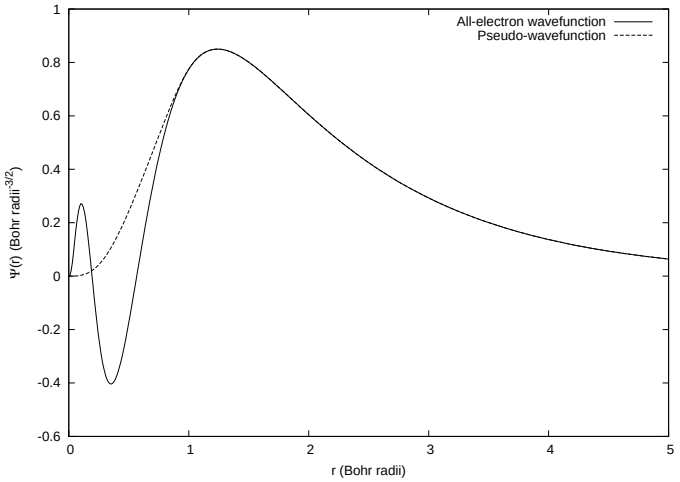

(c)

Figure 5.13: The all–electron and pseudo–wavefunctions for Platinum. (a) $6s$, (b) $5p$, (c) $5d$

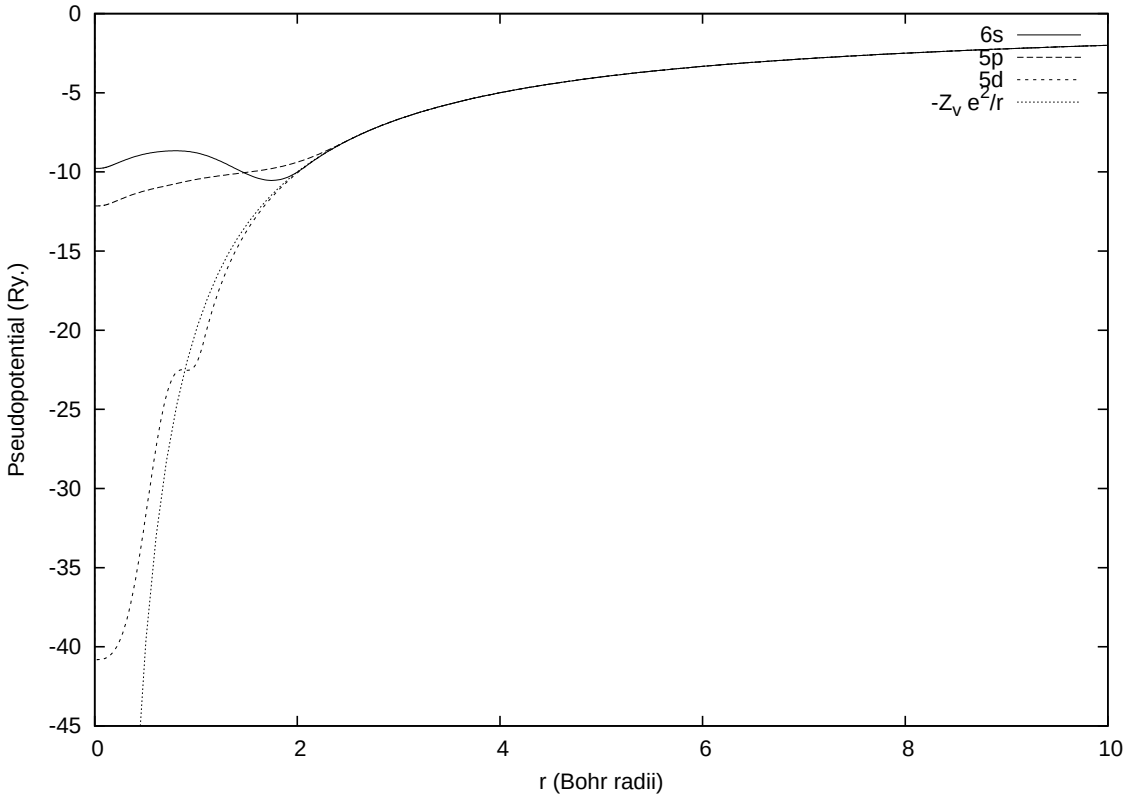

Figure 5.14: The pseudopotential for $l = 0$, 1 and 2 for Platinum.

5.3 Calculational methods

Total energies and structural properties of the $5d$ transition elements are studied by first principles plane–wave basis pseudopotential calculations using BEST(Brookhaven Electronic Structure) codes. The codes, developed between 1993 and 1995 by Chetty and Weinert have been used to successfully predict the energetics of various solid state systems [67, 68]. An Intel Pentium 4 Desktop Computer with a 3.00GHz processor and 2 GBytes of RAM was used to perform the calculations for this work.

The underlying theory in the BEST codes is density functional theory which was discussed in Section 2.2 and the local density approximation which was discussed in Section 2.2.2. The improved norm–conserving pseudopotential of Troullier and Martins [17] type in the fully separable Kleinman–Bylander [64] construction is employed.

It is necessary to investigate the sensitivity of the calculations to the number of momentum space sampling points (k points). Therefore initially we performed calculations in order to check for the convergence of calculated results with respect to the number of k points and the cut–off energy for the plane wave expansion of the wavefunction. In the following pages the results are shown for each of the atoms studied. To obtain convergent results, a large number of k points and a high cut–off energy are required. In our final calculations we have used a $12\times12\times12$ Monkhorst–Pack [42] mesh for the k–space integration a total of 6912 k–points, and a cut–off

energy of 120 Ryd for the wavefunction expansion.

For consistency we have used these values for all of the atoms in our investigation. It is perhaps important to note that the energy is not variable with respect to the k point sampling and therefore the energy does not decrease monotonically.

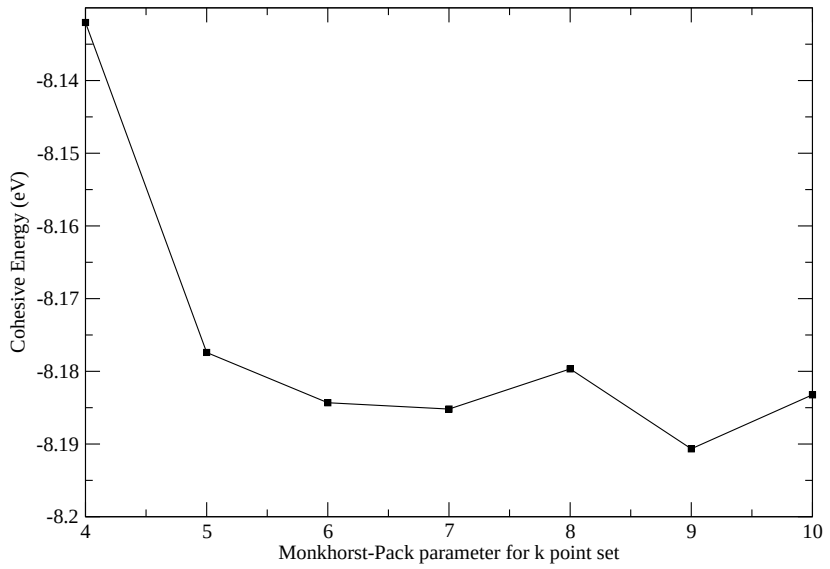

(a) The Monkhorst-Pack parameter for generating special k points

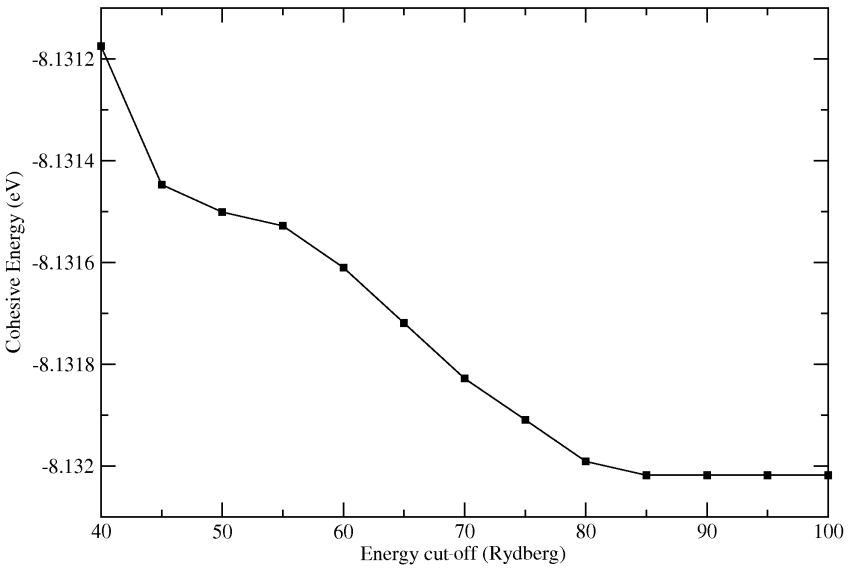

(b) The cut–off energy

Figure 5.15: The convergence of calculated cohesive energies for Hafnium as a function of (a) k points and (b) cut–off energy.

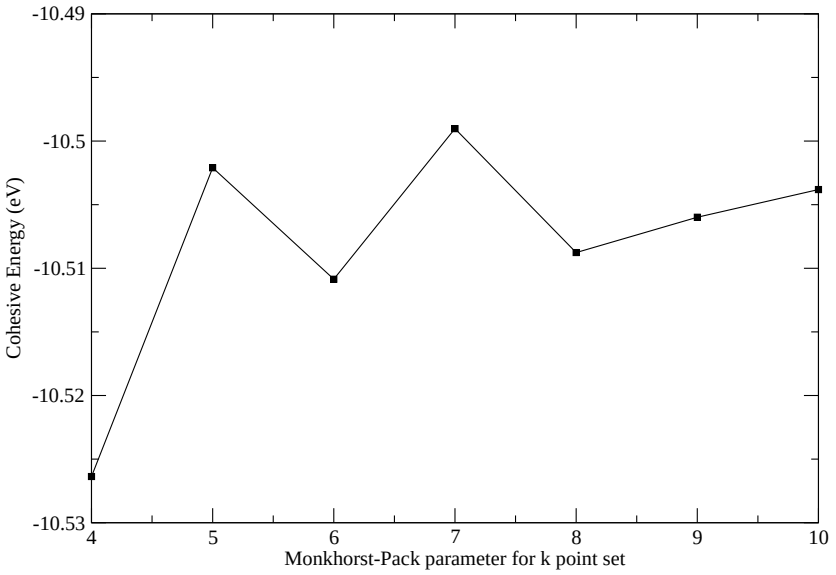

(a) The Monkhorst-Pack parameter for generating special k points

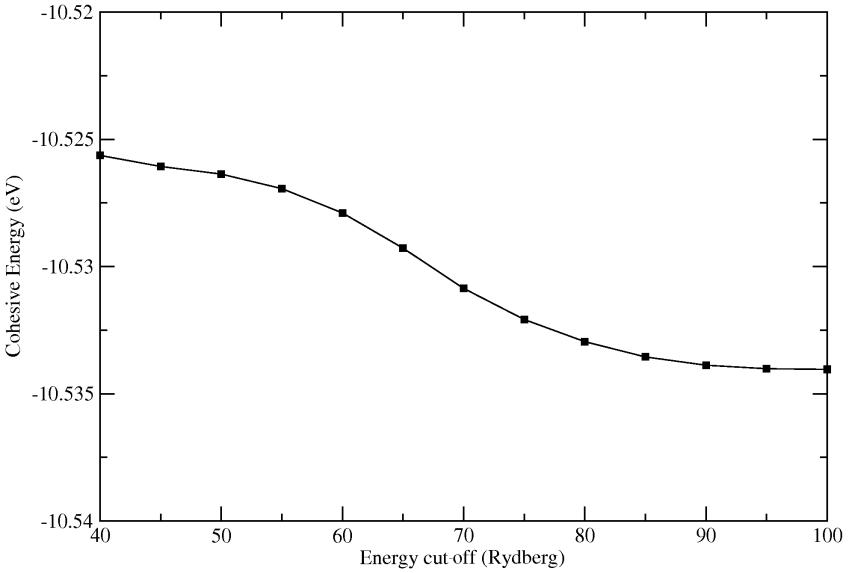

(b) The cut–off energy

Figure 5.16: The convergence of calculated cohesive energies for Tantalum as a function of (a) k points and (b) cut–off energy.

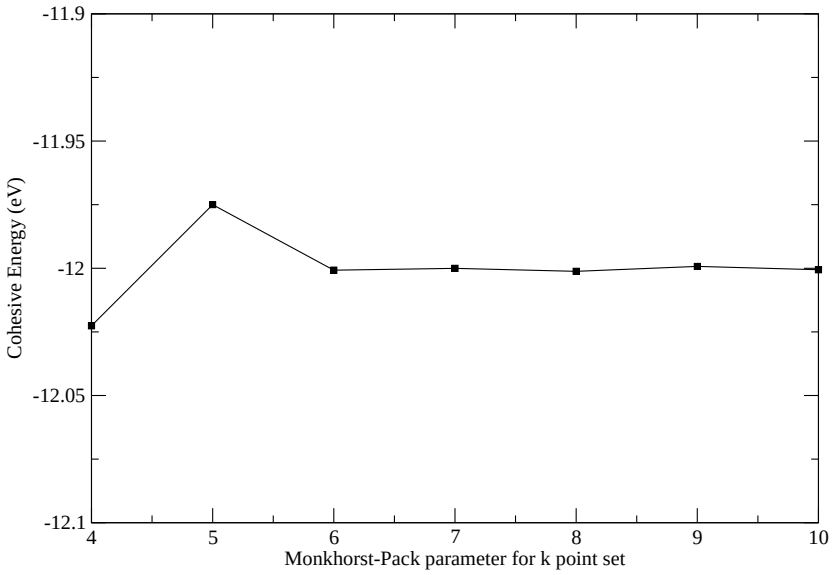

(a) The Monkhorst-Pack parameter for generating special k points

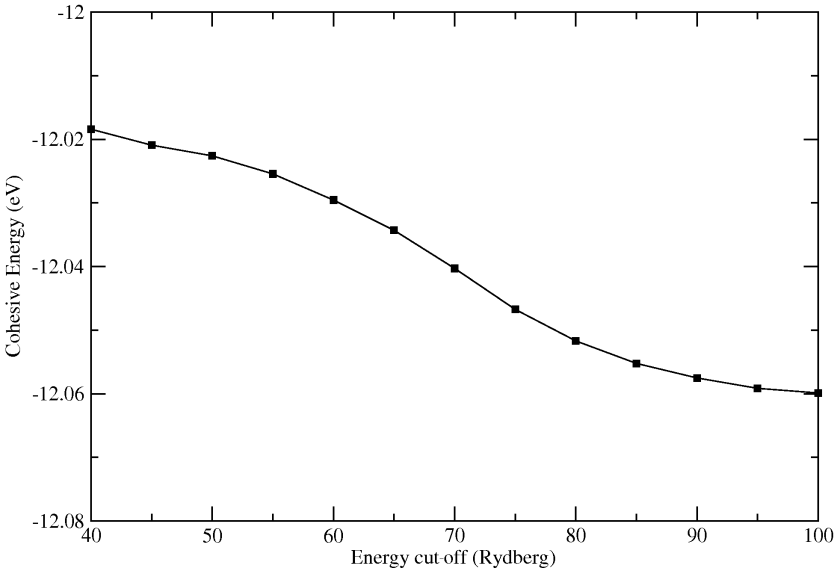

(b) The cut–off energy

Figure 5.17: The convergence of calculated cohesive energies for Tungsten as a function of (a) k points and (b) cut–off energy.

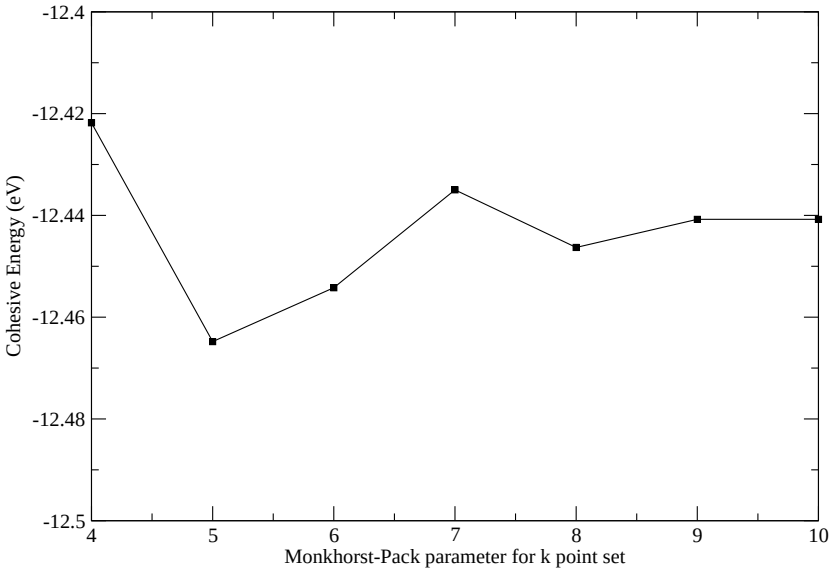

(a) The Monkhorst-Pack parameter for generating special k points

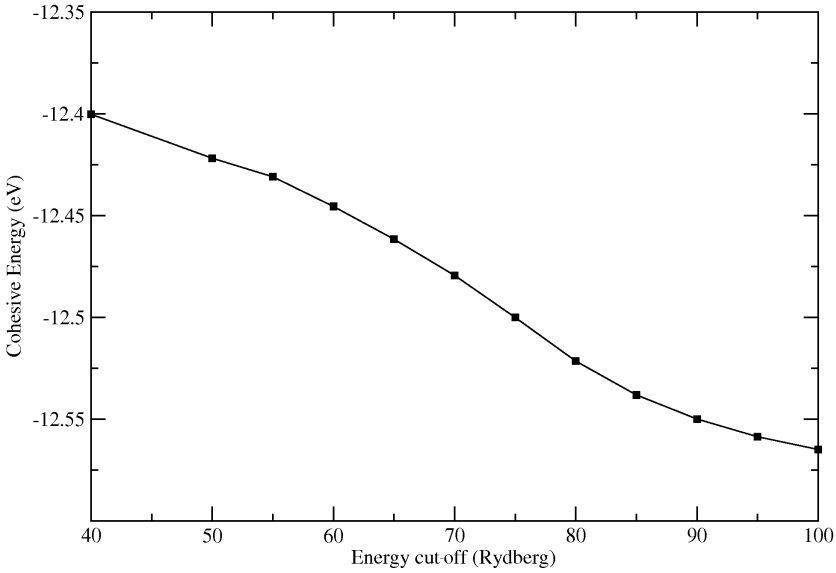

(b) The cut–off energy

Figure 5.18: The convergence of calculated cohesive energies for Rhenium as a function of (a) k points and (b) cut–off energy.

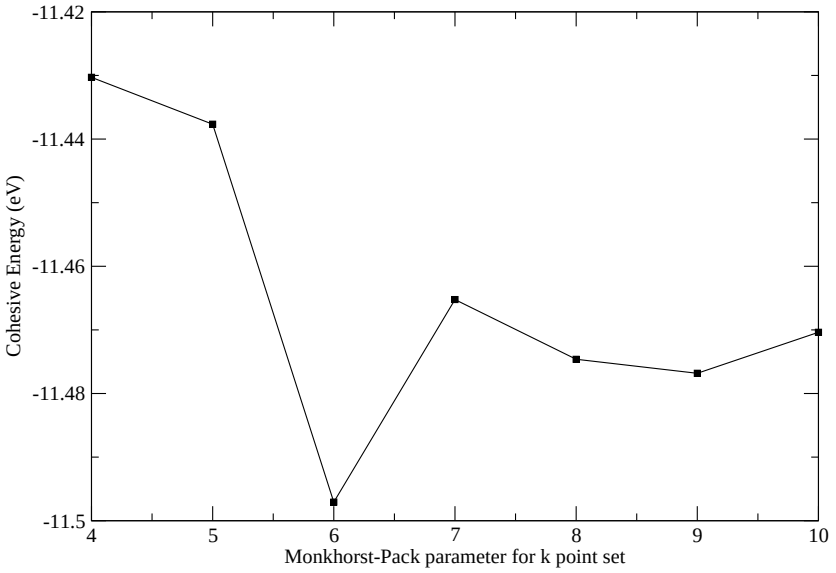

(a) The Monkhorst-Pack parameter for generating special k points

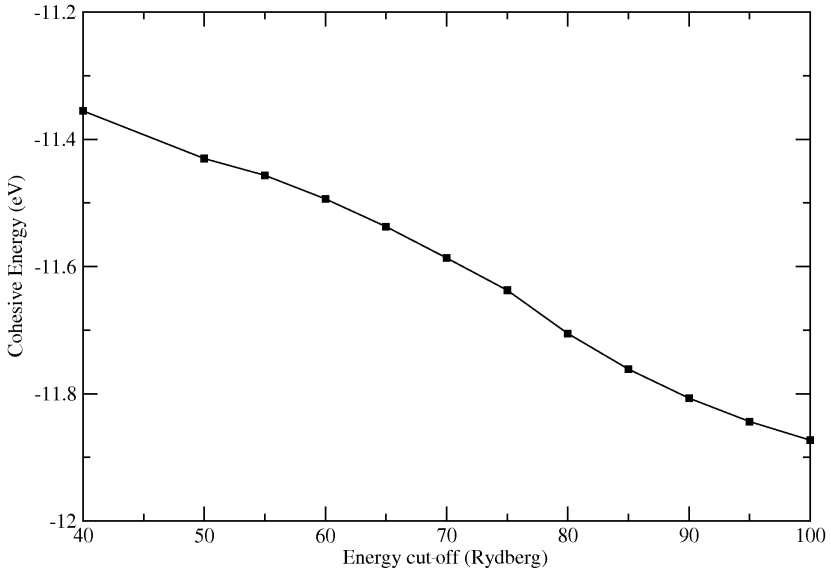

(b) The cut–off energy

Figure 5.19: The convergence of calculated cohesive energies for Osmium as a function of (a) k points and (b) cut–off energy.

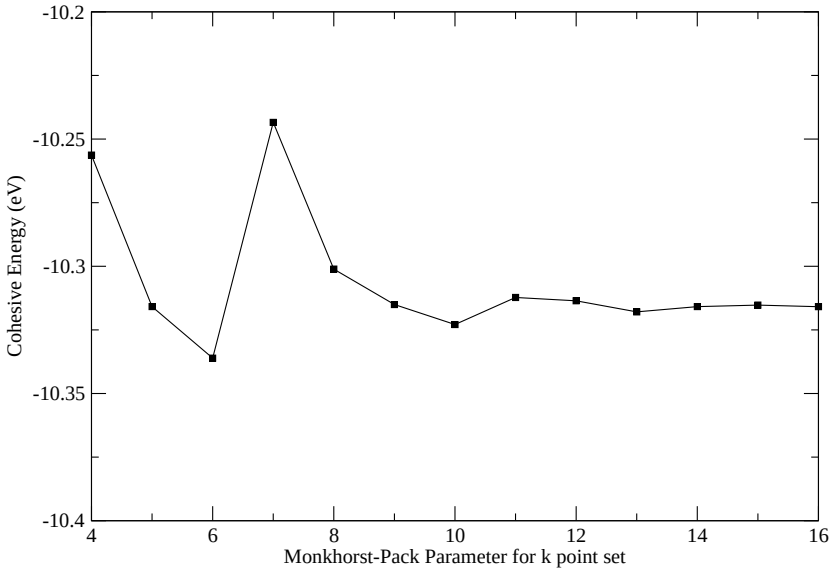

(a) The Monkhorst-Pack parameter for generating special k points

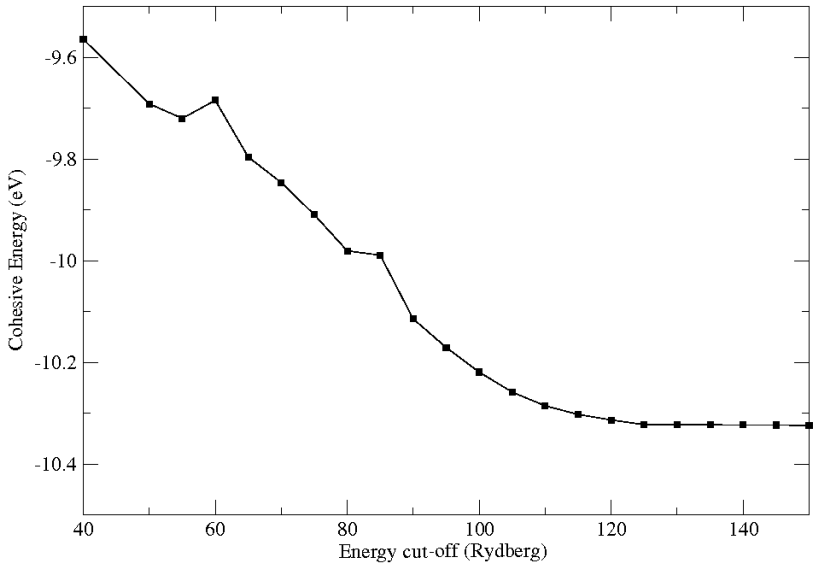

(b) The cut–off energy

Figure 5.20: The convergence of calculated cohesive energies for Iridium as a function of (a) k points and (b) cut–off energy.

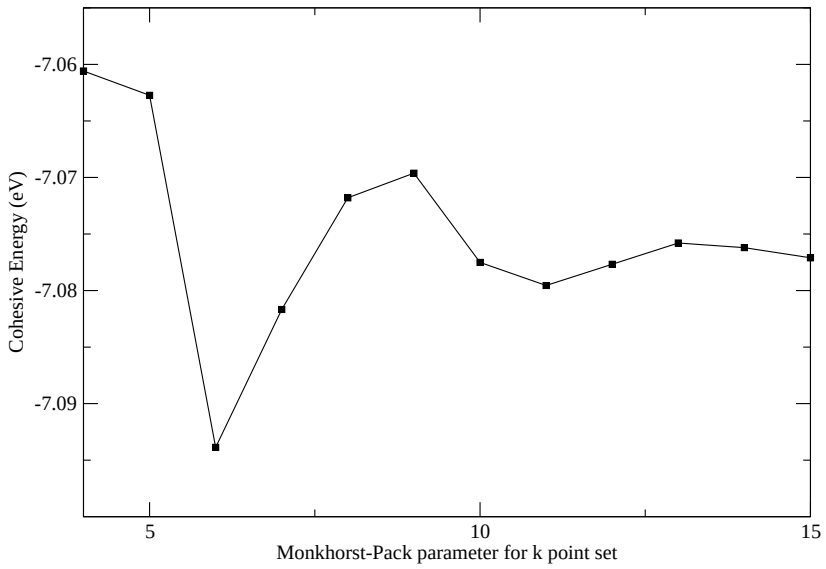

(a) The Monkhorst-Pack parameter for generating special k points

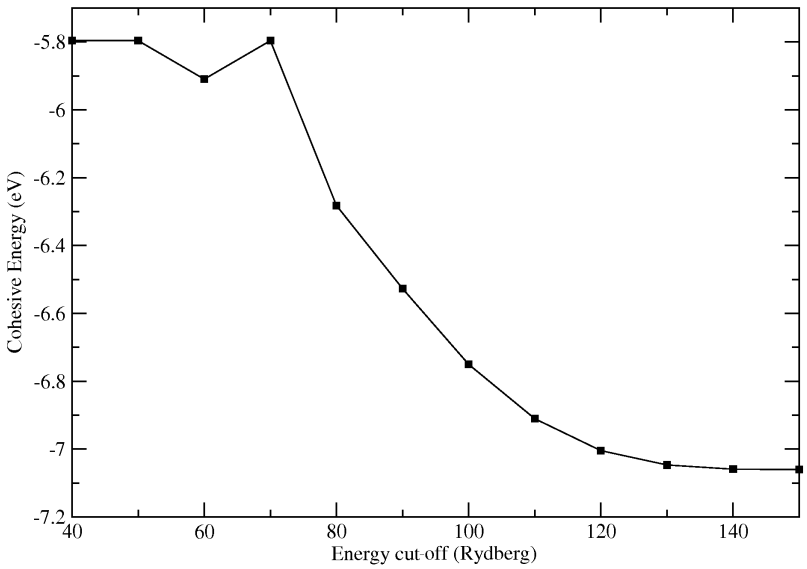

(b) The cut–off energy

Figure 5.21: The convergence of calculated cohesive energies for Platinum as a function of (a) k points and (b) cut–off energy.

5.4 Equation of state

To check the validity of the pseudopotentials generated we refer to both experimental results and to previous all electron calculations. For each of the calculations the angular momentum component $l = 0$ is taken to be the local part. As discussed earlier we have chosen a cut–off energy of 120 Ryd for the plane wave expansion of the wave functions after investigating the convergence of the total energy calculations.

Although only Iridium and Platinum occur in the face–centred cubic structure at standard temperature and pressure we have chosen to perform our calculations for each of the elements in our study in the fcc structure. This is mainly for reasons of consistency between results and so that deviations can be easily compared. For these structures the Brillioun zone sampling has been optimized and Gaussian broadening method [69] for Brillioun zone integration was used.

The equilibrium lattice constant, a_0, is given by the minimum of the total energy, E_{tot}, of the system as a function of the lattice constant a, while the bulk modulus is defined by,

$$B_0 = V_0 \frac{d^2 E_{tot}}{dV^2}\bigg|_{V=V_0}, \tag{5.1}$$

where V is the unit cell–volume, and V_0 is the equilibrium unit–cell volume.

The total energy as a function of volume is obtained by self–consistent total energy calculations. The equilibrium volume, V_0, the bulk modulus at ambient pressure, B_0,

and its first derivative with respect to pressure, B_0', are all estimated by performing a least–squares fit of 10-15 calculated points to the integrated form of the third–order Birch–Murnaghan equation of state [1]

$$E(V) = -\frac{9}{16} B_0 \left[(4 - B_0') \frac{V_0^3}{V^2} - (14 - 3B_0') \frac{V_0^{7/3}}{V^{4/3}} + (16 - 3B_0') \frac{V_0^{5/3}}{V^{2/3}} \right] + E_0. \quad (5.2)$$

The calculated results are shown in Figures 5.22 to 5.28 and the parameters derived from the least–squares fit are listed in Table 5.2 together with other results from the literature.

Our calculated lattice constants for Iridium and Platinum are less than 0.3% greater than the experimental results reported in Ref [5] and the bulk moduli are between 5% and 10% greater than experimental values. In general, LDA calculated bulk moduli typically agree with experimental values to within about 2-5% for transition metals, so differences of order 5% should not be viewed as significant. It is interesting to note that our calculations give lattice constants that are larger than experiment for Ir and Pt. This is unusual as the LDA generally tends to overestimate bond strength and therefore results in slightly small equilibrium lattice constants. This effect could be due to the approximations in the calculations, for example, missing relativistic effects in the scalar relativistic approximation.

In comparison with other calculated results [7] the difference in lattice constant for the $5d$ elements decrease from about 2% smaller for Hf to nearly identical values for Os, Ir and Pt. The difference in bulk moduli on the other hand ranges from about 20% for Hf down to less than 2% for Os and Ir and about 10% for Pt.

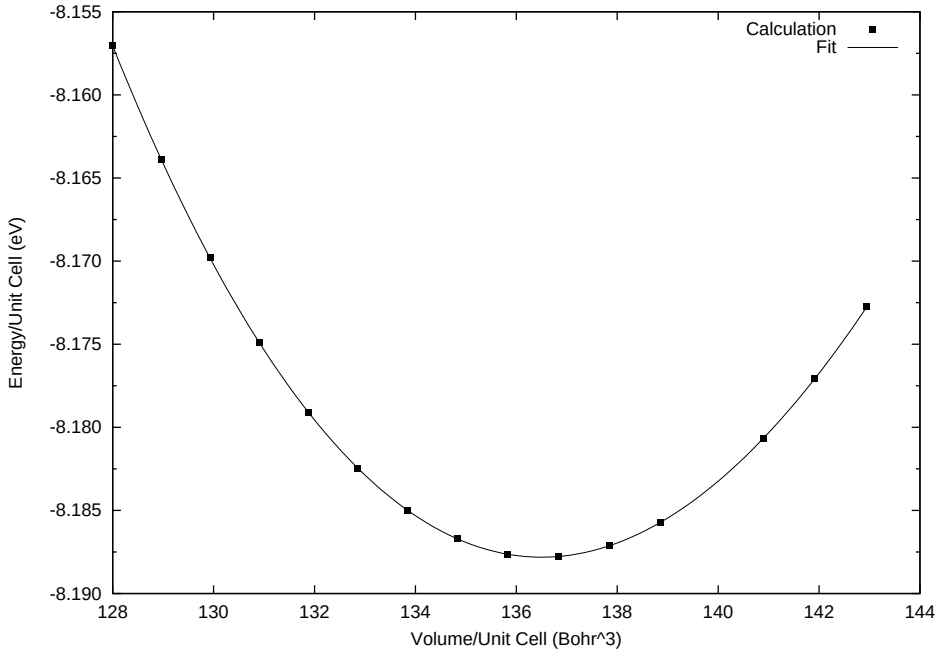

Figure 5.22: Calculated energy versus volume curves for fcc Hafnium. Solid lines are a fit to the third–order Birch-Murnaghan equation of state (5.2).

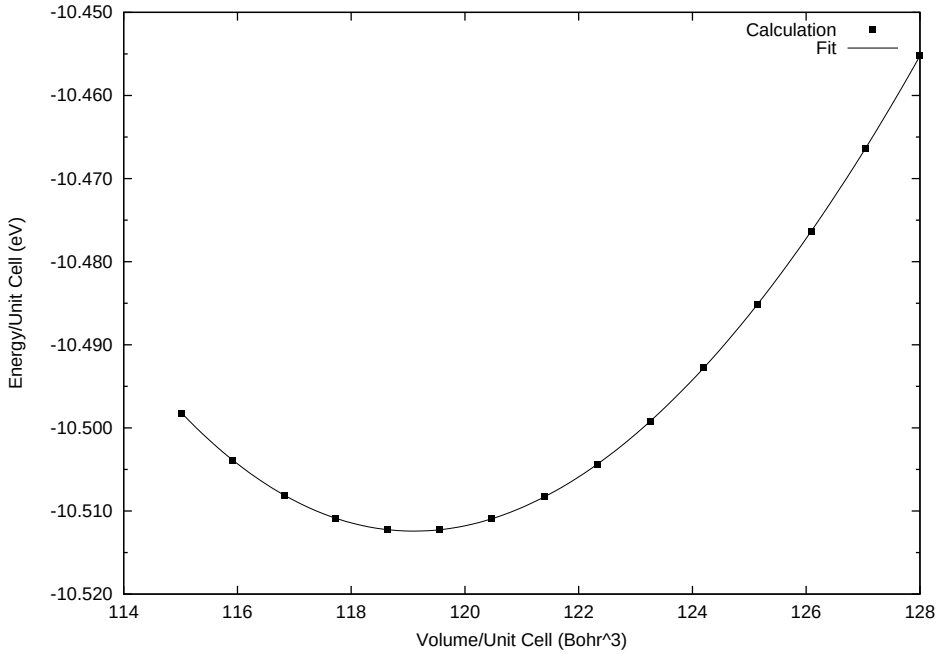

Figure 5.23: Calculated energy versus volume curves for fcc Tantalum. Solid lines are a fit to the third–order Birch-Murnaghan equation of state (5.2).

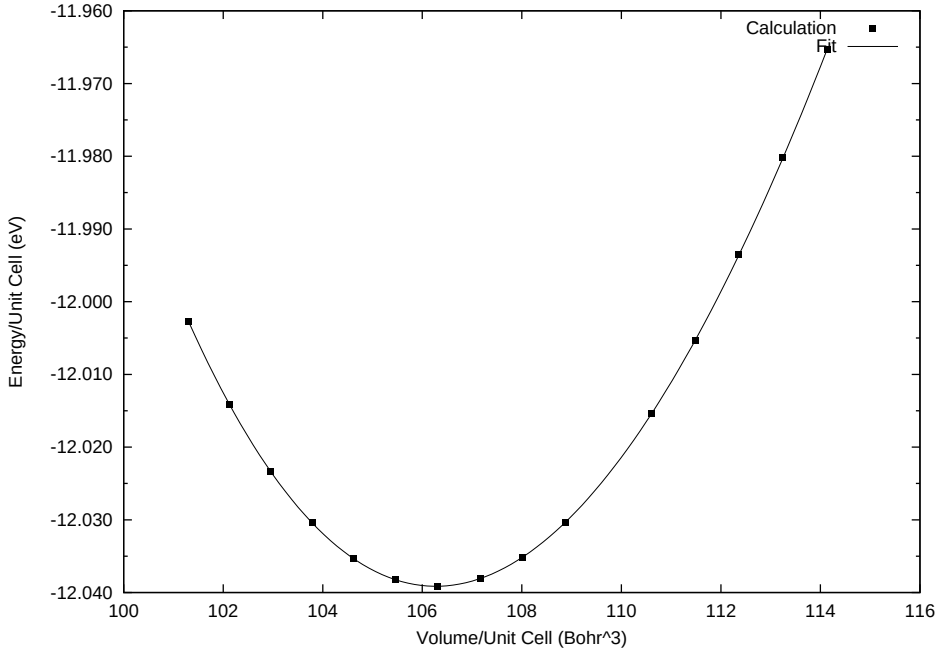

Figure 5.24: Calculated energy versus volume curves for fcc Tungsten. Solid lines are a fit to the third–order Birch-Murnaghan equation of state (5.2).

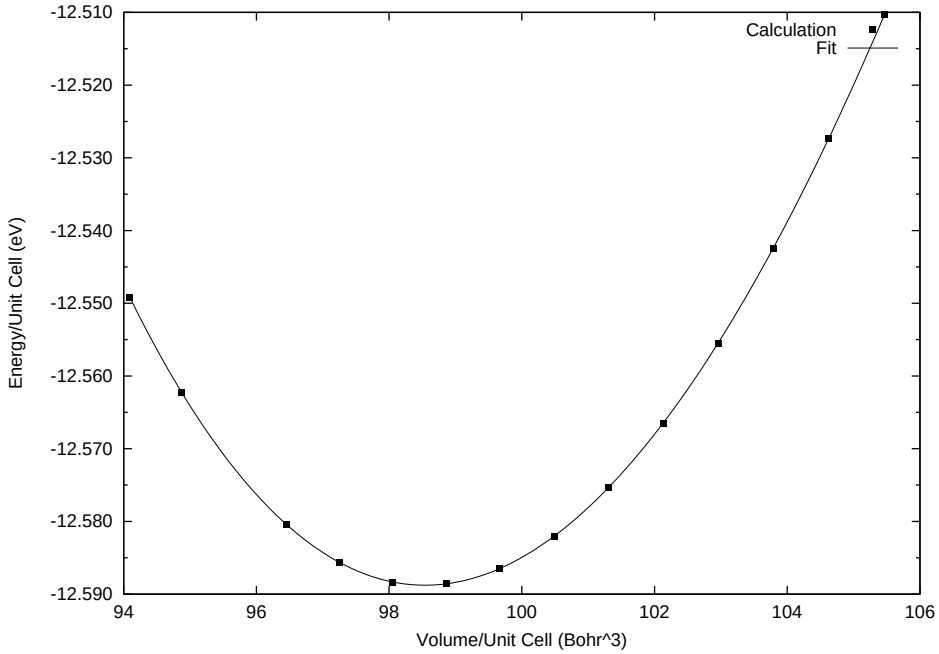

Figure 5.25: Calculated energy versus volume curves for fcc Rhenium. Solid lines are a fit to the third–order Birch-Murnaghan equation of state (5.2).

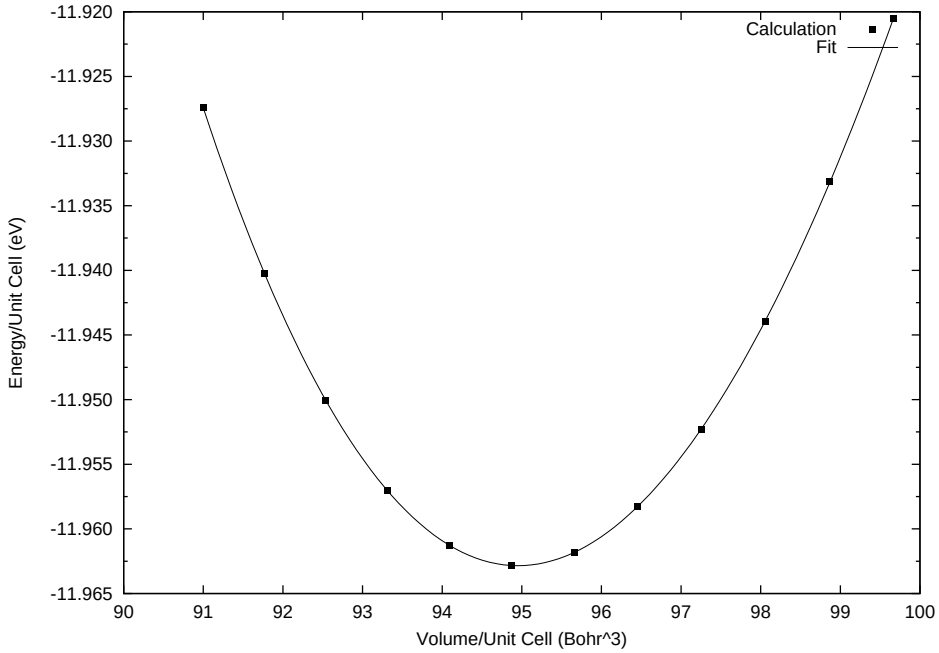

Figure 5.26: Calculated energy versus volume curves for fcc Osmium. Solid lines are a fit to the third–order Birch-Murnaghan equation of state (5.2).

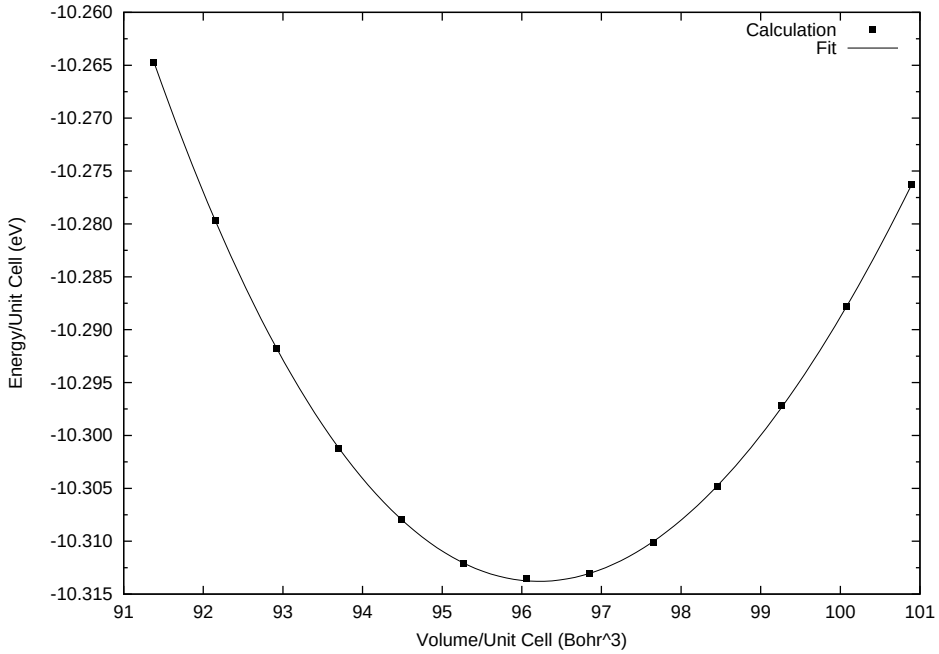

Figure 5.27: Calculated energy versus volume curves for fcc Iridium. Solid lines are a fit to the third–order Birch-Murnaghan equation of state (5.2).

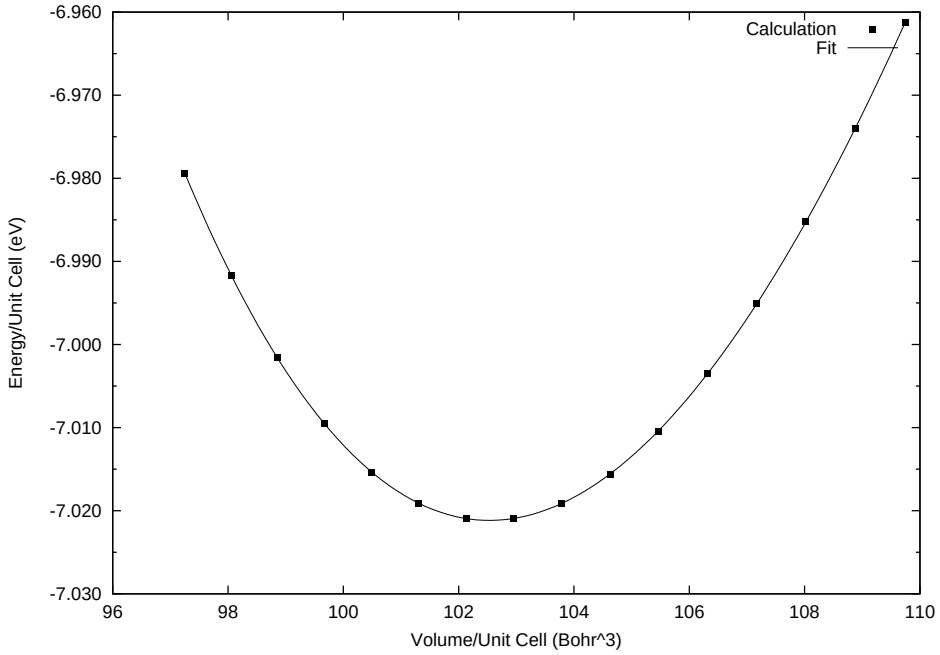

Figure 5.28: Calculated energy versus volume curves for fcc Platinum. Solid lines are a fit to the third–order Birch-Murnaghan equation of state (5.2).

Table 5.2: Calculated and experimental bulk moduli, equilibrium lattice constants and cohesive energies for the $5d$ transition metals. Experimental values are from Ref. [5] and Ref. [6] and the calculated values are from Ref. [7]

	This study			Others			Experimental		
Element	B_0(GPa)	a_0(a.u.)	$E_{coh}(eV)$	B_0(GPa)	a_0(a.u.)	$E_{coh}(eV)$	B_0(GPa)	a_0(a.u.)	$E_{coh}(eV)$
Hf	114	8.17	8.19	143	8.32	1.95	109		
Ta	208	7.81	10.51	248	7.90	4.25			
W	312	7.52	12.04	279	7.60	12.91			
Re	393	7.33	12.59	353	7.37	4.91	365		
Os	429	7.24	11.96	433	7.24	11.74	410		
Ir	393	7.27	10.31	385	7.27	10.23	355	7.26	6.94
Pt	296	7.43	7.02	333	7.43	7.53	283	7.41	5.84

5.5 Cohesive energy

The cohesive energy of a solid is the energy that is required to separate an atom of a certain species from a solid of that species. Cohesive energies are obtained from total–energy calculations as the difference between average energy of the atoms of the bulk solid and the energy of the free atom:

$$E_{coh} = E_{atom} - E_{solid}. \tag{5.3}$$

Our results for the cohesive energy for Iridium and Platinum show the expected overbinding for the LDA when compared to experiment. Experimental results were not available for the other $5d$ elements in the fcc structure. When compared with other LDA calculations however, our results were fairly consistent for the heavier atoms with deviations from the published results becoming extremely large for Hafnium and Tantalum.

5.6 Discussion

The local density approximation has a tendency to overbind bulk systems, i.e. bond strength is overestimated leading to an underestimation of lattice constants and a corresponding overestimation of bulk moduli and cohesive energies. In the systems under consideration there is clear evidence of this overbinding. The lattice constants were in general smaller than other published results except in the cases of Iridium and Platinum in which they were very close to accepted experimental values. The bulk moduli were overestimated in comparison to experimental results in all of the

cases where experimental data was available. The cohesive energies too were overestimated, with the calculated cohesive energy for Iridium being about 50% larger than experiment.

Chapter 6

Including the f component in pseudopotential calculations for the $5d$ transition metals

By definition, all electron calculations describe every atom of an electronic system in order to derive properties of that system. This technique is obviously computationally very expensive but results in accurate results. In an attempt to perform calculations on more complex atoms such as the heavy $5d$ transition atoms the pseudopotential approach treats many of the core electrons as chemically inert in order to simplify the calculation. Generally, this involves treating only the highest s, p, and d orbitals as the valence states and performing calculations to accurately describe them.

Most *ab initio* total–energy pseudopotential calculations assume the behaviour

of the $l = 3$ component of the pseudopotential to be very similar to that of the $l = 0$ component. Therefore calculations to accurately describe the nature of the f component are often neglected. There are several reasons for this:
In most of the $5d$ transition metals the $5f$ orbitals are unbound in the ground state configuration and so are difficult to describe. The $4f$ on the other hand are usually highly localized which makes them difficult to describe accurately using the LDA. Another compelling reason to neglect the f orbitals is the obvious increase in computational demand due to the inclusion of an additional angular momentum component.

The inclusion of the f component has the capability to cause deviations when compared to results obtained in its absence. These deviations, particularly in the $5d$ metals, may greatly affect the nature and behaviour of the atoms being observed. In order to investigate this we have performed calculations on a range of $5d$ transition metals excluding the f component (presented in the previous chapter) and then performed the same range of calculations, this time including the $5f$ component in our pseudopotential generation.

The $5f$ orbitals which we shall be including are unoccupied in the ground state. In order to construct a pseudopotential for these unbound f orbitals we utilize Hamann's procedure for unbound states [70]. Hamann showed that it was not necessary to calculate the pseudopotential for the corresponding bound state and transfer it to a new electronic configuration as had been done previously. He constructed the

pseudopotential using an unbound wave function that has been normalized within a normalization radius and showed that it produced similarly accurate results.

Figures 6.1 to 6.14 illustrate the all–electron and pseudo–wavefunction for each of the elements and the corresponding pseudopotentials that have been generated. One can see that although the unbound wavefunctions are well described, the pseudopotentials required to do so are very deep and will therefore require a large amount of computational resources to utilize. The cut–off radii required to generate these pseudopotentials accurately were also quite small, typically between 0.50 and 1.00 Bohr radii, which is also not ideal for a plane wave expansion as larger cut–off radii are preferable to produce smoother functions.

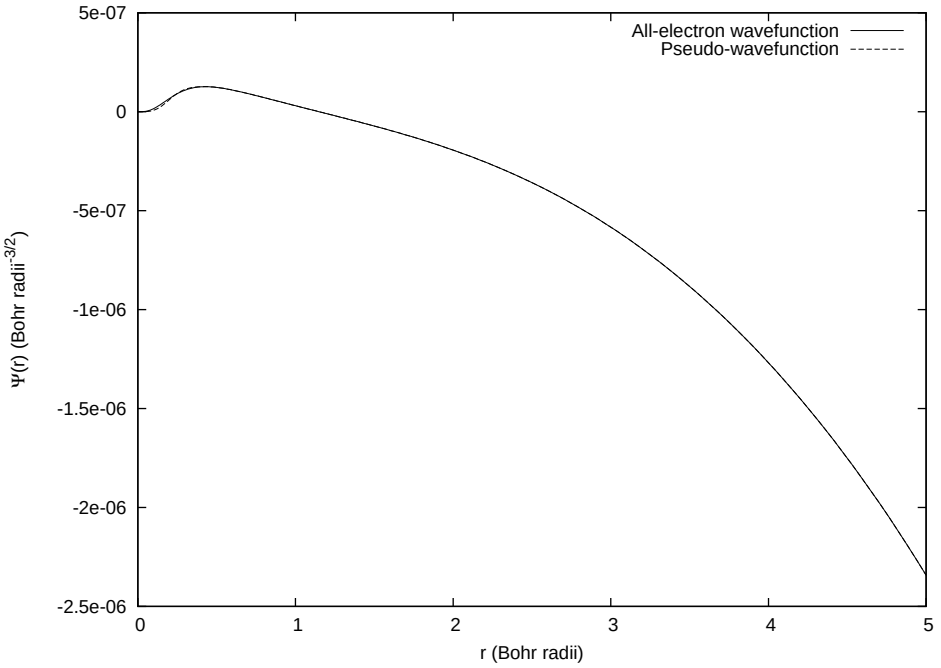

Figure 6.1: The all–electron and pseudo–wavefunctions for the Hafnium $5f$ orbital.

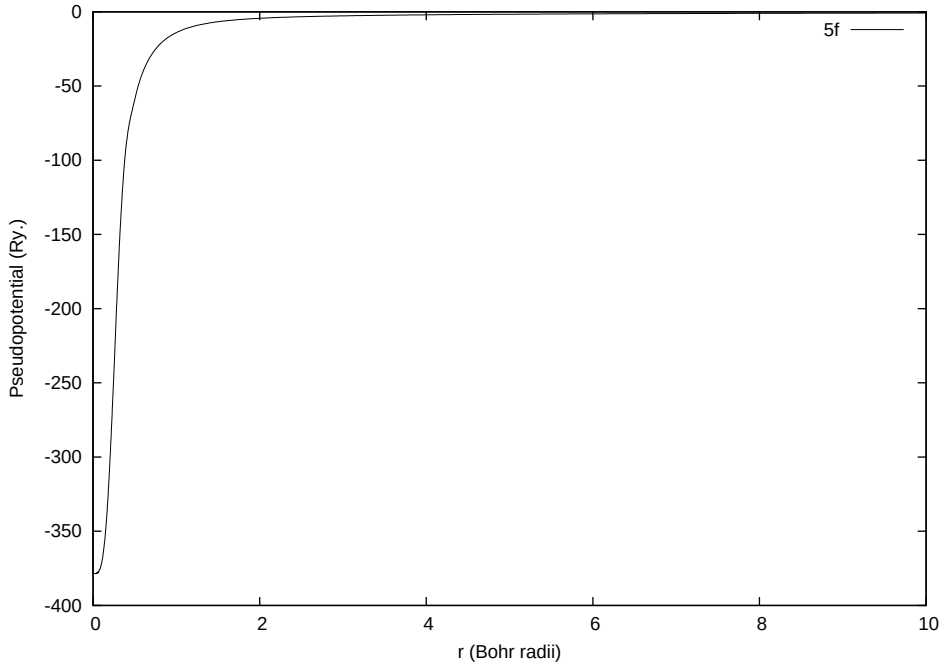

Figure 6.2: The pseudopotential for the $5f$ angular momentum component for Hafnium.

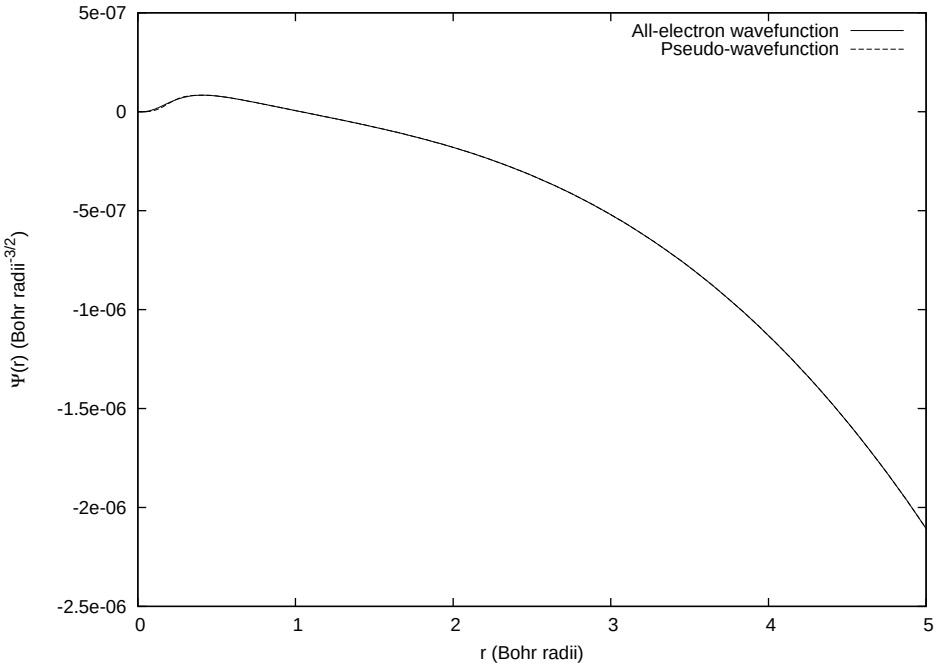

Figure 6.3: The all–electron and pseudo–wavefunctions for the Tantalum $5f$ orbital.

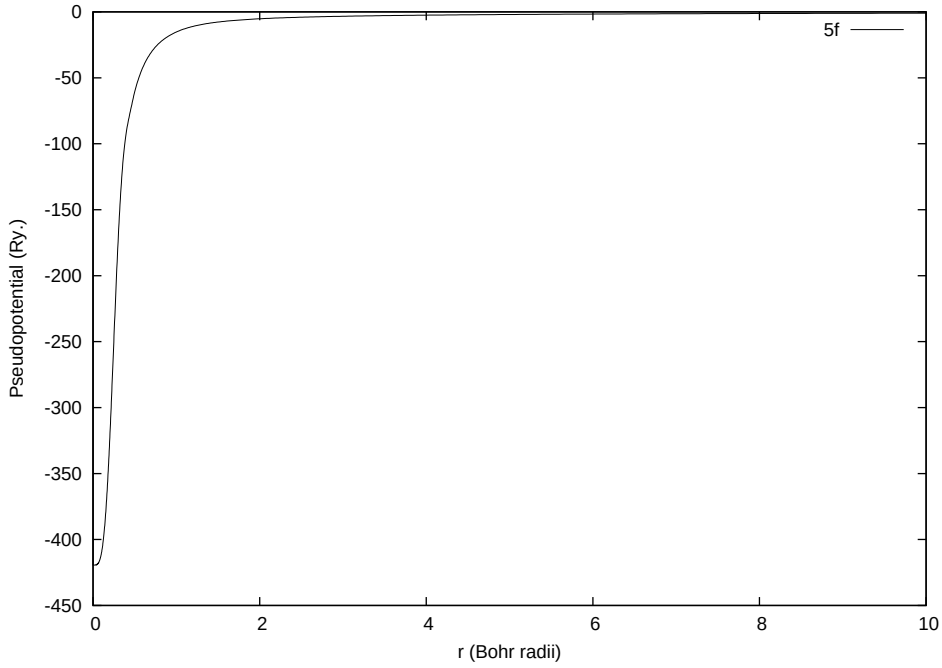

Figure 6.4: The pseudopotential for the $5f$ angular momentum component for Tantalum.

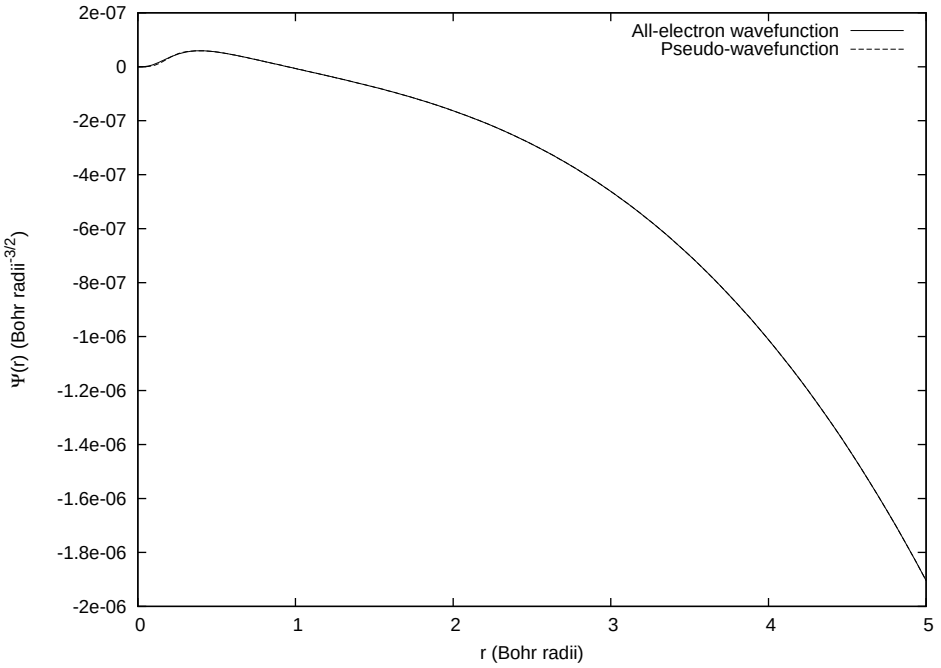

Figure 6.5: The all–electron and pseudo–wavefunctions for the Tungsten $5f$ orbital.

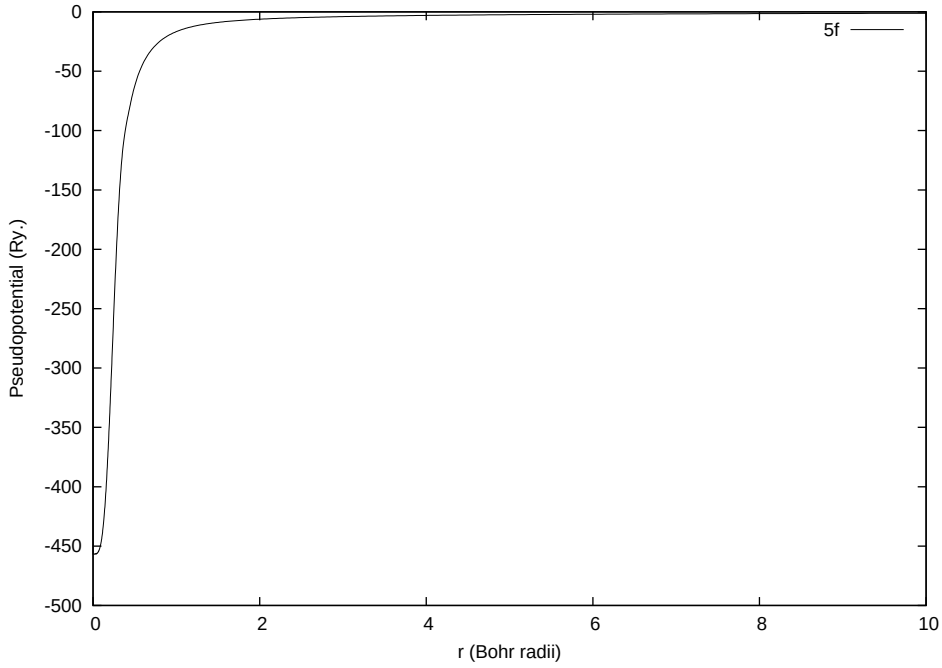

Figure 6.6: The pseudopotential for the $5f$ angular momentum component for Tungsten.

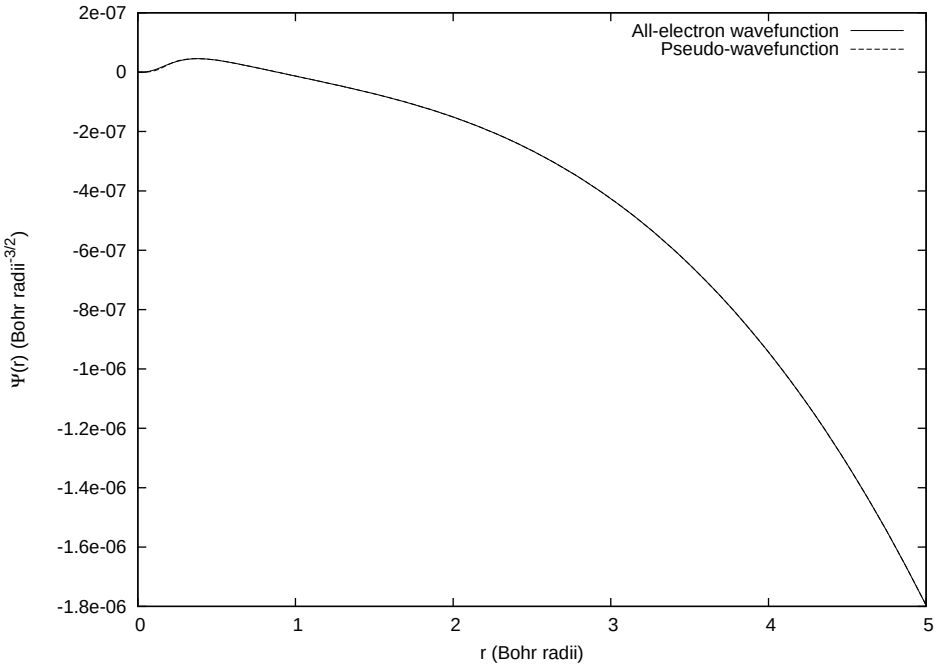

Figure 6.7: The all–electron and pseudo–wavefunctions for the Rhenium $5f$ orbital.

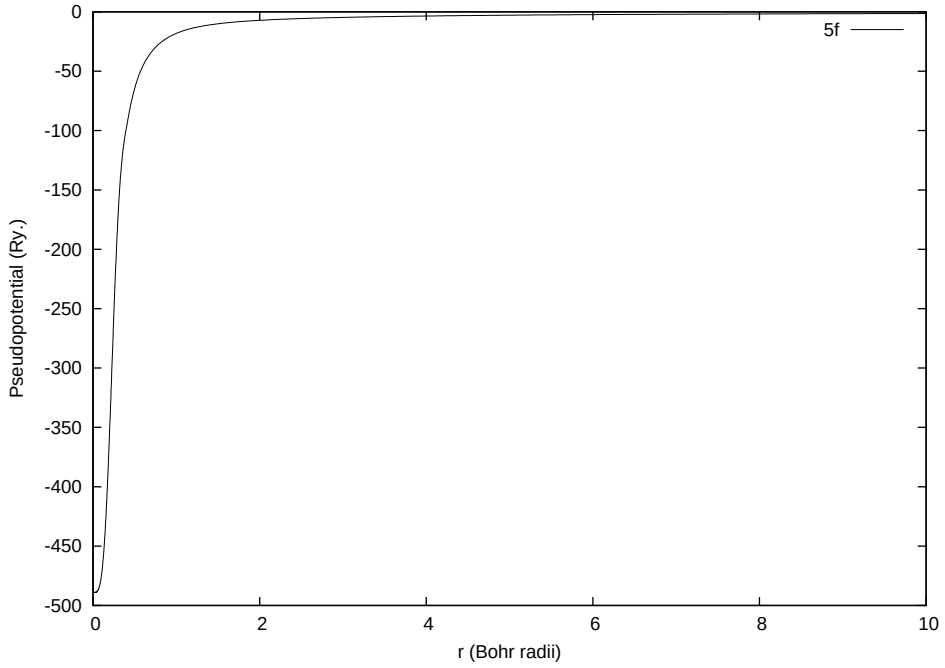

Figure 6.8: The pseudopotential for the $5f$ angular momentum component for Rhenium.

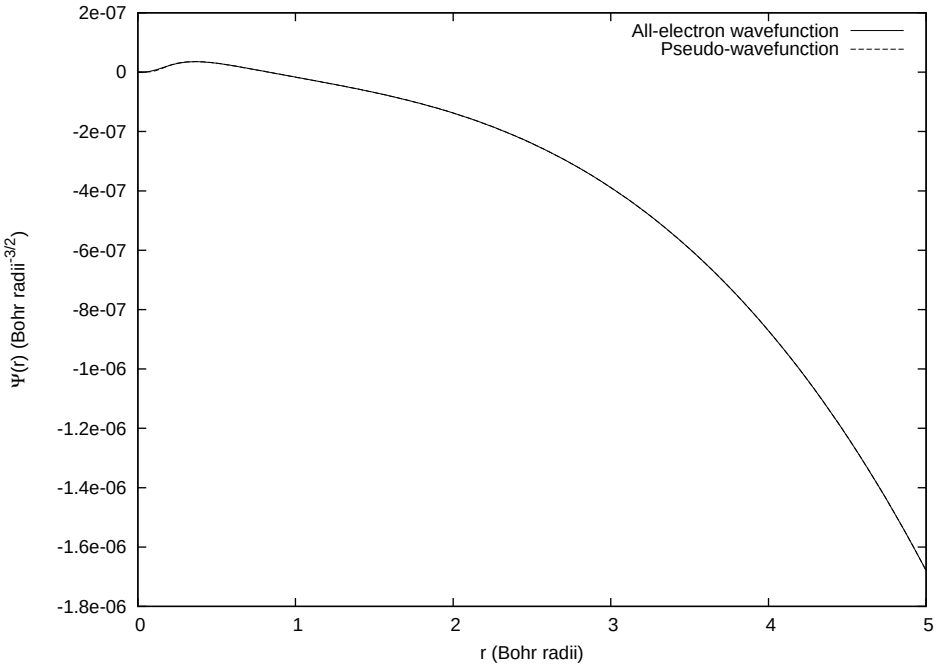

Figure 6.9: The all–electron and pseudo–wavefunctions for the Osmium $5f$ orbital.

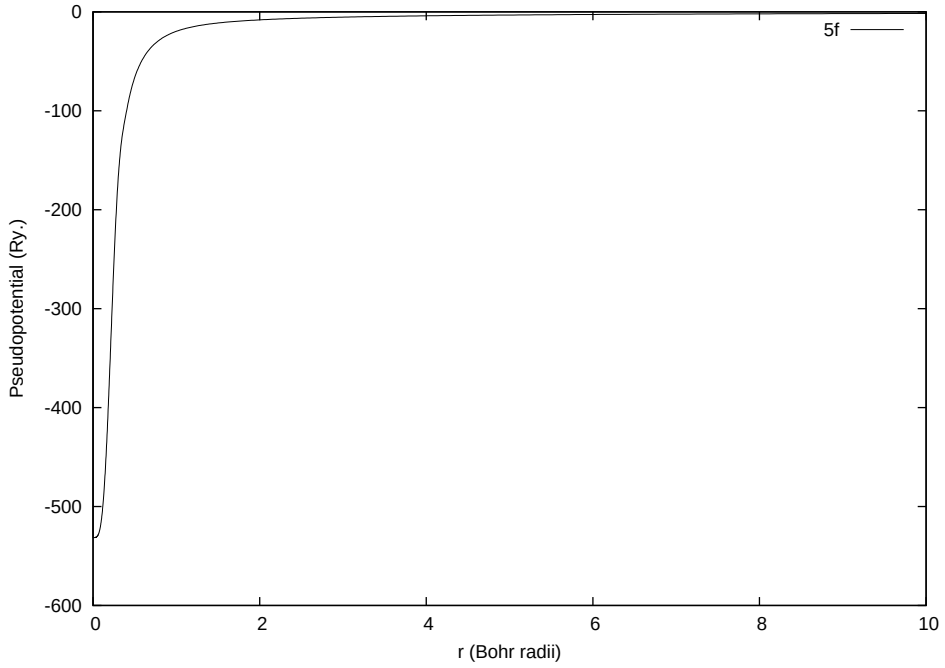

Figure 6.10: The pseudopotential for the $5f$ angular momentum component for Osmium.

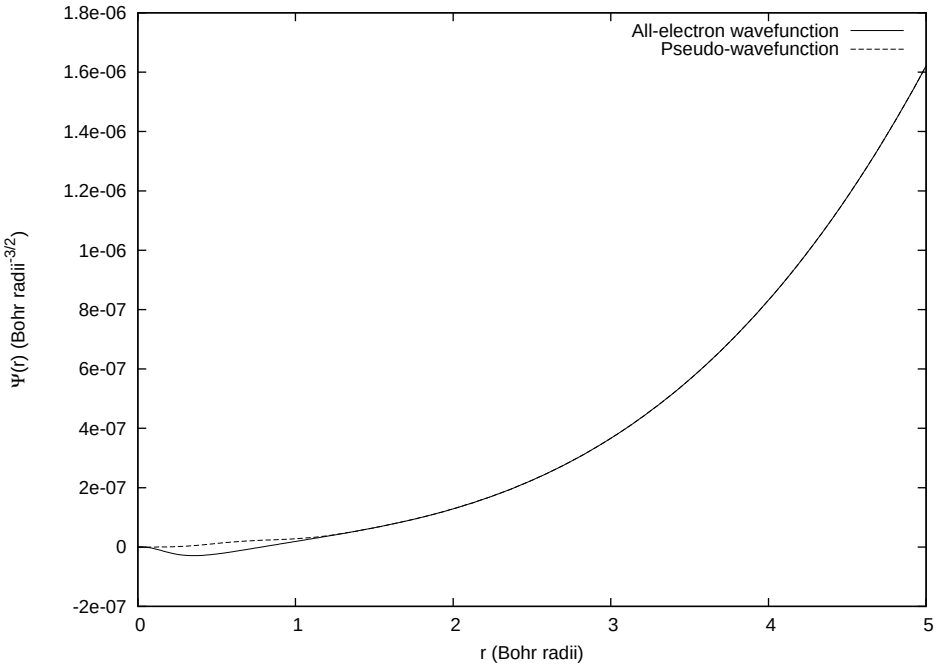

Figure 6.11: The all–electron and pseudo–wavefunctions for the Iridium $5f$ orbital.

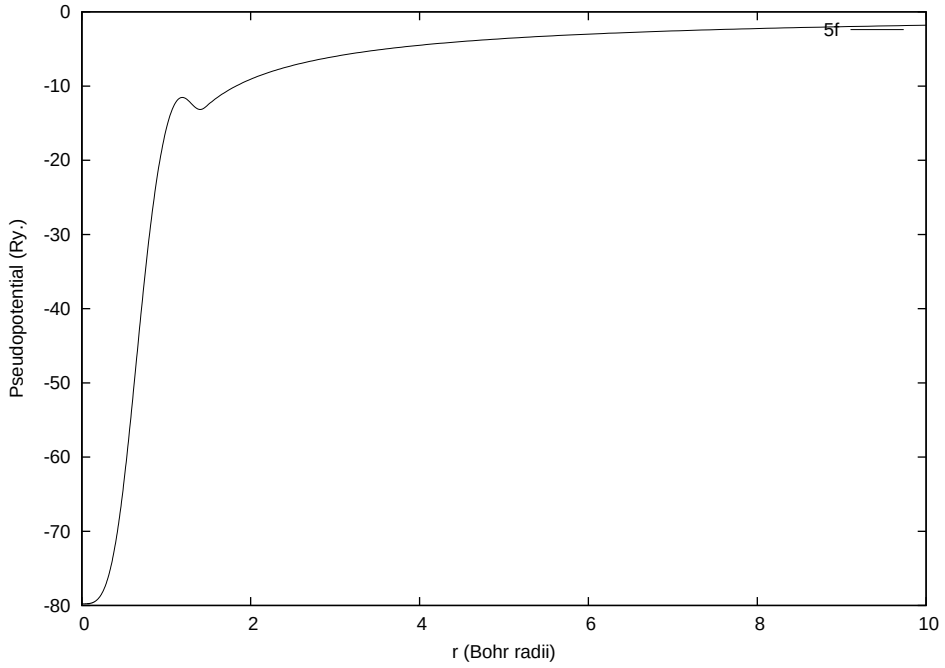

Figure 6.12: The pseudopotential for the $5f$ angular momentum component for Iridium.

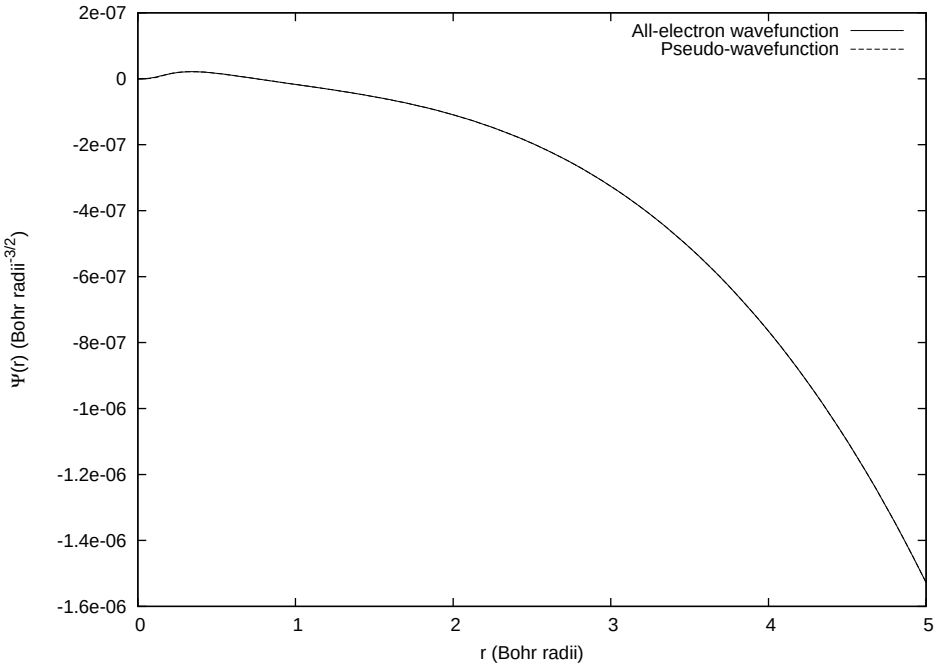

Figure 6.13: The all–electron and pseudo–wavefunctions for the Platinum $5f$ orbital.

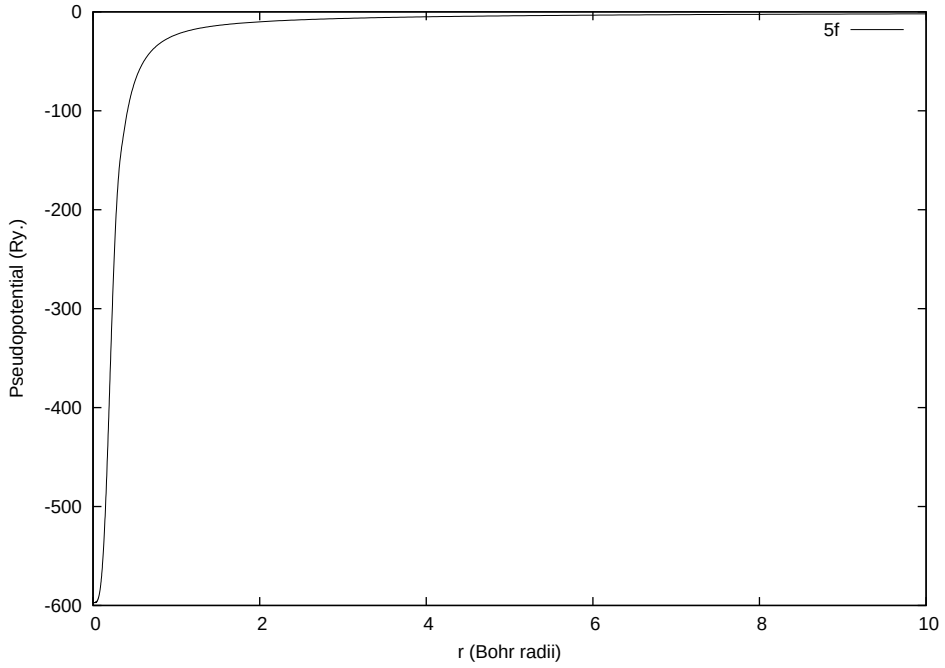

Figure 6.14: The pseudopotential for the $5f$ angular momentum component for Platinum.

6.1 Equation of state

Once again we have utilized the Birch-Murnaghan equation of state (5.2) to obtain the bulk modulus, lattice constant and cohesive energies for each of the $5d$ transition atoms. We have compared them to our previous results from calculations which did not include the f component of the pseudopotential. These results are shown in Table 6.1. Illustrated in Figures 6.15 to 6.21 are the energy versus equilibrium volume plots both including and excluding the $5f$ component.

We observe a clear trend from the energy plots in that the energy per unit cell is decreased by the inclusion of the f component and the energy minimum shifts to a slightly smaller volume per unit cell. Therefore we observe a decrease in lattice constants across the range of atoms. In all cases however the change is small enough to be considered almost negligible, with a maximum decrease of around 0.01 Bohr, which corresponds to a difference of less than one percent. For Iridium and Platinum however, although small, the changes do result in lattice constants which are slightly closer to experimental results than previous calculations.

The changes in the calculated bulk moduli are again small, typically less than 1%. Since errors in bulk moduli of order 5-10% are common and considered acceptable in LDA calculations, changes of less than a percent could essentially be considered negligible. The cohesive energies too have increased by less than one percent.

Table 6.1: Calculated bulk moduli, equilibrium lattice constants and cohesive energies for the 5d transition metals excluding and including the f component.

	Without f			With f		
Element	B_0(GPa)	a_0(a.u.)	$E_{coh}(eV)$	B_0(GPa)	a_0(a.u.)	$E_{coh}(eV)$
Hf	114	8.17	8.19	114	8.17	8.21
Ta	208	7.81	10.51	208	7.80	10.53
W	312	7.52	12.04	311	7.51	12.07
Re	393	7.33	12.59	393	7.32	12.63
Os	429	7.24	11.96	432	7.23	12.02
Ir	393	7.27	10.31	392	7.26	10.37
Pt	296	7.43	7.02	300	7.42	7.06

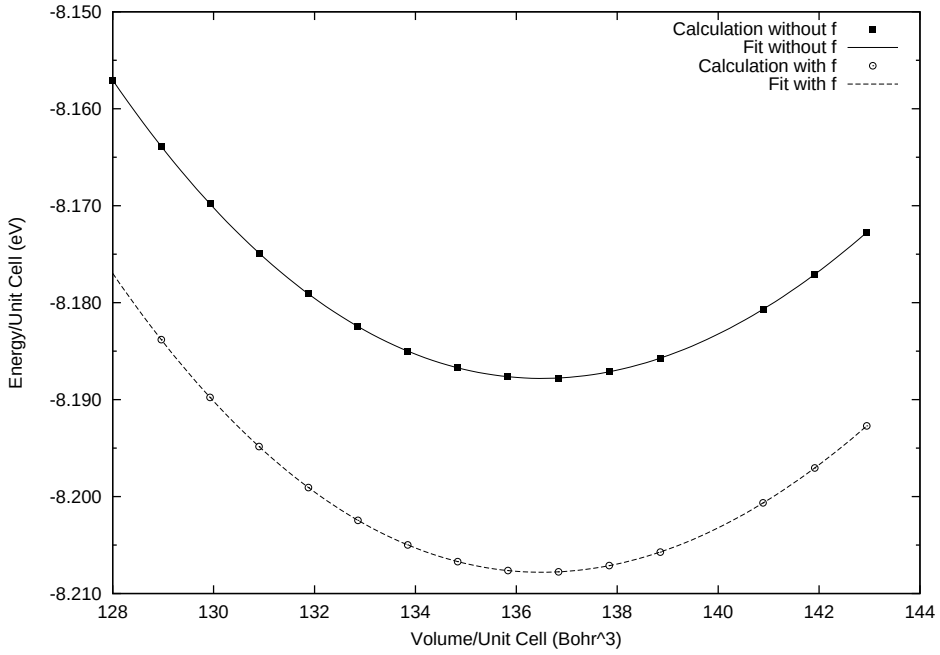

Figure 6.15: Energy versus volume curves for fcc Hafnium calculated with and without the $5f$ component.

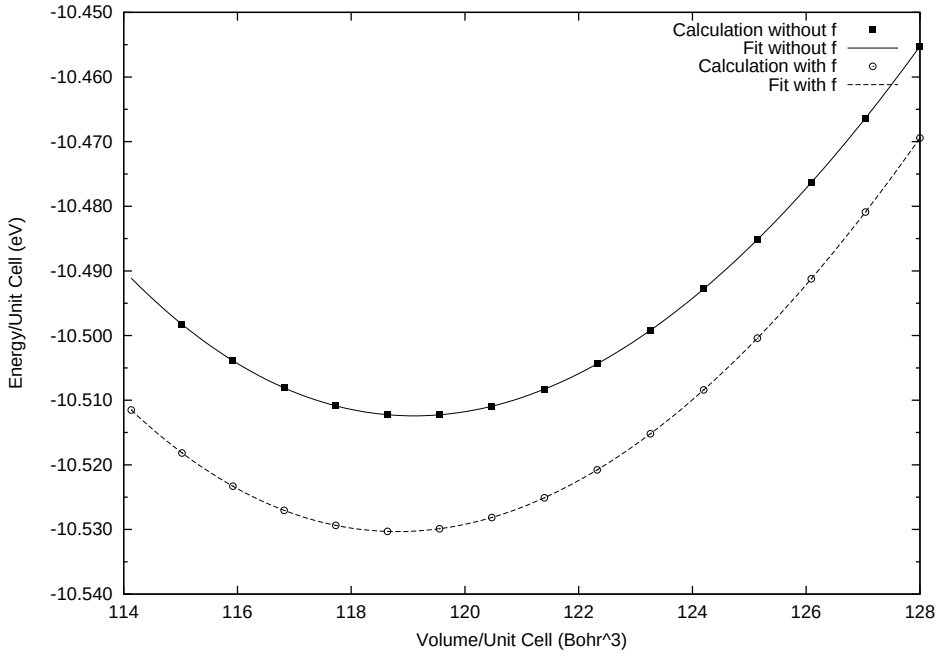

Figure 6.16: Energy versus volume curves for fcc Tantalum calculated with and without the $5f$ component.

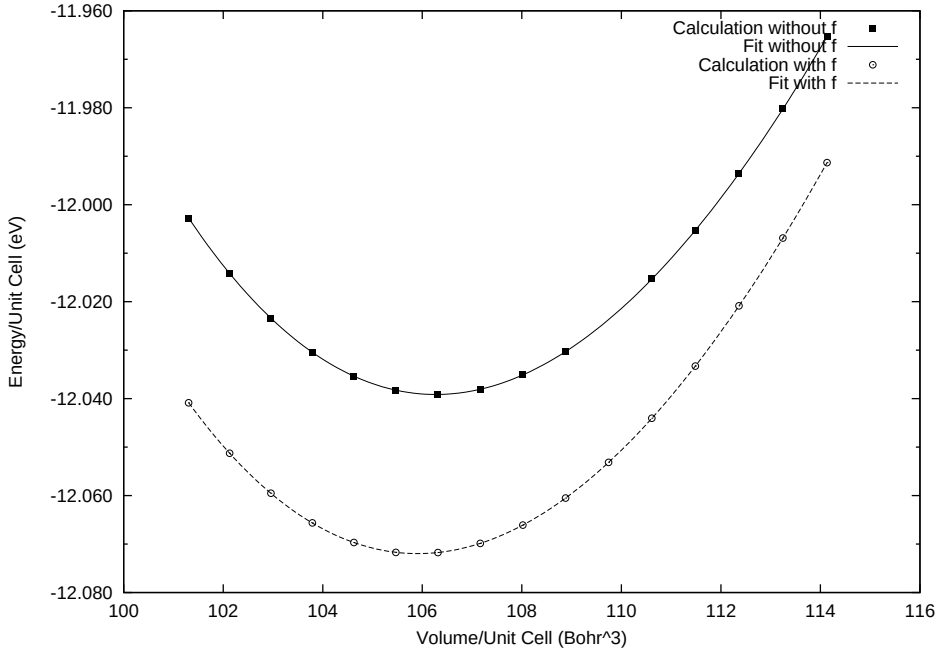

Figure 6.17: Energy versus volume curves for fcc Tungsten calculated with and without the $5f$ component.

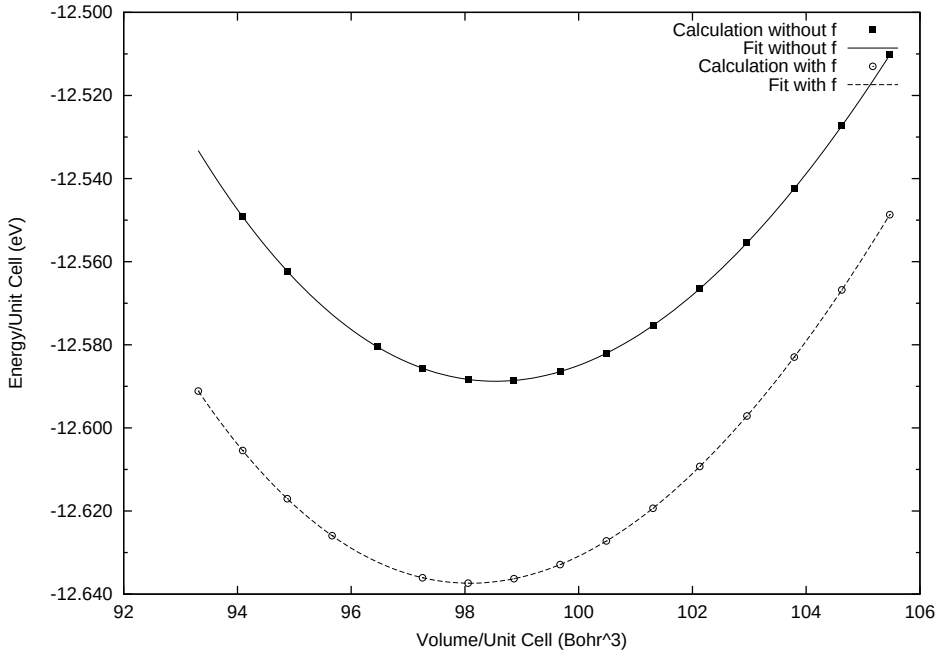

Figure 6.18: Energy versus volume curves for fcc Rhenium calculated with and without the $5f$ component.

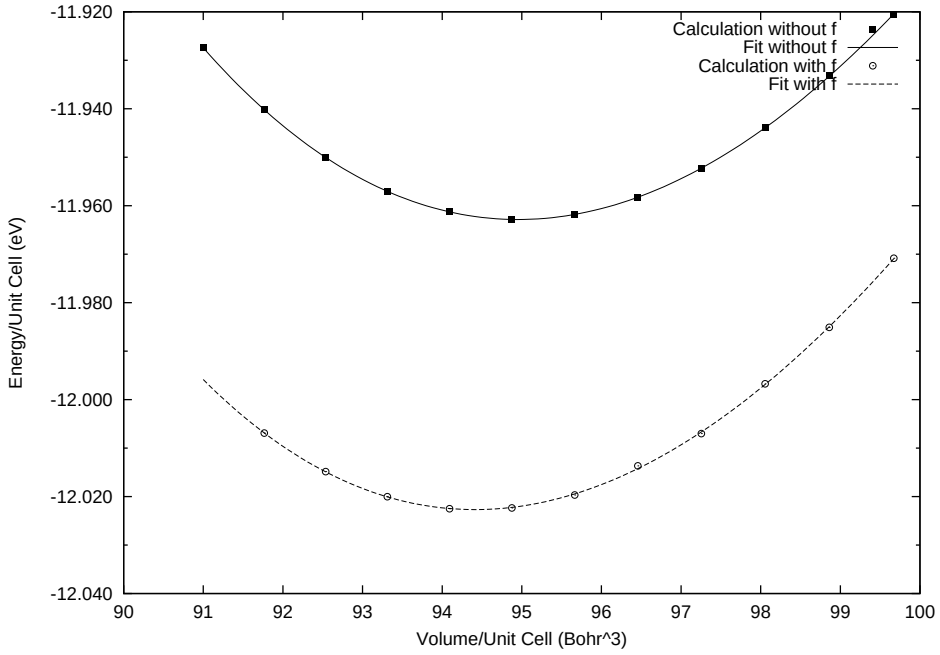

Figure 6.19: Energy versus volume curves for fcc Osmium calculated with and without the $5f$ component.

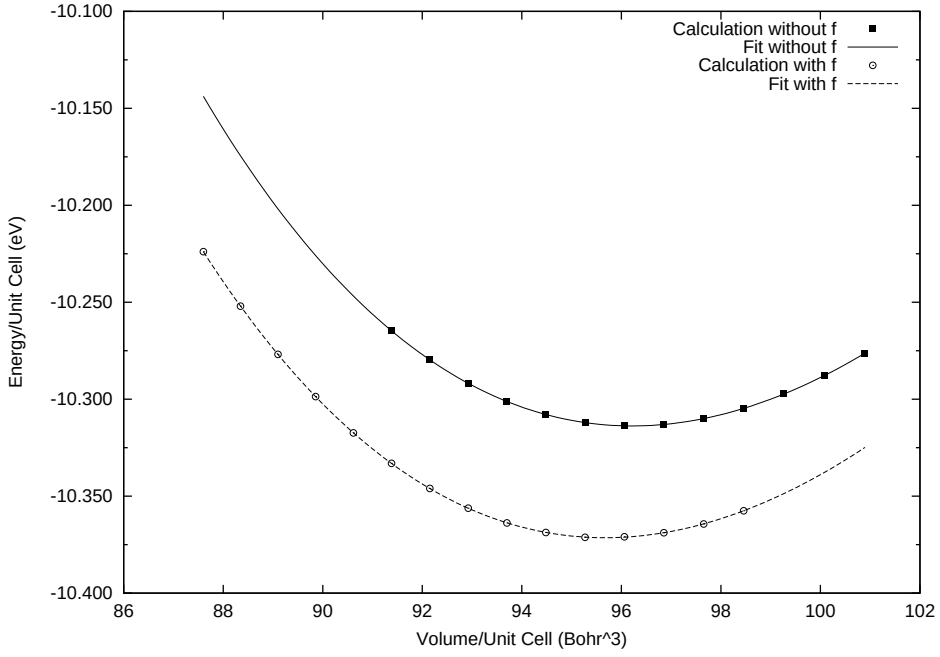

Figure 6.20: Energy versus volume curves for fcc Iridium calculated with and without the $5f$ component.

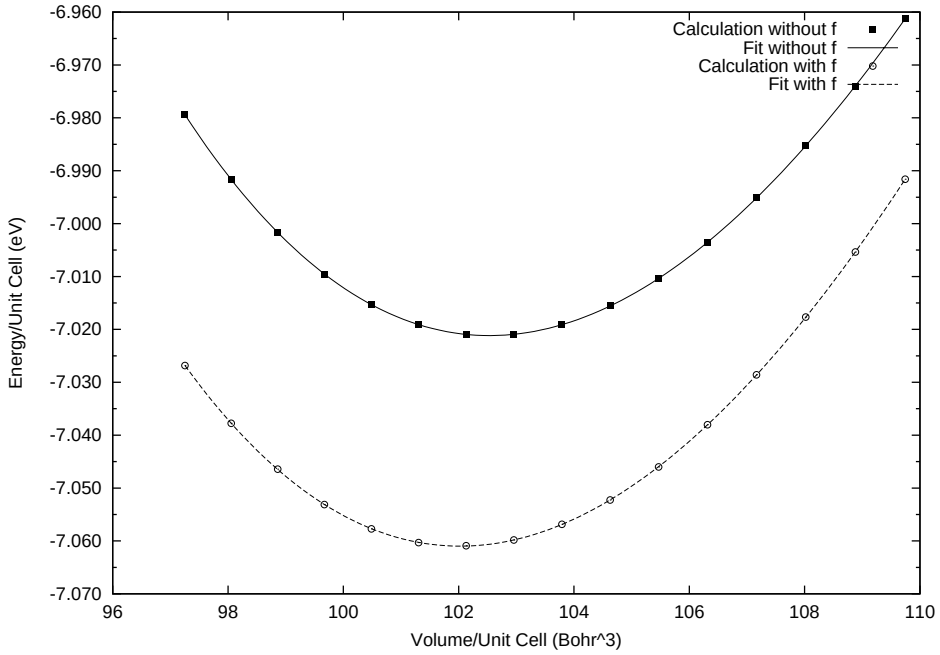

Figure 6.21: Energy versus volume curves for fcc Platinum calculated with and without the $5f$ component.

6.2 Electronic structure

In this section we give a brief description of the changes appearing in electronic structure of the bulk solid due to the inclusion of the $5f$ pseudopotential component. We restrict ourselves to the presentation of the electronic structure of Iridium which shows very similar effects to that of Platinum.

We calculated the electronic band structure and the Fermi level of Iridium at the experimental value for the lattice constant (7.26 a.u.). It is preferable to use experimental values in this case in order to be able to compare our results with both experimental results and other calculations performed at these values. Although, in the case of Iridium, our calculated lattice constant is very similar to that of experiment and would not have resulted in significant deviations. To obtain a self–consistent charge density at the experimental value of the lattice constant, 90 special $\mathbf{k}$ points are used for the integration over the irreducible part of the Brillouin zone.

Figure 6.22 shows the resulting band structure along the high symmetry lines of the irreducible part of the first Brillouin zone plotted for the case including the $5f$ component of the pseudopotential (in dotted lines) and for the case excluding it (solid lines).

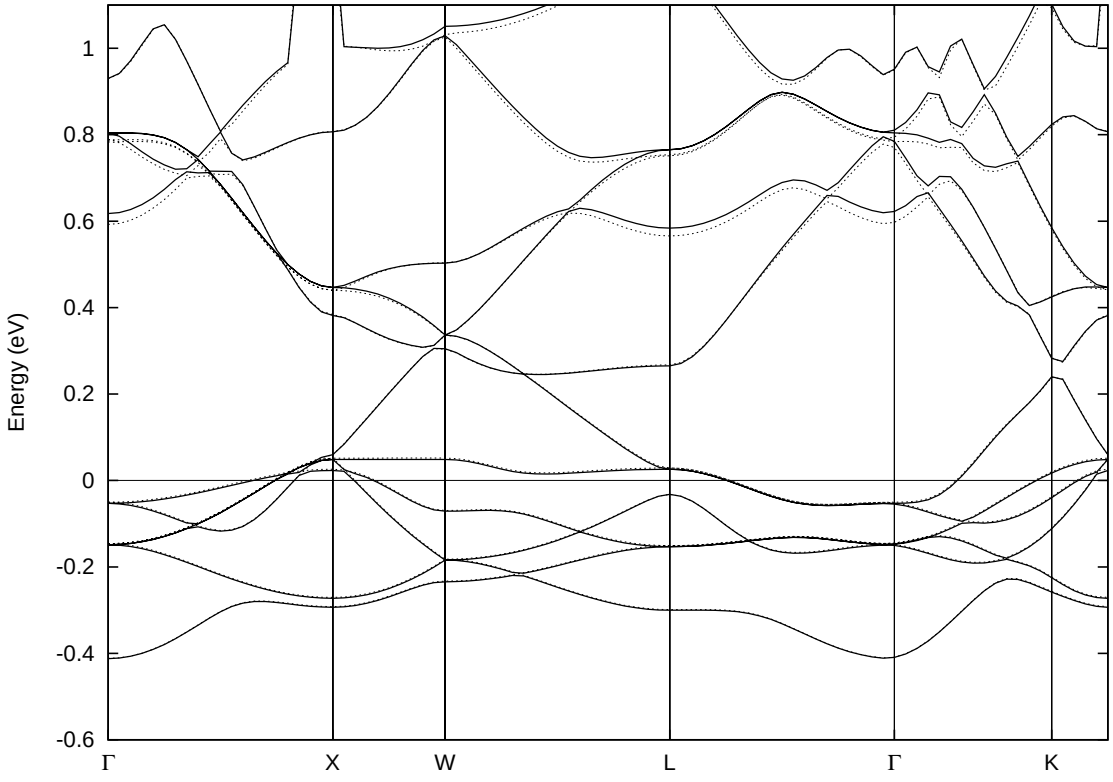

Figure 6.22: Band structures of Iridium along high–symmetry lines of the irreducible part of the first Brillouin zone (see Figure 3.2). This illustrates the differences observed when including the $5f$ component (dotted lines) compared to excluding the $5f$ component (solid lines). The zero of energy is the Fermi level.

We observe almost no change in the band structure near or below the Fermi level. This implies that the occupied states are only of s, p and d character. It is no surprise then that we find little deviation in the bulk properties of the solid when the f component of the pseudopotential is included. Noticeable changes in the band structure near the Fermi level would result in dramatic effects on the calculated physical properties of the elements and since no such changes were observed, we do not expect the physical behaviour of the bulk crystal to be affected.

For higher energy states however, we do see small changes in the band structure as a result of the inclusion of the f component. In Figure 6.22 we observe a slight downward shift in the energy of the bands from about 0.4 eV above the Fermi energy. A downward shift is expected since there is more variational freedom in the occupation of the states with the inclusion of the f pseudopotential. The shifts are largest between the L and Γ point, with a change of about 0.02 eV in energy. Although these changes are relatively small, this is clear evidence of the effect of the $5f$ pseudopotential component on the bands of the system. As mentioned earlier, f orbitals are highly localized. The inclusion of the localized orbitals has resulted in the hybridization of the high energy s, p and d orbitals and the subsequent downward shift in energy of the higher bands. These small shifts are due to the higher energy bands displaying greater f character and localization.

We can therefore clearly discern the effect the inclusion of the $5f$ orbital has had on the band structure and we wish to correlate this with the changes in physical

properties. The fact that the higher energy bands have become slightly more localized due to the inclusion of the f orbital means that the bonds between neighbouring atoms should theoretically be stronger. This strengthening of the bonds is due to the outer electrons becoming more localized and therefore lying between the atoms rather than in a delocalized cloud around it. This increase in bond strength should correspond to the observation of a slightly smaller lattice constant and correspondingly slightly larger bulk moduli and cohesive energies.

As was shown in Table 6.1 this is clearly the case. The lattice constants for the systems under investigation have remained the same or decreased very slightly in every case. The cohesive energies have increased slightly in each case and the bulk modulus has also increased slightly in some cases. These observations are consistent with our explanations on how the bond strength increases with the inclusion of the $5f$ component of the pseudopotential.

6.3 Discussion

As discussed in Section 5.6, the local density approximation tends to overbind bulk solid calculations resulting in underestimated lattice constants and overestimated bulk moduli and cohesive energies. In order to correct for this overbinding one would need to impose an increase in lattice constants and corresponding decreases in bulk modulus and cohesive energy.

What we have observed in these results is a reduction in equilibrium volume and therefore lattice constant, and in general an increase in both the bulk modulus and the cohesive energies. These changes correspond to an increase in the overbinding of the atoms in the bulk solid due to the inclusion of the $5f$ component of the pseudopotential. This can be explained by the increase in the localization of the higher energy orbitals of the electronic structure due to the f orbital. The inclusion of the $5f$ component into the total energy pseudopotential calculation has therefore resulted in a slightly more tightly bound system.

Although this inclusion has not corrected the overbinding of the systems under investigation, the effect of the f component has indeed had a noticeable effect on the electronic structure and bulk properties of the $5d$ transition atoms. Since the deviations are so small we are faced with something of a problem. We have to decide whether the changes observed in the physical properties of these atoms are large enough to warrant the inclusion of the f component in total energy pseudopotential

calculations on the $5d$ transition metal systems.

Obviously the inclusion of another angular momentum component results in a huge increase in computational demand of the total energy calculations. In the case of the unbound $5f$ orbitals the number of plane waves to describe that component is relatively high due to the deep nature of the pseudopotentials describing it. We can therefore safely assume that the inclusion of the $l = 3$ component into the pseudopotential has greatly increased the computational requirements of the total energy pseudopotential calculation. We need to weigh up this increased computational expense with the small deviations in bulk properties observed as a result of this inclusion.

Since we see only minor changes in the lattice constant, bulk modulus and cohesive energy of the transition metals there is of course the the possibility that they are merely due to errors. These errors, such as rounding errors, could be introduced as a result of the increased computational load required by the inclusion of another angular momentum component and the pressure this puts on high precision calculations. The fact that we observe some clear changes in the band structure of Iridium and Platinum as well as systematic changes in energy versus volume plots suggests that the deviations observed were not purely due to computational error but rather to changes in the electronic structure of the solid.

Chapter 7

Conclusions

In this work we employed an *ab initio* pseudopotential within density functional theory and the local density approximation to perform total energy calculations on bulk solids of the $5d$ transition metals. We studied various physical properties of these systems. We utilized the improved Troullier-Martins pseudopotential [17] in a methodology based on the plane–wave pseudopotential approach. The BEST electronic structure codes developed by Chetty *et al* [67] were used to perform these calculations.

We initially took care to construct accurate pseudopotentials for each of the elements under investigation in order to give comparable results and smooth potentials with which we could perform the total energy calculations. This was initially done excluding the unbound f orbitals for the first part of our study.

Once the pseudopotentials had been constructed we proceeded to calculated the

bulk properties of each of the $5d$ transition metals, Hafnium through to Platinum, in the face centered cubic structure by means of the total energy pseudopotential calculation. The results obtained from these calculations were compared with previous theoretical results and experimental results where available. Our results compared fairly well with experiment although the expected overbinding resulting from the local density approximation was clearly observed.

A pseudopotential to describe the unbound $5f$ orbital for each element was then constructed using Hamann's technique [70] for dealing with unbound orbitals. These pseudopotentials were rather deep and required very small real–space cut–off radii to describe the orbital accurately.

The effect of the inclusion of the $l = 3$ angular momentum component was then investigated by the inclusion of the unoccupied $5f$ orbitals in a total energy calculation for each of the systems under investigation. Our results showed only minor changes in the bulk properties of the elements with the lattice constants decreasing slightly and the cohesive energies increasing slightly in most cases. These changes pointed to an increasingly overbound system being described across the range of elements studied. This does not seem to be a result of systematic error but rather a result of small changes in the energy bands of the system resulting from the inclusion of the f channel. No significant changes in the band structure were observed at energies near to the Fermi level and therefore no major changes in bulk properties resulted.

We have seen that the unoccupied $5f$ orbitals have a small but noticeable effect on the physical properties of bulk systems of the $5d$ transition metals. This results in an increased overestimation of the bond strength between atoms in the bulk and therefore smaller lattice constants and larger bulk moduli and cohesive energies. The deviations are however very small and it is therefore difficult to justify the inclusion of the $5f$ orbitals due to the increase in computational expense required to include them especially when one considers the acceptable errors in other approximations utilized.

Future work could involve investigation of the $5d$ metals in their stable crystal structures rather than in the face centered cubic structure in order to investigate the magnitude of deviations in the bulk properties. Similar investigations could also be performed on other elements with unbound f orbitals. In most cases we expect the inclusion of these unbound states would not result in a large enough deviation to warrant the increase in computational demand resulting from their inclusion.

Bibliography

[1] F. Birch. 'Finite strain isotherm and velocities for single-crystal and polycrystalline NaCl at high pressures and 300 k.'. *Journal of Geophysical Research*, **83**:1258–1267, 1978.

[2] Wikipedia contributors. Wikipedia, the free encyclopedia - phonon. *http://en.wikipedia.org/w/index.php?title=Phononoldid=218696757*, 12 June 2008 13:45 UTC.

[3] J. C. Slater. *'Symmetry and Energy Bands in Crystals'*. Dover, New York, 1972.

[4] Ioffe Institute. Semiconductor figures - new semiconductor materials. *http://www.ioffe.ru/SVA/NSM/Semicond/Append/figs/fmd112.gif*, 12 June 2008 14:00 UTC.

[5] M. Korling and J. Haglund. 'Cohesive and electronic properties of transition metals.'. *Phys. Rev. B*, **45**:13293, 1992.

[6] C. Kittel. *'Introduction to Solid State Physics'*. Wiley, New York, 6 edition, 1986.

[7] Naval Research Laboratory. Electronic structure database - centre for computational material science. *http://http://cst-www.nrl.navy.mil/ElectronicStructureDatabase/*, 16 October 2007 11:20 UTC.

[8] S.J. Brodsky *et al.* 'A nonperturbative calculation of the electron's magnetic moment'. *Nuclear Physics B*, **703**:333–362, 2004.

[9] M. C. Payne *et al.* 'Iterative minimization techniques for *ab initio* total–energy calculations: molecular dynamics and conjugate gradients'. *Rev. Mod. Phys.*, **64**:1045–1097, 1992.

[10] M. L. Cohen. 'Dependence of lattice constants and bulk moduli on pseudopotential properties.'. *Phys. Rep.*, **1110**:293, 1984.

[11] W. Pickett. 'Pseudopotential methods in condensed matter applications'. *Comput. Phys. Rep.*, **9**:115, 1989.

[12] J. D. Joannopoulos. *'The Physics of Disordered Materials'*. Plenum, New York, 1985.

[13] D. C. Alan and M. P. Teter. 'Nonlocal pseudopotentials in molecular-dynamical density-functional theory: Application to SiO2'. *Phys. Rev. Lett.*, **59**:1136, 1987.

[14] S. T. Bar-Yam, Y. Pantelides and J. D. Joannopoulos. 'Ab initio pseudopotential solid-state calculations of highly electronegative first-row elements'. *Phys. Rev. B*, **39**:3396, 1989.

[15] A. Rappe *et al.* 'Optimized pseudopotentials'. *Phys. Rev. B*, **41**:1227, 1990.

[16] D. Vanderbilt. 'Soft self-consistent pseudopotentials in a generalized eigenvalue formalism'. *Phys. Rev. B*, **41**:7892, 1990.

[17] N Troullier and J. L. Martins. 'Efficient pseudopotentials for plane–wave calculations'. *Phys. Rev. B*, **43**:1993–2006, 1991.

[18] M Born and J. R. Oppenheimer. 'Zur quantentheorie der molekeln'. *Ann. Physik*, **84**:457, 1927.

[19] D. R. Hartree. 'The wave mechanics of an atom with non-Coulombic central field: parts I, II, III'. *Proc. Cambridge Phil. Soc.*, **24**:89,111,426, 1928.

[20] V. Fock. 'Naherungsmethode zur losung des quantem-mechanischen mehrkorperprobleme'. *Z. Phys.*, **65**:209, 1930.

[21] J. C. Slater. 'The theory of complex spectra'. *Phys. Rev.*, **34**:1293, 1929.

[22] E. P. Wigner. 'On the interaction of electrons in metals'. *Phys. Rev.*, **46**:1002–1011, 1934.

[23] E. P. Wigner. 'Effects of the electron interaction on the energy levels of electrons in metals'. *Trans. Faraday Soc.*, **34**:678, 1938.

[24] M Gell-Mann and K. A. Brueckner. 'Correlation energy of a high-density electron gas'. *Phys. Rev.*, **106**:364, 1957.

[25] G. D. Mahan. *'Many-Particle Physics'*. Kluwer Academic/Plenum Publishers, New York, 3rd edition, 2000.

[26] D. M. Ceperly and B. J. Alder. 'Ground state of the electron gas by a stochastic method'. *Phys. Rev. Lett.*, **45**:566–569, 1980.

[27] L. Hedin and S Lundquist. *'Solid State Physics'*, volume **23**. Academic Press, New York, 1969.

[28] L. H. Thomas. 'The calculation of atomic fields.'. *Proc. Cambridge Phil. Soc.*, **23**:542–548, 1927.

[29] E. Fermi. 'A statistical method for the determination of some properties of atoms. ii. Application to the periodic system of the elements.'. *Z. Phys.*, **48**:73–79, 1928.

[30] P. Hohenberg and W. Kohn. 'Inhomogenous electron gas'. *Phys. Rev. B*, **136**:864–871, 1964.

[31] J. Perdew and A. Zunger. 'Self-interaction correction to density-functional approximations for many-electron systems'. *Phys. Rev. B*, **23**:5048, 1981.

[32] W. Kohn and P. Vashishta. *'Inhomogenous Electron Gas'*. Plenum, New York, 1983.

[33] W. Kohn and L. J. Sham. 'Self-consistent equations including exchange and correlation effects'. *Phys. Rev.*, **140**:A1133–1138, 1965.

[34] M. Levy. 'Universal variational functionals of electron densities, first–order density matrices, and natural spin orbitals and solution of the n-representability problem'. *Proc. Nat. Acad. Sci. USA*, **76**:6062, 1979.

[35] M. Levy and J. P. Perdew. *'Density Functional Methods in Physics'*. Plenum Publishers, New York, 1985.

[36] Richard M. Martin. *'Electronic Structure: Basic Theory and Practical Methods.'*. Cambridge University Press, 1st edition, 2004.

[37] E. Schrödinger. 'An undulatory theory of the mechanics of atoms and molecules'. *Phys. Rev.*, **28**:10491070, 1926.

[38] A. Görling. 'Density functional theory for excited states'. *Phys. Rev.*, **139**:A796–823, 1996.

[39] F. Bloch. 'Über die quantenmechanik der elektronen in kristallgittern.'. *Z. Phys.*, **52**:555–560, 1928.

[40] D.J Chadi and M. L. Cohen. 'Special points in the Brillouin zone'. *Phys. Rev. B*, **8**:5747–5753, 1973.

[41] J. D. Joannopoulos and M. L. Cohen. Electronic charge densities for ZnS in the wurtzite and zincblende structures. *J. Phys. C*, **6**:1572, 1973.

[42] H. J. Monkhorst and J. D. Pack. 'Special points for Brillouin zone integrations.'. *Phys. Rev. B*, **13**:5188–5192, 1976.

[43] J. C. Slater. 'Wavefunctions in a periodic potential.'. *Phys. Rev.*, **51**:846–851, 1937.

[44] W. C. Herring. 'A new method for calculating wavefunctions in crystals'. *Phys. Rev.*, **57**:1169, 1940.

[45] W. C. Herring and A. G. Hill. 'The theoretical constitution of metallic beryllium'. *Phys. Rev.*, **58**:132, 1940.

[46] J. Kohanoff. *'Electronic Structure Calculations for Solids and Molecules'*. Cambridge University Press, New York, 2006.

[47] P. Pulay. 'Ab initio calculation of force constants and equilibrium geometries in polyatomic molecules. i. theory'. *Mol. Phys.*, **17**:197–204, 1969.

[48] J. C. Phillips. 'Energy-band interpolation scheme based on a pseudopotential'. *Phys. Rev.*, **112**:685–695, 1958.

[49] J. C. Phillips and L. Kleinman. 'New method for calculating wave functions in crystals and molecules.'. *Phys. Rev. B*, **116**:287, 1959.

[50] P. W. Anderson. *'Concepts in Solids'*. Benjamin, W. A Inc., New York, 1963.

[51] M. L. Cohen and V. Heine. 'Cancellation of kinetic and potential energy in atoms, molecules, and solids.'. *Phys. Rev.*, **122**:1821, 1961.

[52] N. W. Ashcroft. 'Electron-ion pseudopotentials in metals'. *Phys. Lett.*, **23**:48–53, 1966.

[53] I. V. Abarenkov and V. Heine. 'The model potential for positive ions.'. *Philos. Mag.*, **12**:529, 1965.

[54] A. O. E. Animalu and V. Heine. 'The screened model potential for 25 elements'. *Phil. Mag.*, **12**:1249, 1965.

[55] M. Hamann, D. R. Schlüter and C. Chiang. 'Norm-conserving pseudopotentials.'. *Phys. Rev. Lett.*, **43**:1494, 1979.

[56] W. C. Topp and J. J. Hopfield. 'Chemically motivated pseudopotential for sodium'. *Phys. Rev. B*, **7**:1295–1303, 1973.

[57] R. W. Shaw and J. W. A. Harrison. 'Reformulation of the screened Heine–Abarenkov model potential'. *Phys. Rev.*, **163**:604–611, 1967.

[58] L. I. Schiff. *'Quantum Mechanics'*. McGraw–Hill, New York, 1955.

[59] M. S. Hybertson and S. G. Louie. 'Spin–orbit splitting in semiconductors and insulators from the ab initio pseudopotential'. *Phys. Rev. B*, **34**:2920, 1986.

[60] G. Theurich and N. A. Hill. 'Self–consistent treatment of spin–orbit coupling in solids using relativistic fully seperable ab initio pseudopotentials'. *Phys. Rev. B.*, **64**:073106, 2001.

[61] D. R. Bachelet, G. B. Hamann and M. Schlüter. 'Pseudopotentials that work: from H to Pu.'. *Phys. Rev. B*, **26**:4199, 1982.

[62] A. H. MacDonald and S. H. Vosko. 'A relativistic density functional formalism'. *J. Phys. C*, **12**:2977–2990, 1979.

[63] G. P. Kerker. 'Non–singular atomic pseudopotentials for solid state applications.'. *J. Phys. C*, **13**:L189–L194, 1980.

[64] L. Kleinman and D. M. Bylander. 'Efficacious form for model pseudopotentials.'. *Phys. Rev. Lett.*, **48**:1425, 1982.

[65] P. M. Morse and H. Feshbach. *'Methods of Theoretical Physics, Part I.'*. McGraw-Hill, New York, 1953.

[66] P. Gonze, X. Käckell and M. Scheffler. 'Ghost states for separable norm–conserving *ab initio* pseudopotentials.'. *Phys. Rev. B*, **41**:12264–12267, 1990.

[67] N. Chetty *et al.* 'Vacancies and impurities in aluminum and magnesium'. *Phys. Rev. B*, **52**:6313, 1995.

[68] N. Chetty and M. Weinert. 'Stacking faults in magnesium'. *Phys. Rev. B*, **56**:10844, 1997.

[69] M. Boon *et al.* 'Singular integrals over the Brillouin zone: the analytic-quadratic method for the density of states.'. *J. Phys. C*, **19**:5337, 1986.

[70] D. R. Hamann. 'Generalized norm-conserving pseudopotentials.'. *Phys. Rev. B*, **40**:2980, 1989.